PHASE II REPORT

DETERMINATION OF OPTICAL TECHNOLOGY EXPERIMENTS FOR A SATELLITE

**PREPARED FOR NATIONAL AERONAUTICS AND SPACE ADMINISTRATION
GEORGE C. MARSHALL SPACE FLIGHT CENTER, HUNTSVILLE, ALABAMA**

GPO PRICE $ _____

OTS PRICE(S) $ _____

Hard copy (HC) ___5.00___

Microfiche (MF) ___1.25___

PERKIN-ELMER

PERKIN-ELMER

ELECTRO-OPTICAL DIVISION   NORWALK, CONNECTICUT

ENGINEERING REPORT NO. ___7924___

PHASE II REPORT
DETERMINATION OF OPTICAL TECHNOLOGY
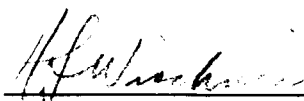EXPERIMENTS FOR A SATELLITE

DATE: FEBRUARY 1965

PREPARED FOR: NATIONAL AERONAUTICS AND SPACE ADMINISTRATION

GEORGE C. MARSHALL SPACE FLIGHT CENTER
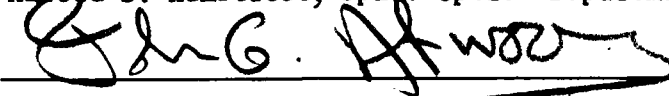
HUNTSVILLE, ALABAMA 35812

Contract: NAS 8-11408
SPO 26471

Herbert F. Wischnia, Project Leader

Harold S. Hemstreet, Space Optics Department Manager

John G. Atwood, Director of Research

Other Project
Participants

R. Arguello
J. Dunn
R. Hufnagel
E. Kerr
S. Meyers
J. Plascyk
E. Schlesinger

TABLE OF CONTENTS

TABLE OF CONTENTS (Continued)

LIST OF IILUSTRATIONS

LIST OF ILLUSTRATIONS (Continued)

LIST OF ILLUSTRATIONS (Continued)

PERKIN ELMER

LIST OF TABLES

PERKIN-ELMER

Optical Technology Satellite

PERKIN ELMER

SECTION I

SUMMARY

This Phase II Report recommends earth satellite experiments which would advance the technology associated with deep space optical communications and diffraction limited optical systems in space. As such, this document is a continuation of the Phase I Report[1] which was submitted to NASA's Marshall Space Flight Center in December 1964. Material presented in the former document is not repeated in this volume. Block diagrams and further system analysis of experiments selected from the 13 experiments identified in the Phase I Report are presented. Cost and schedule information is included based on inputs from Perkin Elmer, Douglas Aircraft Company and Grumman Aircraft Engineering Corporation. Both of the airframe organizations have submitted technical approaches to the Optical Technology Satellite vehicle itself, and these preliminary studies are included as addenda to this volume.

The key issues of aperture size and its effect on channel capacity for a deep space optical communication system have been evaluated for a number of crucial parameters. The Laser Communication Performance curves of the Phase I Report have been computed for diameters of 8, 16, 32 and 64 inches for quantum efficiencies of the detector equal to 8 percent and 100 percent. This family of curves can be found in Section V of this report.

In conclusion, the calculations of channel capacity for a deep space optical communication system of the form indicated for the Optical Technology

---

[1]References can be found starting on page 6-1.

Satellite can provide a communications break-through over microwave communication systems. For a 32-inch aperture system, with a 100-milliwatt laser, the channel capacity calculations indicate a reception on earth at night of 5.2×10^6 bits per second (with a quantum efficiency of the sensor = 100% or a channel capacity of 0.42×10^6 bits per second (quantum efficiency = 8%). Both of these values are for error rates per bit of 10^{-3}. These values of channel capacity can be converted to information bandwidths of 0.5 megacycles and 40 kilocycles respectively at equivalent signal-to-noise ratios of 30 decibels.

As indicated in the Phase I Report, the advancement of space optical technology can be paced by the development of the techniques for the measurement of performance of large diffraction limited telescopes in space. The technique of precisely measuring the Airy disk of the telescope on the earth surface, by means of the transmitting laser at the focal point of the telescope, is an extremely powerful tool. One can readily visualize that this tool can advance the technology of space optics in much the same manner that the Foucault knife edge test advanced the technology of terrestial optics.

At the conclusion of a study project such as this, it is entirely fitting to examine the results of the project in retrospect. While it is clearly too early to determine the real impact these two reports (the Phase I Report and this volume) will have on the advancement of optical technology and optical communication in space, we believe that there are significant contributions in the study:

- The two reports have identified scientific and engineering experiments (to advance optical technology in space) which should be conducted from an earth orbiting satellite.

- The project has developed the critical technical problems of deep space optical communications to the point that they are evident to the equipment engineer. Further, systems, subsystem and component solutions to the difficult problems are presented.

- The derivations of channel capacity as a function of practical hardware parameters should be most useful to future space mission planners in need of high bandwidth. The channel capacities are calculated using Poisson statistical models; and while the communication bandwidths that are computed represent an appreciable breakthrough over present day microwave performance, we believe they are obtainable although they are considerably lower than some of the overly optimistic values that have appeared in the literature.

SECTION II

OVERALL REQUIREMENTS FOR THE OPTICAL
TECHNOLOGY SATELLITE

The basic system elements required to conduct the experiments considered in this program for the Optical Technology Satellite are the typical ingredients for any space borne experiment, i.e., the booster system, the satellite system, the experimental payload (in this case laser telescopes), and the ground station to assist in conducting the experiments and to collect data. Of these system packages, the booster system was not considered during this program, since it is assumed that Saturn IB, Saturn IVB and Centaur propellant stages have the capability to insert the payload into a synchronous orbit.

There is some question regarding the degree of modification of the Centaur to achieve a synchronous orbit. Perkin-Elmer has contacted the Centaur Project Office at NASA's Lewis Research Center and was advised that the basic Centaur configuration could be used for the synchronous orbit requirement with some modification. Lewis Research Center personnel indicated that an original objective of the Centaur was to launch an Advent payload into a 24 hour orbit. The present configuration does not have the Advent mission requirement; instead it is planned to be used with Surveyor. However, modifications to the booster to provide a synchronous orbit capability are feasible.

2.1 SATELLITE REQUIREMENTS SUMMARY

From the experimenter's point of view, the satellite is the bus which carries the payload to the proper location and provides necessary support services. It is apparent to individuals considering the project in its entirety, that the bus and its associated services are the most expensive items. As a consequence, the requirements specified for the vehicle were identified as clearly as possible and reduced in number to only those requirements which are truly essential to serve the payload.

Overall Weight - The weight specification of 6000 pounds overall was furnished to Douglas and Grumman. This was based on a preliminary calculation of overall weight of 5550 pounds by Perkin Elmer. A 10 percent weight contingency was added to establish the 6000 pound requirement. This value is less than the predicted payload capability of the booster system for a synchronous orbit by some 2000 pounds. However, no weights were available on interstage structure between the Centaur, the satellite and the MSFC shroud. Therefore, the two airframe organizations were given the 6000 pound weight figure as a starting point with the information that if the cost, complexity or reliability could be improved, a maximum of an additional 1,000 pounds could be considered in the design approaches.

Overall Volume - Because of the generous proportions of the Saturn booster, the Optical Technology Satellite will not be a high-density payload. The basic requirements issued to the airframe organizations were that the two telescopes must be housed and that there be no interference with the MSFC shroud.

Orbit - The mission performance requirements with respect to the orbit originated in the concept that the satellite should simulate as closely as possible the conditions likely to be encountered in a deep space mission. While the simulation of the deep space parameters need not be exact, the concept requires that the choice of satellite orbit should provide experimental communications conditions which approximate those of deep space. Since the tracking angular rates of a deep space vehicle are relatively low, in the vicinity of 7×10^{-5} radians per second, a low-altitude circular orbit was ruled out due to the excessive angular rates involved.

While a low altitude orbit could provide a period of time during which the angular rates are low by virtue of an ellipticity to the orbit, this orbital approach would permit only a limited time for conducting experiments between a single ground station and the satellite.

A high altitude orbit with ellipticity is a distinct possibility, rather than a circular orbit with an inclination to the ecliptic. However, after independent investigation by the orbital mechanics groups at both Douglas and Grumman, the recommendation (subject to a more detailed study in the future) remains: a sychronous altitude circular orbit with an inclination to the ecliptic of 30 to 60 degrees. The maximum value of inclination permissible depends upon future capabilities of the Centaur as well as the range safety requirements for Cape Kennedy.

Satellite Pointing - The pointing to the apparent ground beacon from the satellite (the up-down error from the line of sight and the left-right error from the line of sight) requires the satellite to orient itself in response

to commands from the sun sensor in the acquisition mode and from the telescope

gimbals during the tracking mode. Since the precision demanded of the satellite

pointing system is not high, a relatively loose tolerance of ± 0.25 degree

was specified.

The pointing requirement for the satellite in rotation about the

line of sight (RLOS) is intimately connected with the approach to acquisition

considered in the Phase I Report. In Appendix B of this report the perform-

ance requirement is derived for rotational steering about the line of sight.

For a selected set of deep space parameters, alignment to within 0.056 degrees

is necessary. Approximately half of this value, ± 0.025 degree, was allocated

to the satellite pointing system.

Thermal Requirements - One of the most difficult technical requirements for

any space vehicle housing a large-aperture, diffraction-limited optical

system is the minimization of thermal gradients in the vicinity of the

telescope. The thermal gradients that exist across the primary mirror cause

loss of figure of the mirror surface. Since the performance of the mirror

must approach theoretical perfection, the tolerance on the thermal environment

of the mirror is correspondingly tight. Even with the utilization of

materials with very low thermal expansion, the amount of deformation per-

mitted is a small fraction of a wavelength.

Based upon experience gained by Perkin-Elmer during the develop-

ment of Stratoscope II with its 36-inch solid fused silica primary mirror,

the thermal specification placed on the satellite in the vicinity of the telescopes was a circumferential thermal gradient of $\pm \frac{1}{4}^{\circ}$ C obtained by passive thermal control only. In our judgement this tolerance specification is most difficult to meet (if possible at all) within the weight and orbit restraints with passive control only. This judgement on achievability of the thermal requirements was transmitted to both Douglas and Grumman with the understanding that if relief from the specification was desired, it could be obtained. However, if relief was sought, a new specification number was to be offered by the airframe group.

A -30°C ambient temperature specification was imposed also. This temperature was based on technical convenience to the experiment payload sensors. Alternate ambient temperatures in the vicinity of the telescopes in the satellite could be accommodated by the payload without technical difficulty.

Satellite Power-Off Residual Angular Rate - A specification of a residual angular rate of 0.1 degree per hour was provided to both Douglas and Grumman. The requirement for this power-off rate arises from the need to have some tracking experiments conducted with the minimum of vibrational disturbance to the payloads.

In the roll about the line of sight axis (RLOS), the subsystem error requirement is 0.05 degree total. The time necessary to conduct the acquisition operation is grossly estimated as being equal to the time it

takes Stratoscope II to conduct its guidance star acquisition operations. This time is about one half hour. Therefore, with the broad similarities between the acquisition approaches of OTS and Stratoscope II, the power-off rate about this axis could be grossly estimated as the 0.05 degree error divided by the 0.5 hour requirement or a power-off rate requirement of 0.1 degree per hour for RLOS.

Satellite Lifetime in Space - A lifetime in space of 1 to 2 years after launch was specified. This requirement originates in the deep space optical communication system considerations. If a future vehicle is to travel inter-planetary distances, travel times involved will necessarily be measured by large fractions of a calendar year. Therefore, equipment lifetimes of one to two years are necessary. The experiment plan is that after the experiments are conducted, perhaps a three month period, the vehicle would be put in a standby mode similar to an interplanetary coast mode. After a three month period in this mode, the experiments would be repeated. This cycle would be repeated every six months for the life of the satellite.

All materials, subsystems, and components should be selected with this lifetime requirements in mind.

Additional Satellite Services - In addition to the key functional requirements described in the preceeding paragraphs, the satellite is expected to provide the microwave transmission link and the electrical power sources. It is believed that space-qualified hardware is obtainable for the microwave system which would be capable of handling telemetry data rates of 200,000 bits per

second. This data rate is adequate for the housekeeping functions of the satellite, the telescope, and the proposed experiments.

Estimates were made on the anticipated power requirements for each telescope in each mode of operation (see Appendix C). The experiment power requirements approximate 300 watts with a duty cycle of 50 percent.

2.2   EXPERIMENTS REQUIREMENTS SUMMARY

The Phase I Report discussed the equipment required to conduct the scientific and engineering experiments recommended by that report. The major items of hardware in the payload are listed below.

(1)   Two 32-inch-Aperture Telescopes

(2)   Diffraction Limited Optical Systems

(3)   Laser Modulators

(4)   0.1 Arc-second Pointing Subsystem

(5)   Coarse Acquisition Subsystem

(6)   Rotational Line of Sight Guidance Subsystem

(7)   Point Ahead Subsystem

(8)   Laser Local Oscillator

(9)   Multiple 10 mw Laser Sources at Different Wavelengths for Transmitters

Although laser sources are considered throughout the Phase I Report, a brief summary is in order. Based upon the communication calculations of Section 8 of the Phase I Report, 10 milliwatts of diffraction-limited laser power on the satellite will produce the very substantial channel capacity

of 7.5×10^{10} bits per second. Ten-milliwatt gas lasers are clearly within the current state of the art. Although a "flight-worthy article" does not exist at present, the weight, size, and power requirements indicate that a gas laser is the logical choice. Different wavelength lasers are indicated for the Scintillation Experiment. A wavelength of 1.15 microns should be used in addition to the 6328Å wavelenth. Also, a solid state diode laser should be tested in space. The gallium arsenide laser seems like a competitive candidate for the gas laser at this time because of its high conversion efficiency ($\sim 20\%$) at a substantial power output (~ 0.5 watt). A third and unspecified laser source is indicated in the Phase I Report for Telescope 2. The laser development activity is moving so fast that the choice of the third laser should be left to as late a period of time as possible. The point that is being made, is that the package design should contain an unmistakable open section so that at the latest practical time, the newest laser development of practical size, weight, reliability, etc., can be included in the space borne instrument.

2.3 GROUND STATION REQUIREMENTS SUMMARY

Location - The very important factors of ground station location are

  (1) a geographical area which has good seeing

  (2) local weather which has a high percentage of unclouded days and nights

  (3) effect on range launch problems

  (4) start-restart requirements of the Centaur stage.

It would be desirable if the ground station could be located in a geographical area which would permit the satellite to be sighted from

other observatories of the world so that the experiments could be conducted by astronomers and scientists from the international community. For example, assume that the ground control station is located in the western United States. With the satellite inclined at an angle of 30 degrees to the ecliptic, and at synchronous altitude, the satellite is in the direct line of sight of observatories 4000 miles away from any point on the trajectory. The ground control station in Western Unites States, as an example, could set up an experiment sequence for the satellite so that an experiment could be conducted with an observatory in Chile in the Andes Mountains. The observatory in Chile would require very little ground equipment to act as a ground tracking beacon for the satellite guidance system. The equipment required uses a 2-inch diameter telescope with a relatively low power laser (about 0.5 watts), a system for controlling the hour angle and declination angle of the laser telescope, and any special experimental equipment.

If the ground control station is located in the Ascension Islands instead of Western United States, then observatories in Europe and Africa could participate in the experiments. However, the trade-offs of Centaur modifications and personnel and equipment travel costs would require additional study.

It should be noted that these international experiment operations apply more readily to a satellite in a circular orbit at synchronous altitude with a stored ΔV. This alternate approach would simulate deep space angular rates by utilizing the cold gas jets on the satellite in such a manner that the satellite is given an additional trust increment, or ΔV, on

command. If this approach were to prove more feasible economically for the satellite than the inclined 24 hour orbit, then this same equipment could be utilized to shift the satellite to the vicinity of some foreign observatories.

Equipment - The major equipment groups required for the ground control station follow:

   (1) 30-inch Aperture Telescope

   (2) Optical Tracking Receiver Subsystem

   (3) Transmit Laser Beacon Subsystem

   (4) Laser Modulator Subsystem

   (5) Point Ahead Subsystem

   (6) 4 Auxilliary 12-inch Aperture Receiving Telescopes (for intensity measurements)

   (7) 6 Auxilliary 2-inch Aperture Transmitting Telescopes (with lasers)

   (8) 1 Mobile 2-inch Aperture Transmitting Telescope (with 0.5-watt laser)

   (9) Operational and Control Consoles (for the satellite and experiments)

   (10) Ephemeris Display Equipment

   (11) Data Processing Facilities

   (12) Satellite Diagnostic Display Equipment

   (13) Data Recording Facilities

   (14) Microwave Transmitting and Receiving Equipment

2.4 OPTICAL TECHNOLOGY SATELLITE COST SUMMARY

Perkin Elmer has prepared budgetary cost estimates for the payloads and associated equipment necessary to produce the experimental equipment identified in the Phase I Report. In addition, Douglas and Grumman have prepared budgetary cost estimates for the satellite itself. The basis for the satellite costs can be found in the Douglas and Grumman technical approaches which are attached to this Phase II Report as addenda.

Total Program Estimates - The budgetary costs presented in Table 2 - 1 are arithmetic averages of the independent estimates by the two airframe organization plus the appropriate experiments estimates. These costs are based on a launch schedule of 3 to 3 1/2 years after program start up.

TABLE 2 - 1		
Phase I	Period of Time (Months)	Estimate (Millions)
Satellite and Payloads Initial Engineering, Design, Experimental Test Rigs and Breadboards	0 - 12	$5.7
Phase II Final Engineering, Manufacturing and Testing of Models and Flight Qualification Unit	9 - 26	$34.0
Phase III Flight Unit Manufacturing and Testing	10 - 37	$18.2
Equipment Costs Range From		$50 to $62

Experiments Estimates - The budgetary costs for the satellite payloads and associated equipment were prepared by Perkin Elmer based on the selected experiments identified in the Phase I Report. The estimates were assembled from individual hardware item estimates, where available, and from breakdowns for each phase of the program (See Table 2 - 2). The costs are based on a schedule which would permit the airframe organization to assemble and test the entire satellite so that a launch date of 3 to 3 1/2 years could be attained. The program schedule for the experiments equipment is shown in Figure 2 - 1, while the schedule for the vehicle can be found on page 3-2 of the Grumman document. The Douglas schedule which was submitted to Perkin-Elmer also indicated a 3-year launch date after go-ahead.

Figure 2-1. Experiments Development Schedule

TABLE 2 - 2

BUDGETARY ESTIMATE - EXPERIMENTS

(Dollars In Thousands)

Task No.	Task Description	Engr.	Mfg.	Materials	Other Direct Costs	Total Dollars
1.	Design of Space-Borne Equipment (Generation 1)	$1,900	$600	$800	$ 85	$3,385
2.	Thermal, Structural, Form & Fit Models	-	200	120	5	325
3.	Reliability Testing of Subsystem & Components	100	260	175	10	545
4.	Design, Development, & Build 2 Engineering Models (Generation 2) (1 unit for Flight Qualification Test)	1,750	1,340	1,400	80	4,570
5.	Flight Unit, Manufacturing Assemble and Test	300	690	700	40	1,730
6.	Manufacturing and Field Support Spares		175	100	8	283
7.	Field Operations During Integration, Test and Check-out	313			82	395
8.	Documentation & Special Reproduction Charges				150	150
9.	Special Facilities				200	200
10.	Engineering Support During Delivery of Flight Unit	344	125	125	30	624
		$4,707	$3,390	$3,420	$ 690	$12,207

SECTION III

CONFIGURATION SUMMARY

3.1 OPTICAL CONFIGURATION

This portion of the study defines the basic optical system, including the main telescope with its required optical guidance systems. The space allocation in the satellite provides an over-all length of 10 feet and a diameter of 40 inches. The dimensional allocations are important to the optical design considerations and have influenced the suitable lens form investigations. The overall arrangement is shown in the Frontispiece.

Functionally, the optical system contains three separate channels:

(1) A fine guidance channel with precise line of sight pointing capabilities.

(2) A coarse guidance channel with a larger field of view but with less stringent pointing requirements.

(3) A transmit laser channel with precise pointing.

The functions are performed by the main telescope optical system although each channel requires special purpose optical elements. The fine system is optically coupled to both an image dividing prism and, by means of a beam splitter, to the laser transmitter. The transmitted laser beam enters the optical system from behind the primary mirror and passes through the fine guidance system. The 32-inch diameter primary mirror acts as the transmit laser antenna with a beam spread of 0.2 arc-second. The field of view for this fine guidance system is 2 arc-minutes.

The coarse channel has a one degree field of view, and it must lock onto the earth beacon and center it in the telescope so that the earth beacon image enters the fine guidance system field of 2 arc-minutes.

For the purpose of determining some of the specific optical components required for these functions, the complete optical system must be considered as comprising three distinct optical units; a main telescope consisting of primary and secondary, a fine transfer unit, and a coarse transfer unit. The optical design requirements for each of these units have been individually considered.

Main Telescope - A 32-inch aperture has been established as a requirement from photometry and bandwidth calculations. This aperture size immediately limits the selection of possible lens forms to those which are either entirely reflective or catadioptric. In addition to the aperture, optical parameters including the fields of view and image quality have been determined by system requirements. Thus, the optical characteristics which will assist in the determination of the system form are:

(1) field of view

(2) image quality

(3) relative aperture

(4) color correction

(5) obscuration ratio

(6) sensitivity of system to alignment

Field of View - The field of view requirements have been set at 2 minutes of arc for the fine channel and one degree for the coarse channel.

Image Quality - Image quality requirements have been established as a beam spread of 0.2 arc-second for the f/70 system over the central 2 minute area of the field; this corresponds to diffraction limited performance.

The region of the field beyond one minute off-axis to 1/2 degree is less critical, since its use is limited to coarse guidance.

Relative Aperture - The main telescope's relative aperture is determined by the system's overall length limitations. However, the optical form should minimize the system sensitivity to mechanical and thermal disturbances in space so that focus and alignment are maintained. In addition, the primary mirror speed is a factor in establishing the system speed since there are manufacturing constraints on f/D when figuring diffraction limited mirrors.

Color Correction - Since monocromatic light will be used at the 6328Å and 8400Å* wavelengths, all refracting optics must be corrected for this spectral region. Color correction for the primary mirror is automatically obtained, since reflective optics are used.

Obscuration Ratio - The diameter of the secondary mirror should be held to a minimum to reduce transmission losses, and to maintain favorable sine wave response characteristics. Restricting the maximum diameter of the secondary to about 6 inches keeps the transmission losses to less than 4 percent, while the frequency response characteristics are not appreciably altered from those of an unobscured system.

Sensitivity of System to Alignment - In addition to the parameters listed above, the sensitivity of the entire lens to misalignment of its components is a design consideration which influences the selection of a final form.

---

*If argon ion lasers are used as ground beacons, the wavelength would be 4880Å or 5145Å instead of 8400Å.

<u>Coarse Optical System Image Dividing Mirror</u> - This mirror has the function of dividing the 1-degree field into four quadrants. The ground beacon image is dissected by the four elements of the mirror. The budles of rays from each quadrant element pass through four individual field lenses, are reflected from a single folding mirror, and then pass through four individual transfer lenses to four photomultiplier tubes as shown in Figure 3-1. The up-down and left-right signals are developed from the signals received by the four photomultipliers into acquisition commands for the coarse acquisition subsystem. The control signals will drive the ground beacon image to the center of the image dividing mirror. A central hole approximately 0.4 inch in diameter is cored in the segmented mirror to permit the central portion of the field to pass through to the fine guidance optics.

This overall arrangement for the coarse guidance optical elements has evolved from considerations of alignment factors. The present arrangement is relatively insensitive to misalignment of the field lenses, the folding flat, the transfer lenses and the photomultiplier tubes. It is sensitive to the placement of the four quadrant mirror surfaces to each other and to the alignment of the hole cored into the center of the image dividing mirror. However, the location of this mirror is directly behind the primary and this vicinity is most duitable for equipment with alignment requirements.

The image diameter corresponding to a 1-degree field of view at the image dividing mirror is 8.4 inches. The overall length of the mirror is

PERKIN-ELMER
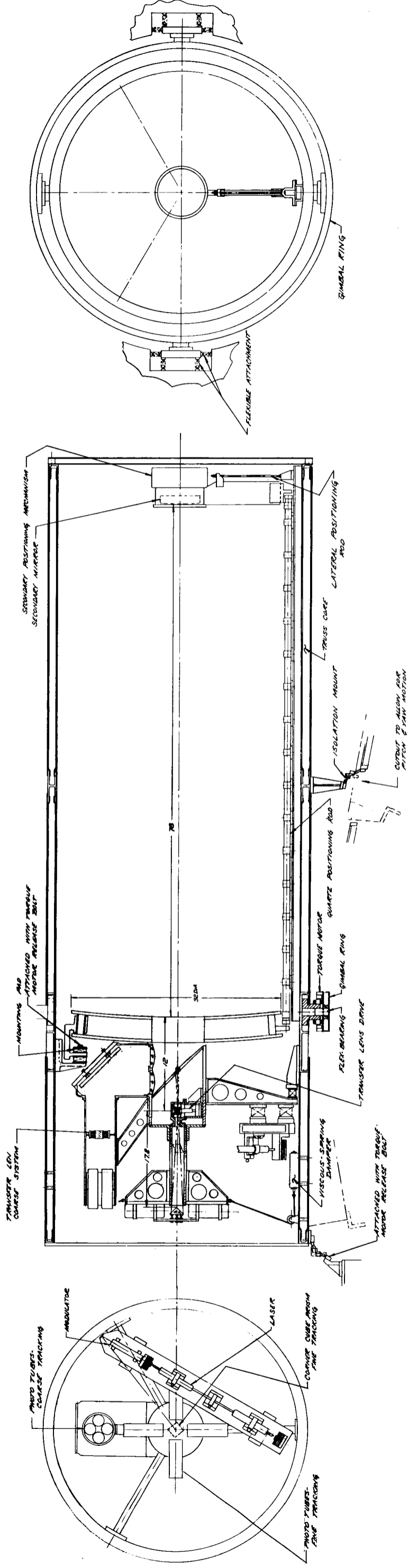
Figure 3-1. Overall Arrangement of OTS Optical System

3-5.

12 inches, and the 0.4 inch elliptical hole in the mirror corresponds to a 2-minute field stop.

Consideration of Basic Lens Forms - From an optical system point of view, the all reflective lens forms are most attractive because these forms are inherently free of chromatic aberration. Even though the optical system will be used with laser sources, different wavelengths are required. One length is indicated for the spaceborne laser transmitter and a different wavelength is used for the ground beacon. Also, the Scintillation Experiment will use multiple laser wavelengths. Thus, chromatic aberration is a consideration even though monochromatic sources are used.

The reflective lens forms are desirable as well because of their lightweight and basic ruggedness. Large refractive elements can be designed and manufactured, but all factors considered, the reflective forms represent the more suitable choice.

The most promising lens forms for the OTS Mission are the well known Gregorian and Cassegrain configurations. The Stratoscope II Telescope utilizes a Gregorian form while the Princeton Experimental Package of OAO is a Cassegrain. The choice of these two spaceborne large aperture optical systems are based on similar considerations of optical performance as well as relative insensitivity to alignment problems.

Gregorian Form - The Gregorian lens uses a paraboloidal primary mirror combined with an ellipsoidal secondary in order to achieve the necessary optical correction. The concave ellipsoidal mirror is located behind the focus of the primary. This extends the overall system length an amount which depends upon

3-7

the magnification factor selected for the secondary mirror. An f/4 primary mirror speed gives a primary focal length of 128 inches. This exceeds the desired OTS overall system length of 120 inches. Increasing the primary mirror speed to f/3 reduces the primary focus to a point 96 inches from the mirror vertex. However, even the f/3 relative aperture does not reduce the system length sufficiently to permit an in-line secondary mirror even with the necessary additional transfer optics.

A folded arrangement in the basic Gregorian form whereby a flat mirror is located in the primary's convergent beam and the ellipsoidal secondary axis is placed perpendicular to the main system's optical axis has been considered as a method of reducing the tube length. Unfortunately, this arrangement, while within the length limitation using an f/3 primary, presents severe mechanical support and alignment problems. Consequently, it has been eliminated from further consideration in favor of the more easily aligned in-line telescope form. This narrows the selection of a suitable lens form to the Cassegrain or one of its modifications.

Cassegrain Form Consideration - The true Cassegrain lens employs a convex secondary mirror located before the focus of the primary; this location substantially shortens the system's tube length. For example, if an f/4 primary and a 6 inch diameter secondary are taken as a starting point, then the system length, primary to secondary vertex distance, is approximately 104 inches in the Cassegrain compared with over 150 inches for a Gregorian system. If an f/3 primary is used, the length is reduced to 75 inches. Since the length of the main telescope is of major concern, every reasonable effort should be made to limit its length. While an f/3 paraboloidal mirror of 32 inches diameter is

not an easy fabrication task, especially if figured to a $\lambda/50$, the problems presented are not insoluble. Paraboloidal mirrors of this, and larger diameters, have been successfully fabricated to a relative aperture approaching f/3. A $\lambda/50$, f/3 mirror of this size is known to be within the current state of the art. Since length requires f/3, an f/3 primary mirror speed has been used as a design parameter for the OTS.

Lens Form Factors - Another characteristic which influences the choice of the mirror forms is the main telescope f number. This value is established by determining the location of the system focus. It is desirable from the mechanical point of view to locate the transfer lens optics for both channels to the rear of the primary mirror's support. This means locating the main system's focus approximately 12 inches in back of the primary mirror vertex. At this location the mechanical support for precise optical alignment is excellent. This focus location combined with the secondary diameter of 6 inches yields a primary-secondary speed of f/15.

Several other design factors also bear on the establishment of the primary-secondary speed. These factors are associated with providing an f/70 convergence at the fine channel image dividing prism. Large transfer lens magnifications are undesirable,* and in order to keep the transfer magnification less than 5, a main system relative aperture of f/14, or slower is necessary. (The f/15 speed set above requires a 4.67X transfer lens.)

---

*Large transfer lens magnification makes the system excessively sensitive to small motions of the transfer lens servo.

with the present 4.7X fine transfer lens a 0.001-inch lateral displacement at the main system focus will result in a 0.0047-inch displacement at the final image plane. Longitudinal displacement of 0.001 inch at the main focus will result in a focal shift of approximately 0.022 inch at the final image. These values are not disproportionately large and are within the allowable range for maintaining performance.

<u>Cassegrain Lens Form</u> - In summary, the main system will be an f/15 Cassegrain configuration with a 32-inch diameter primary mirror and 6-inch diameter secondary mirror. The mirror vertex separation is 78 inches with the focus located 90 inches from the secondary mirror. This basic configuration is shown in Figure 3-2.

The system parameters established above permit several possible lens forms to be used in the Cassegrain arrangement; the true Cassegrain, aplanatic Cassegrain, and Dall-Kirkham telescopes.

The true Cassegrain has a paraboloidal primary and hyperboloidal secondary and is completely corrected for axial spherical aberration by this combination. An alternate form known as the aplanatic Cassegrain, or Ritchey-Chretien lens, employs the same basic mirror forms - that is a hyperbolic primary and hyperbolic secondary. These mirror contours are aspheric and depart from true conics. These departures provide correction for coma as well as spherical aberration, and consequently the form is capable of good performance over a wider field of view than the true Cassegrain. A third form known as the Dall-Kirkham is also a possible choice. In this form an ellipsoidal primary mirror combines with a spherical secondary to provide spherical aberration
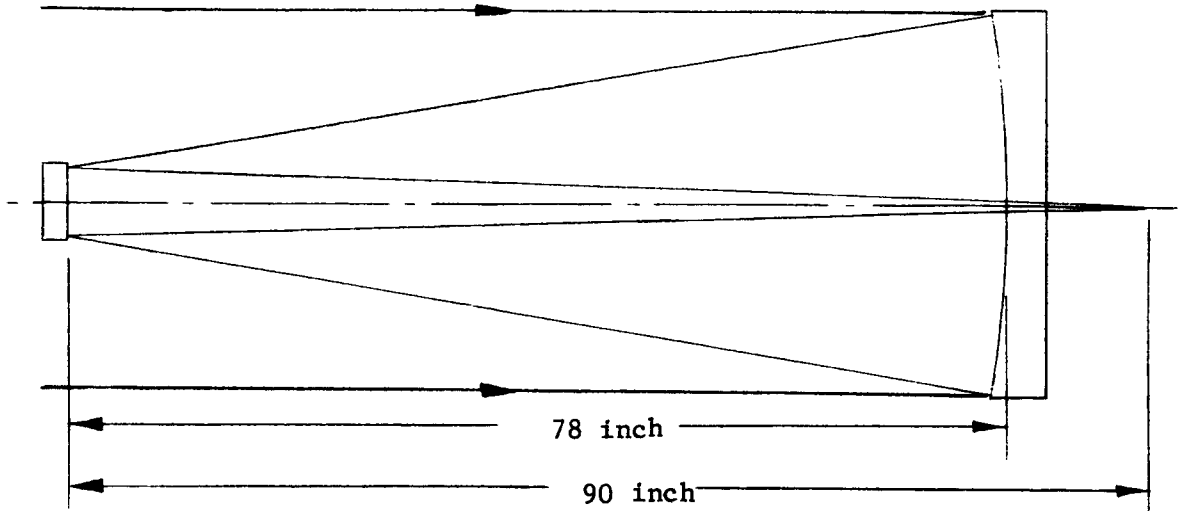
Field Angle	Image Size
2 Minutes	0.27 inch
1 Degree	8.38 inch

E.F.L. = 480.0 inch = 40 feet

Figure 3-2. Main Unit Optical System
(f/15 Cassegrain Type Configuration
With 32" Diameter f/3 Primary)

correction. The fabrication advantages offered by the Dall-Kirkham's spherical secondary are distinct, and in addition there are advantages in alignment and test which support this lens form.

The inherent performance capabilities of each of these lenses including sensitivity to optical alignment is the final basis for selection. Their optical fabrication and test problems may later control the selection of the final form if serious problems arise in these areas.

Axially, the optical capabilities of each of the three systems are equivalent; each is free of chromatic and spherical aberration. It is the field rays in the presence of element decentration which must be considered in order to demonstrate the superiority of one of the lenses. Off-axis, the first aberration to limit performance is that of coma. For the true Cassegrain and Dall-Kirkham lenses this aberration restricts the usable field. For the aplanatic Cassegrain the third order coma is completely corrected and astigmatism limits the useful field.

The true Cassegrain offers no optical advantage over the Dall-Kirkham and it is more difficult to fabricate. The comparison of the lens forms, therefore, can be reduced further to that between the aplanatic Cassegrain and the Dall-Kirkham.

An optical comparison between the aplanatic Cassegrain and Dall-Kirkham lenses has been made for rays entering the primary mirrors at two field angles. The aberration curves (h versus tan U') for each of the lenses for centered and decentered conditions have been plotted in Figures 3-3 through 3-6 for the OTS.
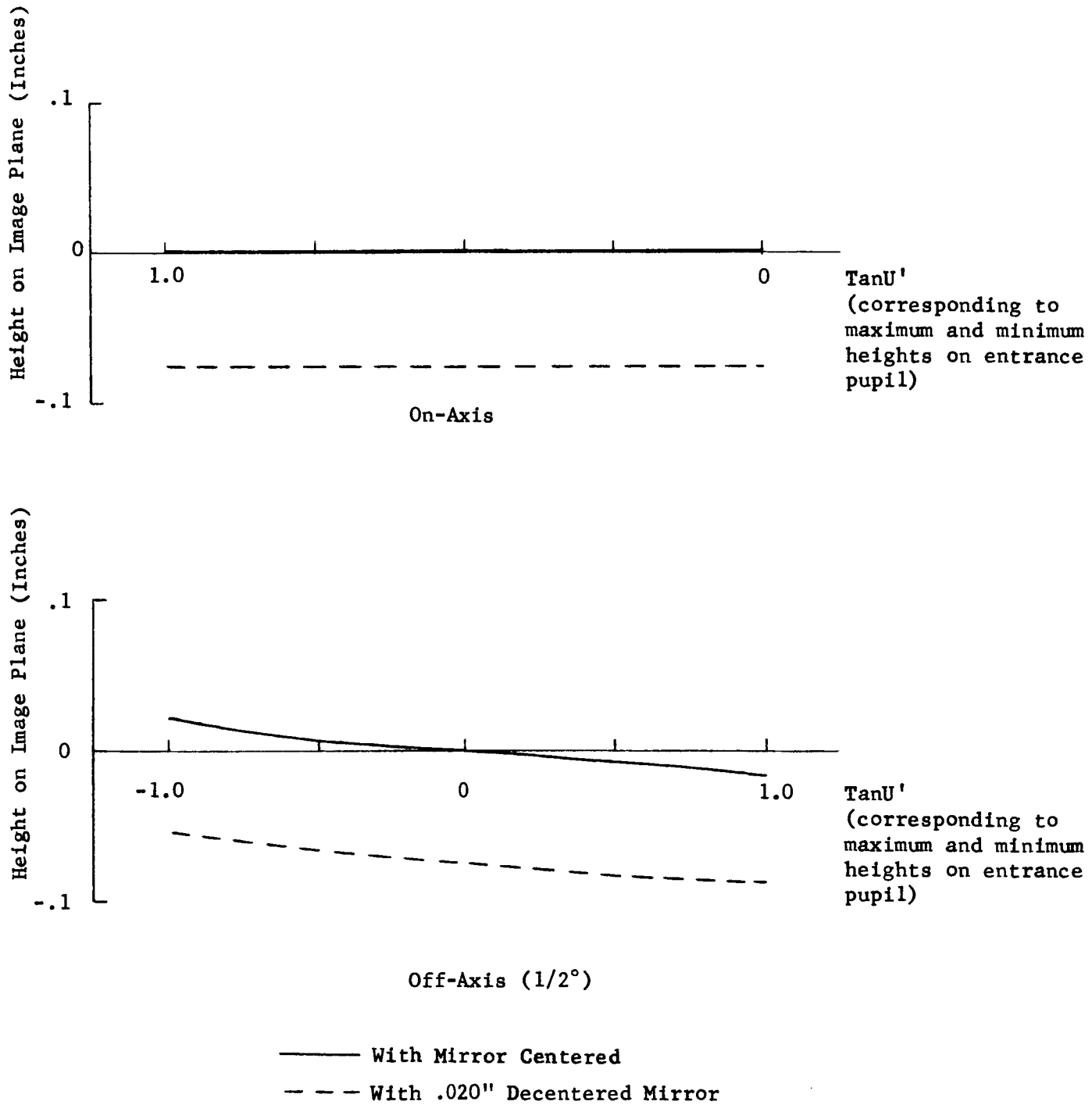
Figure 3-3. Aberration Curves of Ritchey-Chretien
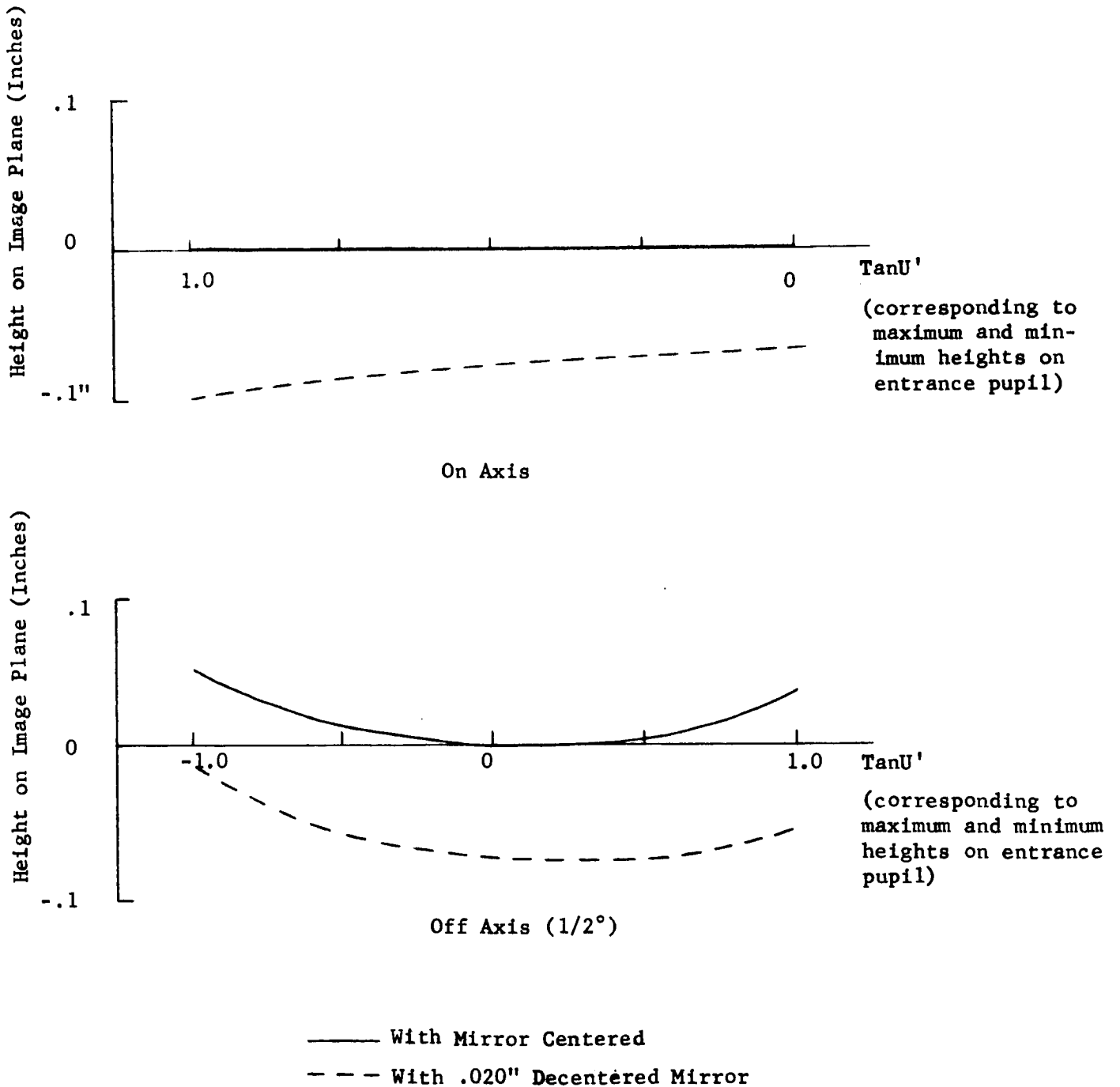
Figure 3-4. Aberration Curves of Dall-Kirkham Lens

PERKIN ELMER

Ritchey-Chretien Lens

1 Minute of Arc Off-Axis

(corresponding to maximum and minimum heights on entrance pupil)

Dall-Kirkham Lens

1 Minute of Arc Off-Axis

(corresponding to maximum and minimum heights on entrance pupil)
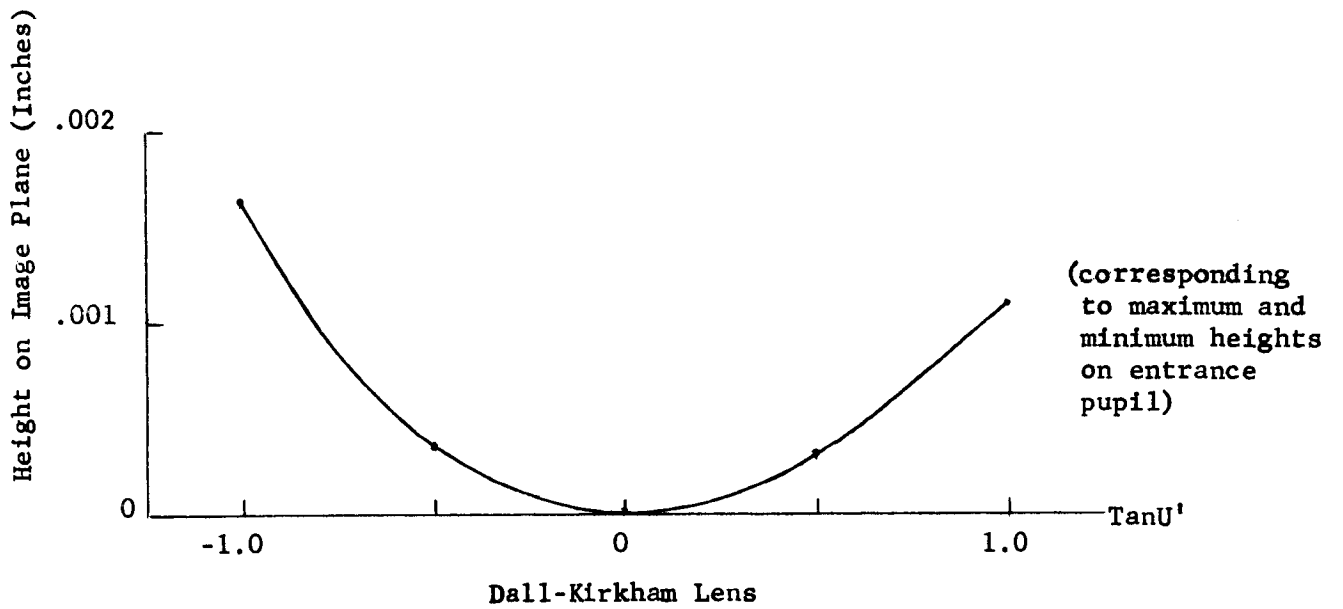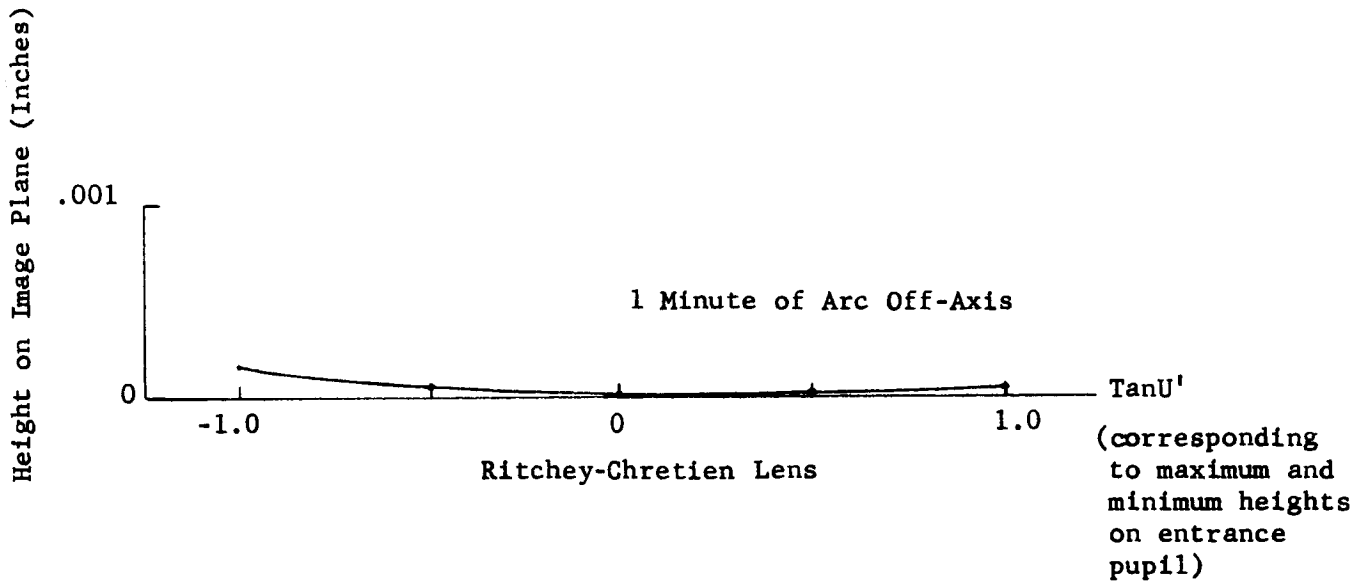
Figure 3-5. Aberration Curves of Centered Systems
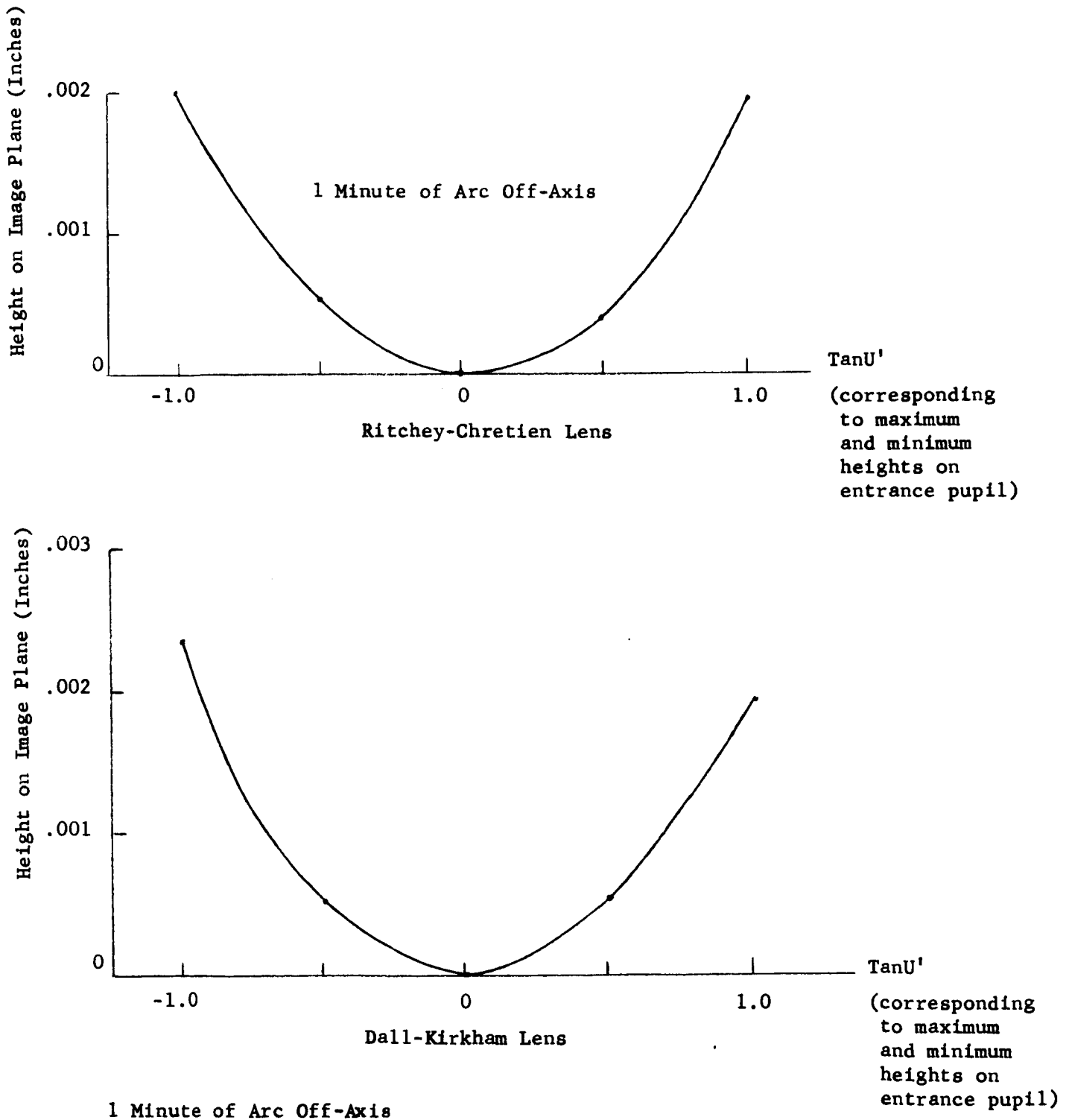
Figure 3-6. Aberration Curves of .020 Inch
Decentered Secondary Mirror System

The curves plot height on the image plane, h, versus the tangent U' of the angle that the ray makes with the optical axis leaving the system. Differences in the ray heights indicate the extent of the blur circle.

The Ritchey-Chretien lens is naturally superior for the centered mirrors. It is of interest to compare these two systems in the presence of decentration. Figures 3-3 and 3-4 also show the aberration curves for the two systems when their secondary mirrors are displaced laterally from the optical axis by 0.020 inch. For 1 minute of arc off-axis, the performance of the aplanatic system is just slightly better than the Dall-Kirkham as shown in Figures 3-5 and 3-6 and in actual operation the performance difference probably would not be seen.

The aberration curves of Figures 3-3 and 3-4 include the centered and decentered cases when the field angle is increased to 1/2 degree. At the increased field angle the Ritchey-Chretien system is far superior[*] for both the centered and decentered cases and its use for the main telescope system assures system performance through both the fine and coarse channels.

Unless unusual manufacturing problems arise because of scattered light problems, the Richey-Chretien lens form will be used.

Fine Channel Transfer Lens - At the main telescope focus the linear field which corresponds to 2 arc-minutes is approximately 0.28 inch. Because of this small image, a field lens at this location can be completely avoided. However, a

---

[*]Superiority of a lens form is indicated by the straightness of the curve. Image displacements, as such, are not important since compensating transfer lens shifts are practical.

transfer lens will be used to decrease the f/15 convergence of the main tele-scope to an f/70 cone at the final image location. This convergent relation-ship establishes the lens magnification at 4.67X and results in a 1.3-inch diameter field at the corner cube. This size assists in establishing the size of the corner cube prism at 1.5 inches.

Dimensional limitations require the use of a transfer lens which has a short conjugate distance, i.e., the distance from the main system focal point to the final image at the prism. Shortening this distance increases the lens field of view requirements and increases the difficulties of providing high performance. A reasonable compromise value for this distance appears to be approximately 17.8 inches. A 5-degree field of view for the lens results. This field of view is safely within the performance capabilities of a high per-formance transfer lens and at the same time the length is reasonable.

Relative aperture is determined by the established long and short conjugate convergences. These require an f/11.8 (infinity based) speed.

In summation, the transfer lens requires an f/11.8 relative aper-ture and a 4.67 magnification. The required conjugate distance is 17.8 inches and the corresponding angular coverage is approximately 5 degrees. The lens will be designed for diffraction limited performance in the 6328Å and 8400Å* spectral regions.

---

*See footnote page 3-3.

Fine Channel Auxiliary Optics - Several additional optical components will
be required to transfer the output beam from the laser to the focus of
the main telescope. This includes a beam-splitter. A straight-through
optical path to the fine channel image dividing prism, and a reflected path
for the laser beam will be provided by this element. (The glass path through
the beam splitter will be considered in the final correction of the transfer
lens aberrations.)

In order to provide the required point ahead capabilities,
deviation to the laser beam will be introduced by means of a Risley prism. Rotation
of the prism elements will produce the required amount of beam deviation. It
will be necessary to allow for the optical path through this prism in focussing
the laser assembly so that its focal position is precisely conjugate with the
focus at the image dissector prism.

Coarse Channel Optical Train - The function of the transfer lens in this
channel will be to increase the f/3 convergence to f/4 at the photomulti-
pliers, this dictates a 3.75X demagnification. The linear dimensions of the
main system's image, which corresponds to a 1 degree field of view, is 8.38
inches and the use of four individual field lenses (one for each quadrant of
the coarse image dividing mirror) will be necessary to keep the transfer lens
size reasonably small . The field lenses are located at the main system's
focus and will image the primary mirror, which is the system's entrance
pupil, into the pupil of the transfer lenses.

The available space for the image transfer determines the con-
jugate distance for the coarse channel transfer lens. Since the image

quality requirements are less stringent than for the fine channel lens, the field angle may be substantially increased without adversely affecting the performance.

A conjugate distance of approximately 32 inches has been taken. This requires an angular field of view of approximately 20 degrees, and an infinity-based relative aperture of approximately f/3.2. These requirements can be met by the use of a Biotar type lens containing 6 or 8 optical elements.

3.2 MECHANICAL ARRANGEMENT

The optical configuration (Section 3.1) basically establishes the telescope's general arrangement. The light but rigid aluminum structure shown in Figure 3-1 has channel section rings to provide hard points for mounting of major components within the tube. These rings are positioned by longerons. The entire structure can then be stiffened by truss-core sandwich panels between the rings and longerons. The units will be assembled by welding rather than brazing or riveting, since the use of brazing for this type of structure is difficult to control, and the use of rivets results in structural hysteresis after exposure to severe dynamic environment.

The centerline distance between the facing surfaces of the primary and secondary mirror is 78 inches. The indicated design of the primary mirror is of eggcrate construction. The diameter of the mirror is

32 inches with a 4-inch thickness. The mirror is mounted to a circular ring of aluminum alloy using lateral positioning links of titanium alloy. As shown in Figure 3-1, these links also serve as connecting links to isolator pads during launch. The links are released from these pads after launch by a simple and reliable motor release mechanism. When these links are released, the primary mirror is pulled into contact with the fused quartz positioning rods. The positioning links are pivoted on ball joints at the housing and at the mirror so the mirror is free to move up and down with a rotation about the line of sight.

The secondary mirror is mounted within an axial focusing device which positions the mirror to allow for refocusing. The axial focusing device is a sealed unit utilizing a bellows to allow for axial movement. The focusing group containing the secondary mirror is mounted with a hub supported by a three legged spider structure. The legs of the spider are mounted on isolator pads during launch. The entire assembly is positioned laterally by three tension members. After launch, the legs of the spider are disengaged from the mounting pads as shown in Figure 3-1. Springs pull the legs of the spider into engagement with the quartz rods, thus axially positioning the secondary mirror with respect to the primary mirror. The tension members position the mirror laterally. Since quartz rods are the same material as the primary and secondary mirrors, they help insure that correct focus is maintained when all the elements are close to the same temperature.

Mounted behind the primary mirror are the coarse and fine tracking systems as shown in Figure 3-1. A more detailed sketch of this region is presented in Figure 3-7. The fine tracking system consists of a moveable

transfer lens, transfer lens servo actuator, image dividing prism, four photo-multiplier tubes,[*] a dichroic beam splitter, and the transmit laser. All these elements are mounted in one rigid 20-inch long package. Alignment of these elements is critical. This mounting structure consists basically of a central aluminum alloy tube in which the aforementioned elements are mounted.

The transfer lens drive system is a two-axis drive unit which is housed in a segmented cylindrical housing mounted from the center tublar structure. This servo drive actuator is basically an armature with a square fitting over a field magnet. The armature is designed to move in a lateral direction. Mounted on the same armature sleeve is another winding which serves as a tachometer to feed a velocity signal to the servo system used to control the movement of the armature. The two axis servo system provides for positing the transfer lens in accord with the control signals from the photo-multiplier sensors.

The image dividing prism and phototube(s) are mounted as one unit on a rigid structure at the end of the center structural tube. The dichroic is housed within the structural tube which has an opening to permit the en-trance of the laser beam. A larger diameter tube is mounted perpendicular to the lower end of the main support tube. This tube mounts the coarse image dividing mirror and the coarse field lenses.

---

[*] Although four individual photomultiplier tubes are shown, the single 4 quadrant photomultiplier tube similar to ITT F 4002 has good possibilities of reducing overall complexities. The comparative reliabilities and performance factors would require detailed engineering examination and exhaustive flight quali-fication testing.

PERKIN-ELMER
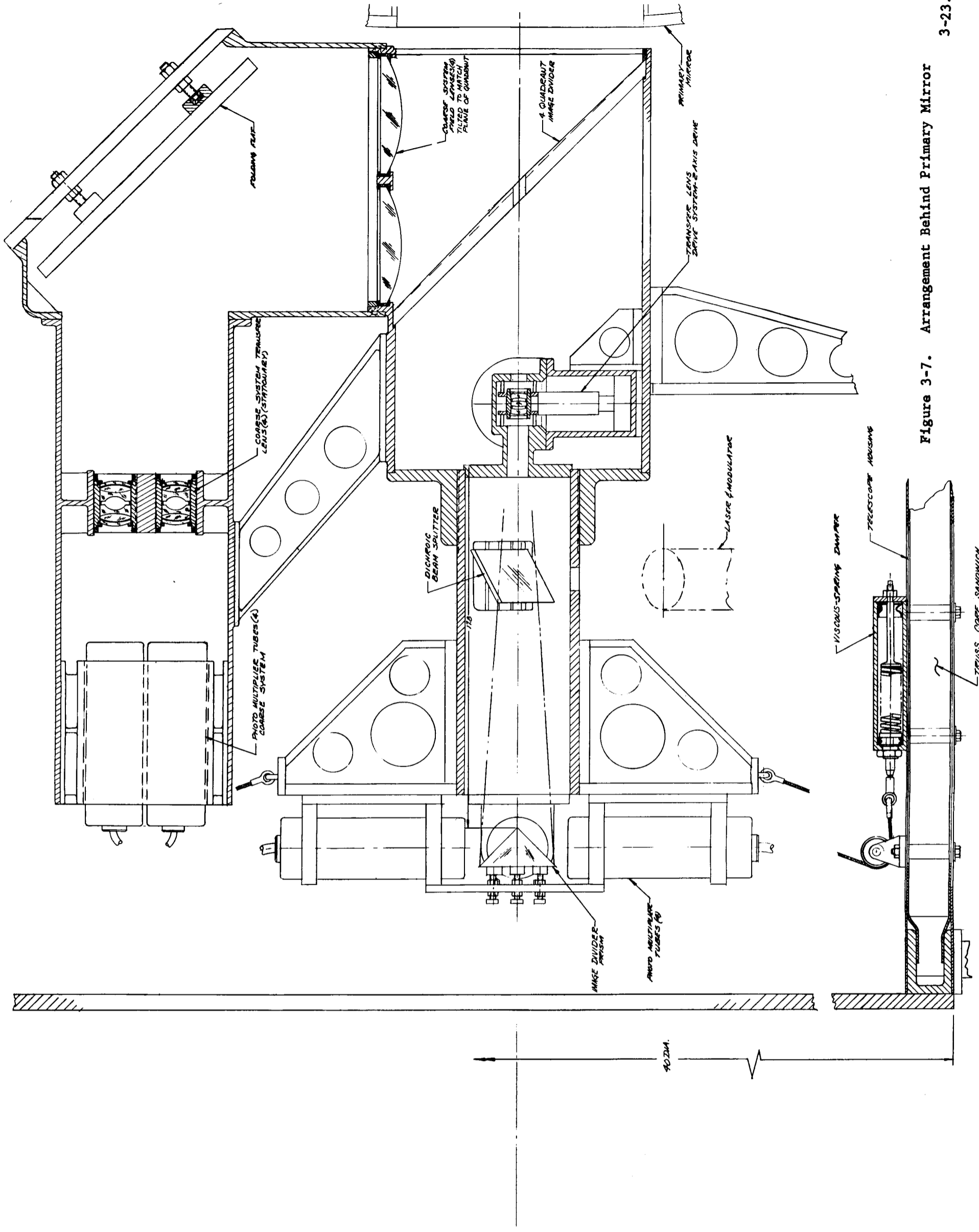
Figure 3-7. Arrangement Behind Primary Mirror

A three-legged spider mounts the tubular structure at the lower end of the tube. This spider is held to the telescope housing with shock isolator pads. At the top of the center tube beneath the phototubes are three aluminum gussets welded to the tube and the mounting plate for the photo tubes. This stiffens the entire assembly in the lateral and axial directions. A cable from each gusset connects to a spring damper on the housing wall. The damper has true viscous damping with very little hysteresis which provides good returnability. The cable from the gusset passes over a pulley on the housing wall and then attaches to the damper. The angle of the cable and the spring rate of the unit are selected to provide that the required spring rate in the three principal directions is obtained and that the elastic center of these dampers and the shock isolator pads at the lower end coincides with the center of gravity of the unit. This will prevent coupling of the dynamic loads and minimize rotational response.

The laser unit and modulator are positioned on a platform across the lower mounting spiders. Depending upon the ultimate fragility of the laser, isolator pads might be added between the laser mount and the spiders to further soften the system. Since the laser will be a source of heat, a means of dissipating this heat is required to avoid thermal problems in the nearby optical elements. A passive approach to avoid thermal problems using super insulation and special heat conductors should be used. Low conductivity pads are used to mount the laser to the spiders. Shock isolation pads, if required, can serve this purpose. The high thermal conductivity path will provide heat removal from the laser unit through the telescope housing and into the satellite heat sink. Flexible copper straps have been successfully used by Perkin-Elmer for similar applications.

The entire telescope structure is connected to gimbals. These gimbals have flexure blades supported on a plate which in turn is soft mounted to the satellite. Pitch and yaw motion are obtained by means of torque motors mounted in the gimbal ring and connected to the telescope structure and satellite respectively. This configuration is shown in an end view on Figure 3-1.

An initial design of the gimbal ring was developed, controlled by rigidity and weight. For a rotational structural frequency of 5 cps, the weight was calculated to be 12.1 pounds.

The gimbal ring is shown to scale in Figures 3-1 and Figure 3-8 shows the assembly of the pitch torque motor and flex bearing mounted in the gimbal ring. An aluminum hub which is bolted to a ring in the housing structure mounts the flex bearing and rotor of the torque motor to the telescope. The housing of the motor is bolted to the gimbal frame. The plate mounting the yaw gimbal to the spacecraft is held to the spacecraft by flexible attachments which can provide sufficient stiffness to avoid stability problems during the tracking procedures while in orbit. This mounting must be sufficiently compliant so that during the launch the dynamic loads will be reacted principally by the much stiffer isolation mounts shown in Figure 3-1. This arrangement avoids the need to capture the gimbal ring in orbit after the isolation mounts are released.

The entire telescope housing is mounted on four flexible mounts to provide attenuation of the launch environment (Figure 3-9). Four ladder type isolator mounts are shown positioned so that the elastic center will concide

TELESCOPE I HOUSING

GIMBAL RING

TORQUE MOTOR

FLEXURAL PIVOT

FLEXURAL PIVOT RETAINER CAP

1.5

1

6

Z

Z
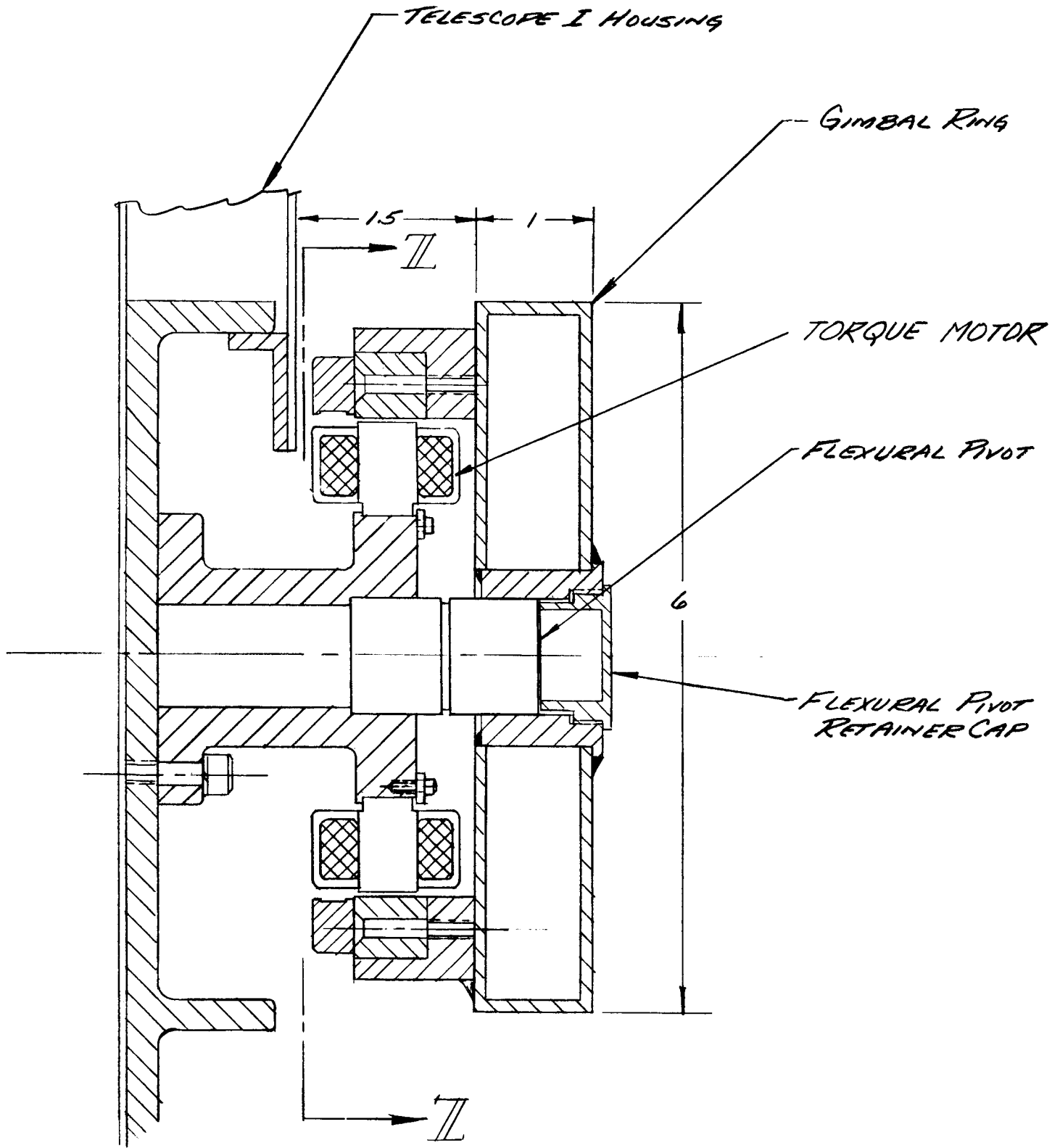
Figure 3-8. Gimbal Mounting

PERKIN-ELMER

TELESCOPE HOUSING

MOUNTS PRELOADED TO PROVIDE A RELEASE FORCE

SATELLITE RIB
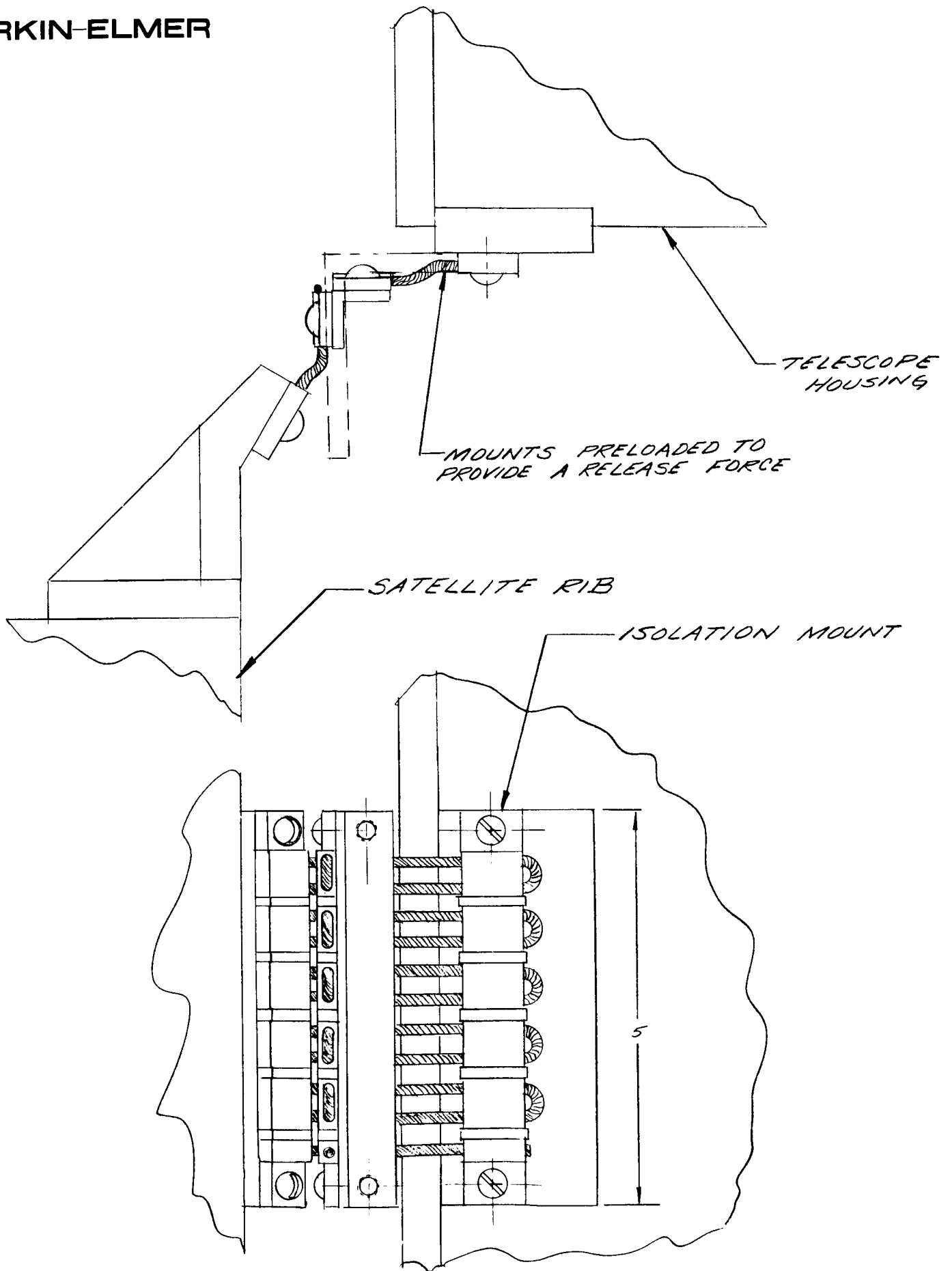
ISOLATION MOUNT

Figure 3-9.   Isolation Arrangement

with the cg of the complete telescope system. The mounts are initially preloaded so that when released after launch they snap away from their mounting positions on the satellite. The part of the isolator attached to the satellite is secured with motor release bolts. The clearance in the satellite structure is adequate so that the telescope can rotate ±10 degrees about both the pitch and yaw axes.

The dynamics of the telescope structure and its mounts are considered in Appendix E.

3.3 THERMAL CONSIDERATIONS FOR THE OTS

In the near future the optical performance of a 32-inch diameter fused quartz primary mirror of eggcrate construction must be measured as a function of thermal environment. However, certain calculations and experiments performed at Perkin-Elmer with the Stratoscope II 36-inch solid fused quartz primary mirror yielded results of enough interest to present the data in this report even though there are differences between the two mirrors (i.e., solid versus eggcrate and 36-inch diameter). For example, certain Stratoscope II calculations indicated that to maintain the mirror figure to within $\frac{\lambda}{30}$, the maximum axial temperature difference should not exceed 5.5°F, while the circumferential gradient calculation indicated a requirement for 0.36°F. Extending this data to the 32-inch primary mirror of the OTS 32-inch primary, it seems necessary to control the temperature distribution in the mirror in a similar manner. Thus, a 3°C thermal gradient axially and a 0.25°C thermal gradient circumferentially are useful initial numbers to consider until precise calculations and measurements can be made for the OTS vehicle and telescope.

To further illustrate the critical nature of the thermal control problem on the OTS, two germane calculations from Stratoscope II are presented in graphical form. Figure 3-10 shows the variation of the temperature of the front face and that of the rear face of a 36-inch mirror with time assuming an initial ambient of -55°F in the telescope. After an initial rise, the temperatures of both faces continuously decline and it is apparent from this graph that after 20 hours, thermal equilibrium is still not reached. These data indicate the need for opening the telescope capping shutter on OTS well in advance of time zero. Note also that the temperature difference between the front face and the rear face of the mirror, ΔT_{FR} does not increase continually, but reaches its maximum value of -5.9°F and then starts to decline, after about 18 hours as shown in Figure 3-11. Again, the analogous OTS situation would be the opening of the capping shutter once the satellite is on station.

The thermal control approach for the OTS Telescope is an extension of the Princeton Experimental Package Orbiting Astronomical Observatory technique of utilizing superinsulation radiation barriers (emissivity $\sim$.01).

The inner layer of this insulation which is blackened to limit light scatter can be applied in blankets to the interior of the telescope housing. This technique minimizes the heat transfer into or out of the tube to assist in the controlled thermal decoupling between the telescope optical elements and the satellite. Heat sources within the telescope housing such as the laser and laser modulator are provided with a good conducting path through the super insulation so that the satellite structure acts as the heat sink.
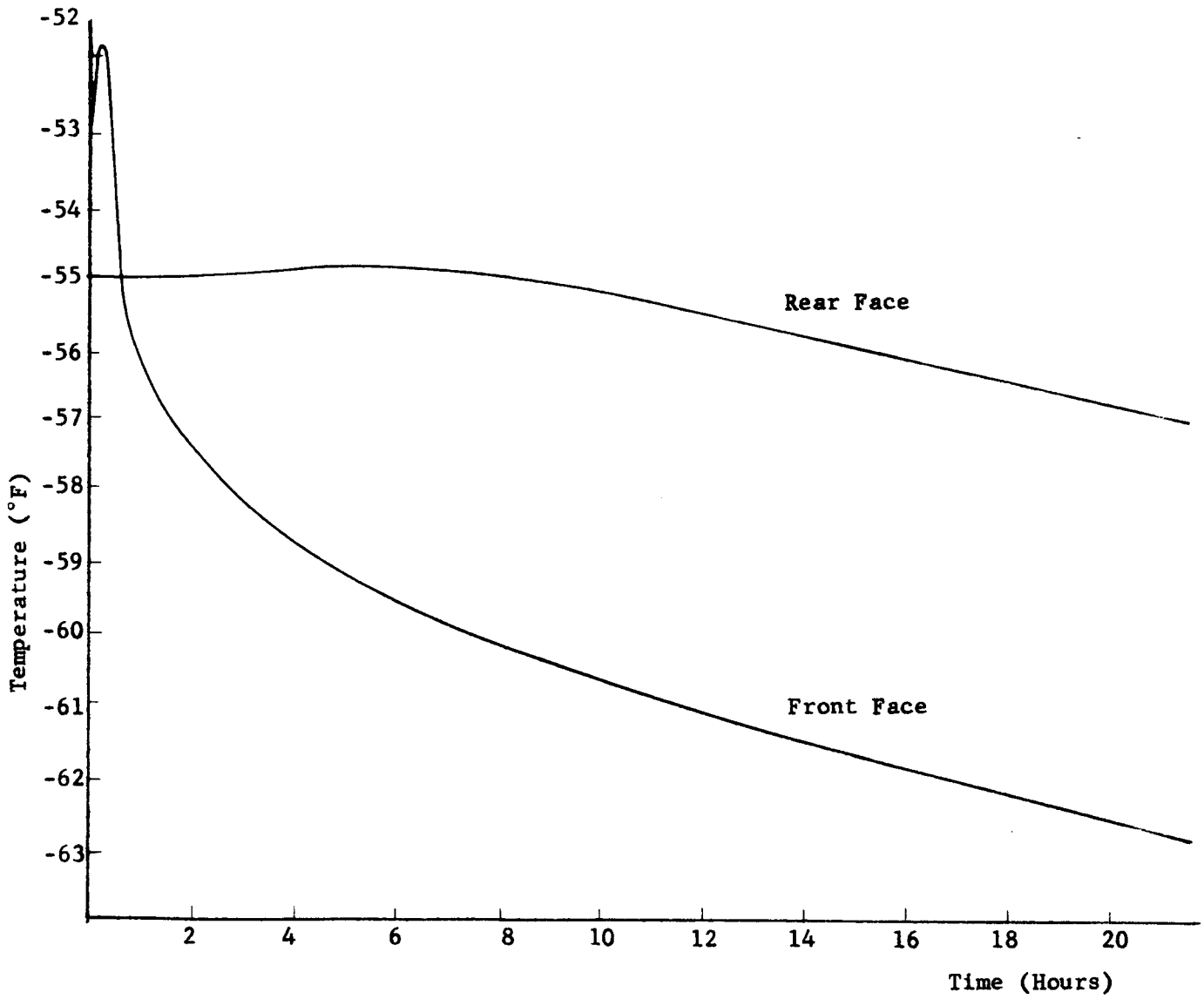
Figure 3-10. Calculated Temperature of the Front Face and the Rear
Face of a 36-Inch Solid Fused Quartz Primary Mirror as
a Function of Time
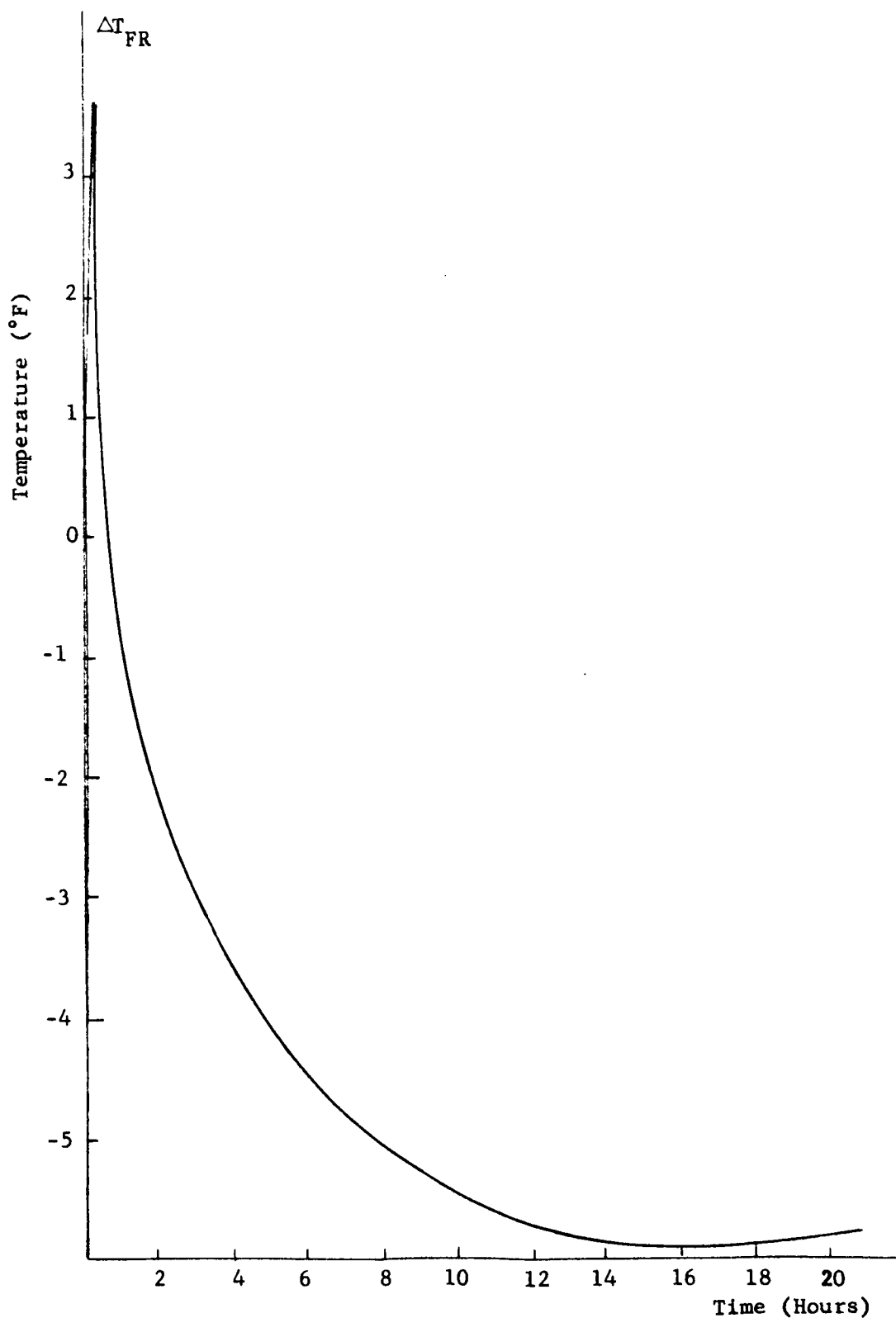
Figure 3-11. Calculated Temperature Difference Between the Front
Face and the Rear Face of a 36-Inch Solid Fused
Quartz Primary Mirror as a Function of Time

SECTION IV

ADDITIONAL EXPERIMENT DISCUSSION
AND ANALYSIS OF SELECTED EXPERIMENTS

4.1 ATMOSPHERIC SCINTILLATION AND IMAGE JITTER

This experiment originally had as its objective the measurement of the amplitude and frequency distribution of light intensity from a coherent source as sensed after passing through the whole atmosphere.[1] It is felt that data on angle arrival fluctuations should also be collected since it will be useful for the evaluation of tracking system performance. It was also suggested that scintillation measurements be carried out both from the earth to the satellite and from the satellite to the earth, for (at least) two aperture sizes, for (at least) two laser frequencies, for daytime and nighttime operation, for various meteorological conditions and slant angles.

It is felt that this experiment should be conducted on board a synchronous satellite rather than an airborne balloon since this would provide for the first time two-way measurements of intensity and angular fluctuations of a coherent source through the entire length of the atmosphere. The experiment allows one to study the different effects in the two directions of atmospheric disturbances on laser light.

The Experiment Satellite-To-Earth Link - Attention will first be focussed on the satellite transmitter configuration. Two possible laser wavelengths have been considered for this experiment. The first is 6328Å He-Ne laser wavelength,

and the second laser wavelength (1.15μ) has been chosen to be at about twice the 6328Å wavelength in order to obtain a significant wavelength dependent change in intensity scintillation.

One useful measure of the effect of atmospheric turbulence, i.e., index of the severity of the interference caused by turbulence, is the ratio of mean square value of the fluctuations about an average value to the square of the average value. This measure has the useful property of being independent of the type of encoding or modulation of information contained in the optical signal. It is of the form that will describe the random noise-like behavior of the interference. The conventional percent type modulation although useful for instantaneous measurements depends on the instant that the measurement is made and does not average over a time sufficiently long to describe average effects.

The index proposed should be relatively easy to measure, which enhances its utility for the envisioned experiment.

The radiant power from a laser beacon which impinges on a detector and is converted into an electrical signal is given by I (t). Then the average of I (t) is:

$$\overline{I\,(t)} = \lim_{T \to \infty} \frac{1}{2T} \int_{-T}^{T} I(t)\, dt$$

and the rms value of the fluctuations about this average is:

$$\overline{I^2\,(t)} = \lim_{T \to \infty} \frac{1}{2T} \int_{-T}^{T} \left[I\,(t) - \overline{I}\,(t) \right]^2 dt$$

the modulation index M is then given by:

$$M = \overline{I^2(t)} \Big/ \left[\overline{I(t)} \right]^2 = \overline{V^2(t)} \Big/ \left[\overline{V(t)} \right]^2$$

since the output voltage V (t) of a photodetector is proportional to the radiant power.

To facilitate the measurements of any index of turbulence against a fluctuating background it is desirable to have the laser transmitter system provide a constant average power level during scintillation measurements. This will allow the fluctuation values to be referenced against a relatively steady level. The pulse code modulation satellite transmitter configuration utilizing polarization modulation (PCM-PL) shown in Figure 4-1 can be used for this experiment. An adequate low frequency tracking signature can be obtained from the satellite PCM-PL system by sending a few thousand words of all right-circular polarization followed by a few thousand words of all left-circular polarization, (constant signal level). The satellite laser transmitter power level should also be monitored during this experiment, and sent via the microwave telemetry link to the earth terminal.

The earth receiver configuration shown in Figure 4-2 consists of the basic PCM-PL receiving system with separate channels for: detecting laser beacon intensity fluctuations, detecting an adjacent star's intensity fluctuations, and determining low and high frequency image motion components for both the satellite beacon and starlight. It is an engineering choice whether there should be two separately synchronized aperture controls for the beacon and stellar channel or one aperture control in front of both channels to allow scintillation measurement at several aperture diameters. The scintillation
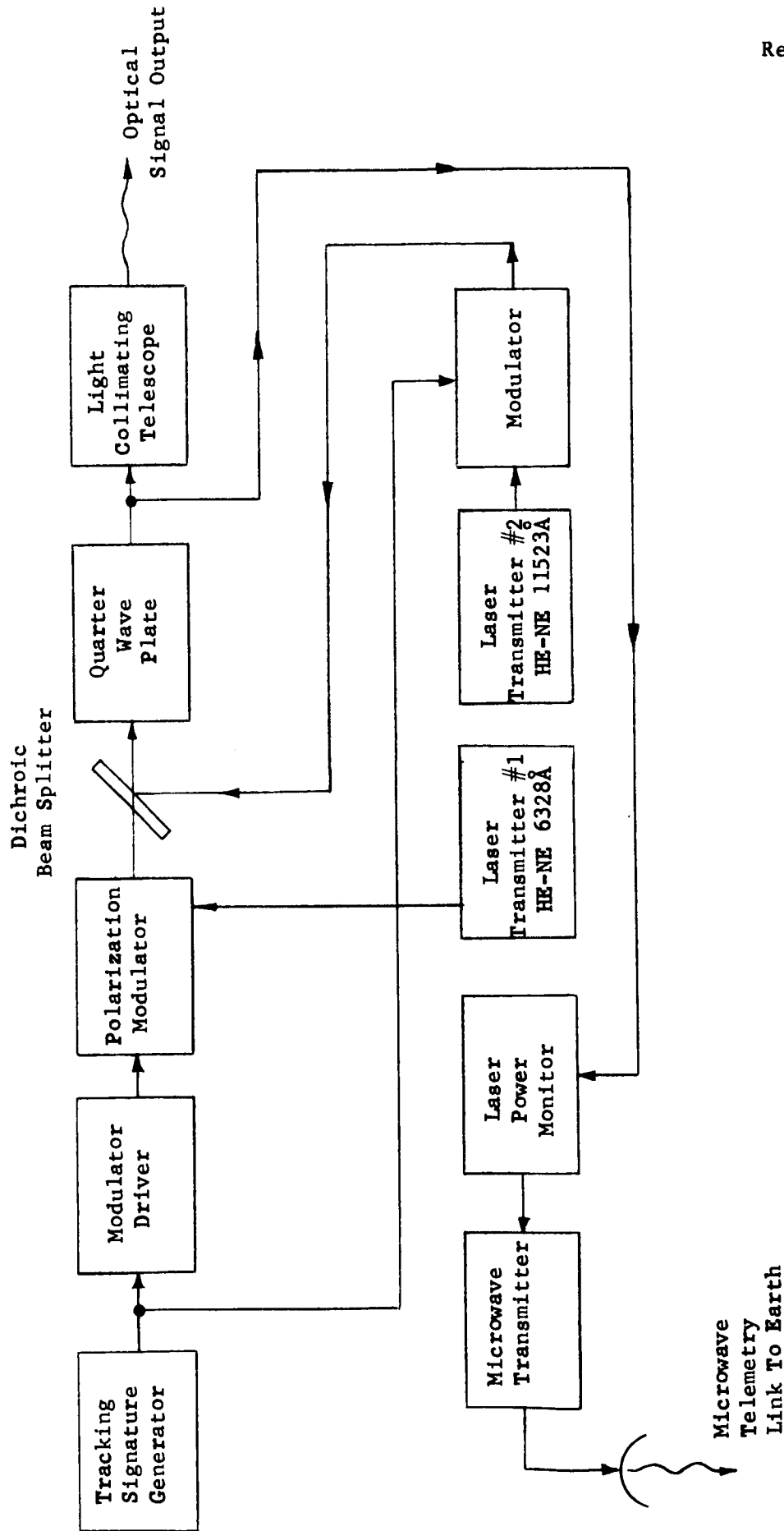
Figure 4-1. Block Diagram Of Scintillation Experiment (Satellite-To-Earth Link) Satellite Transmitter Configuration
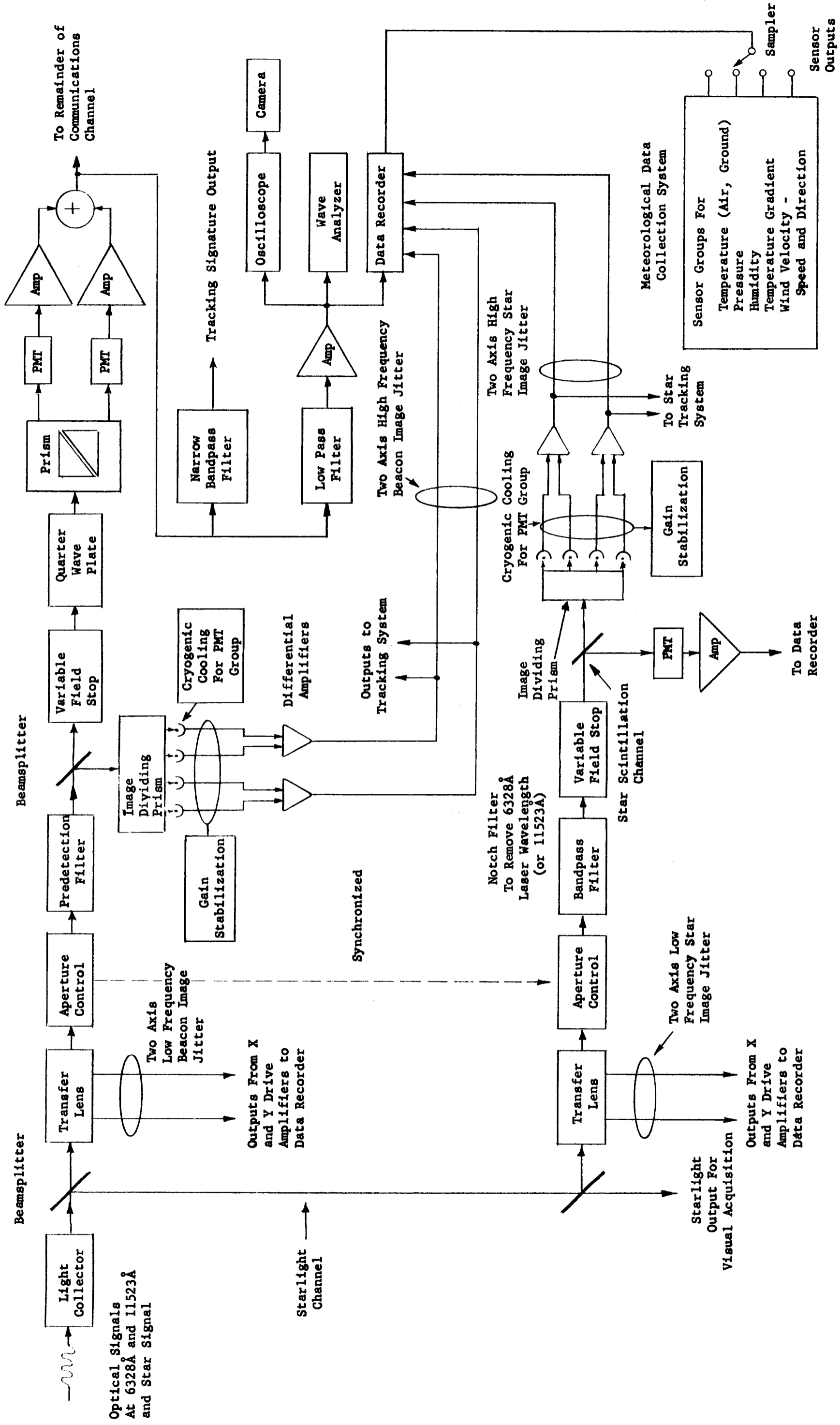
Figure 4-2. Block Diagram of Scintillation Experiment - Earth Receiver Configuration (Satellite to Earth Link)

data and the tracking signature will pass through the light collector, aperture control unit, predetection filter, variable field stop, and then on through the polarization resolving optics, photomultipliers, amplifiers and difference circuits. At this juncture the tracking signature can be extracted through a narrow bandpass filter, and the scintillation data can be extracted through a low pass filter amplifier combination.

The power spectral density of the intensity fluctuations measured by a wave analyzer will provide an indication of the frequency content of the scintillation. The power spectral density measurements can be made with various aperture diameters and under different meteorological conditions. The index of turbulence M can be determined from plots of the power spectrum. The index M can then be related to aperture diameter and correlated to corner breakpoint frequencies of the spectrum.

Oscilloscope and camera recording of the scintillation waveform will also be provided, as well as other recording apparatus. The scintillation data will be correlated with various outputs of the meteorological data collection system.

Statistical measurements of the thermal microstructure at the earth terminal should also be recorded. Various Rawinsonde systems* employing balloons to measure temperature and humidity at various altitudes could be employed at the ground terminal where the experiment is to be conducted.

---

*This equipment should be obtainable as GFE from U.S. Army Signal Corps.

The altitude information can be used together with humidity, and temperature data to obtain pressure. Slant range of the balloon can be employed to obtain wind zone velocity.

There will be simultaneous ground recording of the scintillation of a star and satellite laser beacon. The star will be chosen to be close in elevation angle to the satellite laser beacon so as to allow a comparison of the effects of the atmospheric fluctuations over approximately equal zenith distances. For the 60 degree inclination satellite orbit under consideration, it is felt that a one degree star field will be adequate to compensate for the differential in angular rates of the satellite and star, and insure enough time on both targets to obtain meaningful scintillation and image jitter data.

An optical pickoff is also provided for visual acquisition of the star.

Satellite laser beacon and stellar low frequency two axis image jitter data can be derived from the two transfer lenses' x and y drive amplifier outputs. The high frequency beacon two axis image jitter is taken from the fine tracking difference amplifier outputs. Similarly the high frequency stellar two axis image jitter is taken from the star tracking difference amplifier outputs. The image jitter amplitude, and power spectral density can also be correlated with intensity fluctuation data.

Earth-to-Satellite Link - Refer to Figures 4-3 and 4-4 for block diagrams of the earth transmitter and satellite receiver configurations respectively. A gallium arsenide laser at 8400Å which would have to be cryogenically cooled,
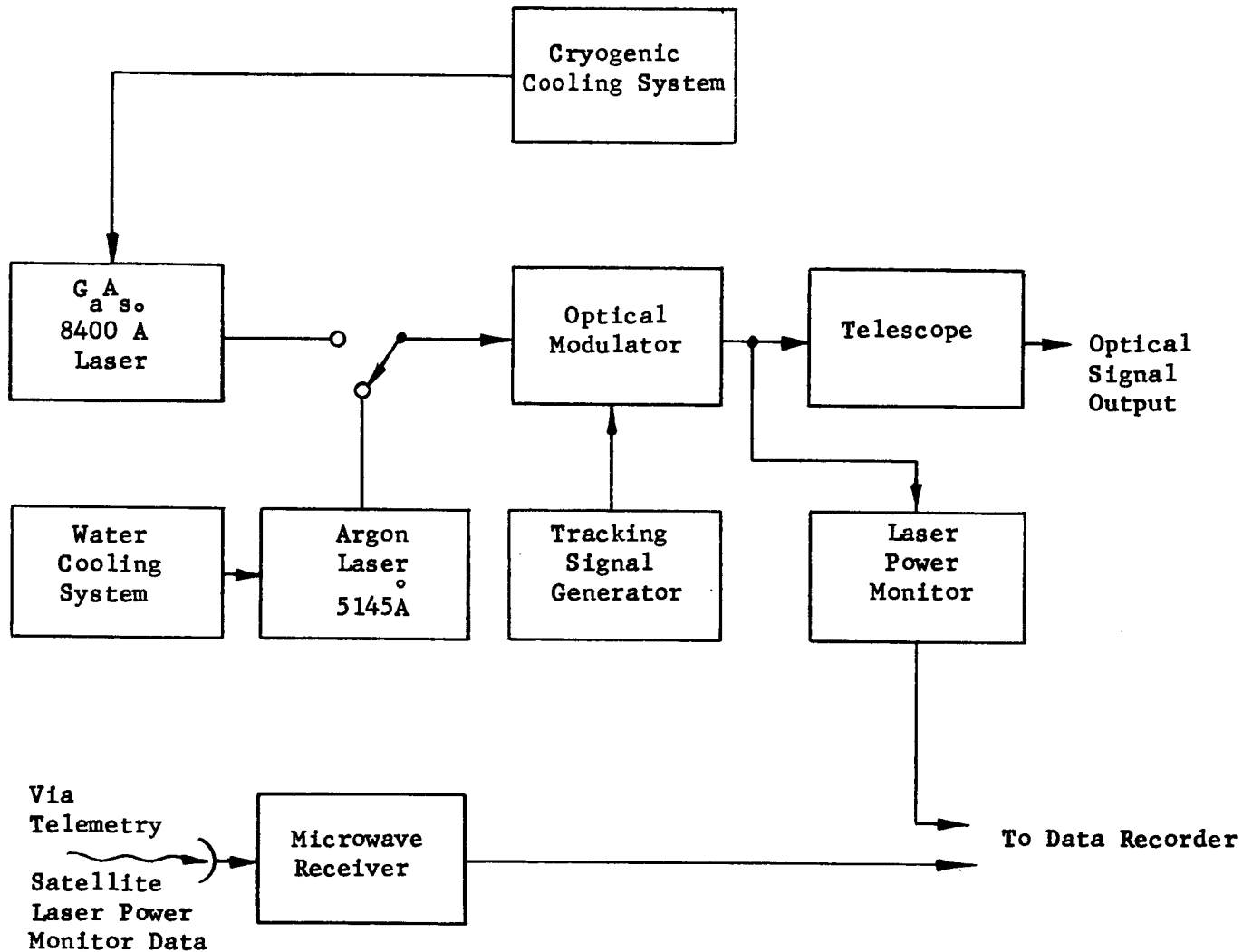
Figure 4-3. Block Diagram of Scintillation Experiment
Earth Transmitter Configuration (Earth-to-
Satellite Link)
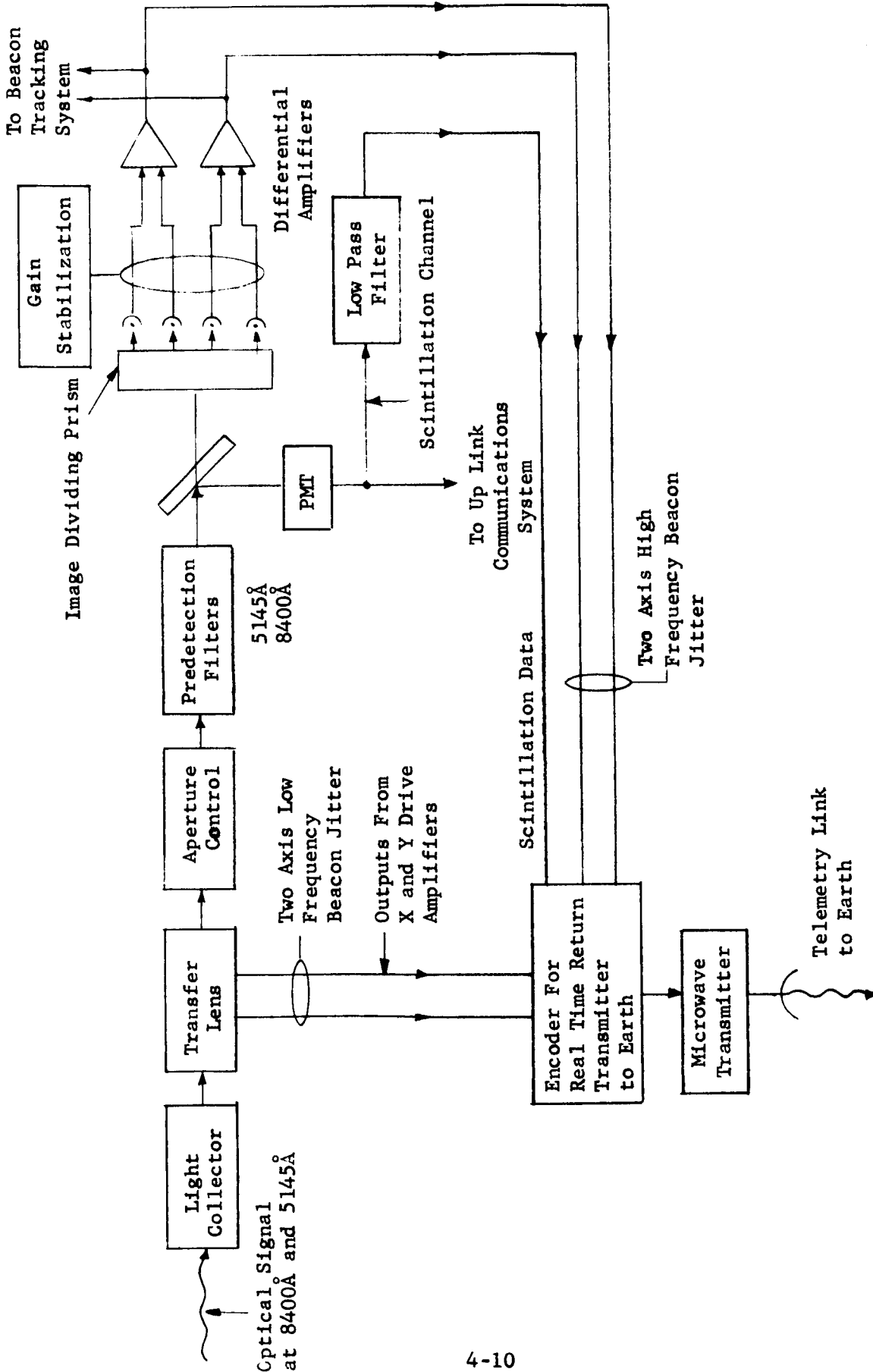
Figure 4-4. Block Diagram of Scintillation Experiment Satellite Receiver Configuration (Earth to Satellite Link)

and/or an argon laser at 5145Å will be required for the experiment to obtain scintillation and angle of arrival data in the near infrared region and in the visible region.

Efficient high power operation of the 8400Å GaAs diode laser requires that it be kept at cryogenic temperatures. This can be accomplished by open cycle or closed cycle liquid evaporation systems. The engineering choice as to the applicable technique is dependent upon system requirements and economic factors. The cryogenic refrigerator must bring the diode down to its operating temperature, dissipate the heat generated by the diode and any heat that leaks into the unit through the thermal insulation and/or wiring. By far the largest contribution to the heat load is that dissipated by the diode itself.

Ground laser power will be monitored to insure the constant average power level required for the scintillation modulation index determination. Also, a low frequency tracking signature will be provided.

The satellite receiver system will detect the ground laser beacon signal and modulated ground tracking signature. The received laser signal will pass through a transfer lens, aperture control system and then into the two predetection filters (one at 8400Å and one filter at 5145Å). At the output of the predetection filter the scintillation pickoff signal will be shunted through a low pass filter and then encoded for microwave real time return transmission to earth. The output of the satellite transfer lens x and y drive amplifiers will give an indication of the two axis low frequency image jitter. This data will also be encoded in a format suitable for real time return transmission.

The output of the fine tracking loop difference amplifier will represent the high frequency image jitter information and this data will also be sent to earth via the microwave telemetry link.

Effect of Aperture and Zenith Angle on Scintillation - In general, for large telescope apertures one receives an image that is stationary but not sharp in definition, and for small apertures a sharp image is obtained but its position and intensity varies in a random manner.

If I (y, z) is the intensity of the light wave on the surface of the objective, then the total light flux P through the objective is given by:[2]

$$P = \int\int_{\Sigma} I\,(y,z)\,dy\,dz$$

where Σ is the surface of the objective. It has been shown by Tatarski[2] that I (y, z) has a log normal distribution. Experimental evidence from starlight observations has led to the conclusion that P also has a log normal distribution.

Tatarski has further concluded that where the diameter of the telescope diaphragm exceeds the atmospheric correlation distance of the fluctuations, the variations of the total light flux through the telescope are weakened considerably. This is due to the fact that for telescope diameters greater than the correlation distance, several field "inhomogeneities" with different algebraic signs are located within the aperture, and these practically compensate one another.

Taken from the data of the Perkins Observatory, Table 4-1 shows how the relative fluctuations in intensity, σ_p, varies as a function of aperture and season.[2] σ_p and P are related as follows:

$$\sigma_p{}^2 = \overline{(p-\bar{p})^2} \Big/ \Big[\,\overline{P}\,\Big]^2$$

TABLE 4-1
SEASONAL STARLIGHT FLUX DEVIATIONS VERSUS DIAMETER OF RECEIVING APERTURE

Aperture Diameter Diaphragm in Inches	Intensity Deviation σP	
	Winter	Summer
1	0.476	0.373
3	0.346	0.250
6	0.189	0.160
12.5	0.098	0.080

Tatarski further points out that the magnitude of the fluctuations of stellar light flux passing through the aperture of a telescope, besides depending on the size of the aperture is a function of the zenith distance of the star and the meteorological conditions. Figure 4-5 taken from Reference 3 is a plot of measured stellar intensity spectra for 4 inch and 15 inch apertures taken at small zenith angles during different times of the year 1953. The corresponding relative stellar intensity fluctuation versus telescope aperture diameter measured by Ellison and Seddon and reported by Reiger in Reference 3 is shown in Figure 4-6. Figures 4-7 and 4-8 show the zenith distance dependence for a 3-inch and 12.5-inch aperture system. It appears that from both a theoretical and experimental point of view that for zenith angles which are not

The Scintillation of Starlight
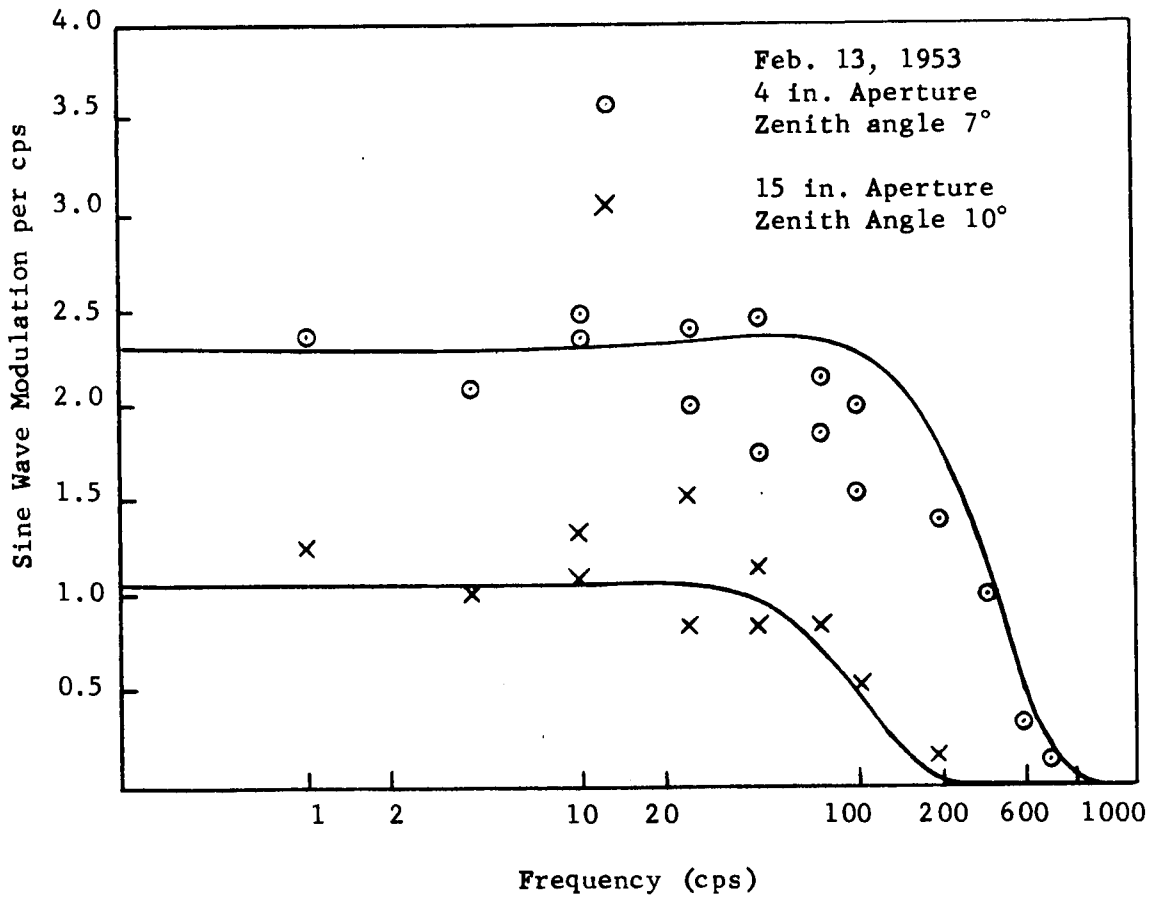
Figure 4-5.   Starlight Intensity Spectra
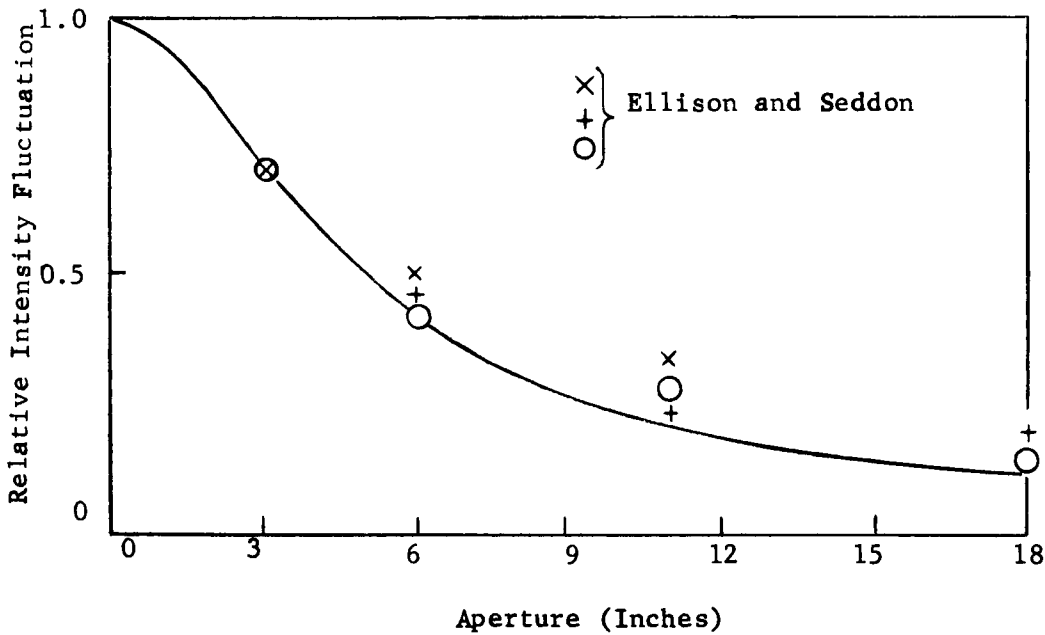
Figure 4-6. Scintillation Versus Telescope Aperture
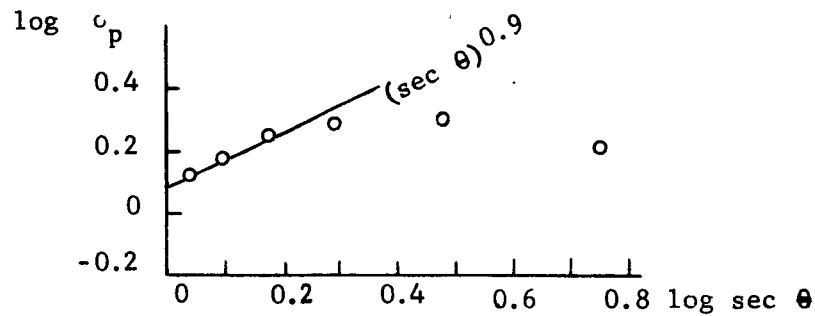
Figure 4-7. Dependence of the amount of twink-
ling on the zenith distance when
the telescope diaphragm has a dia-
meter of three inches.
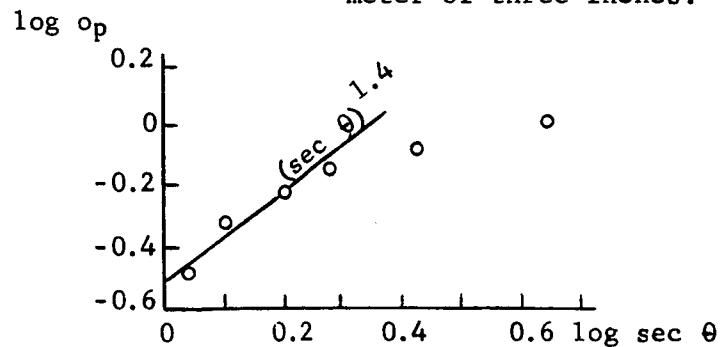
Figure 4-8. Dependence of the amount of twink-
ling on the zenith distance when
the telescope diaphragm has a dia-
meter of 12.5 inches.

very large, the rms intensity fluctuation varies approximately as the secant of the zenith angle.

At this point it is important to note that the data on intensity fluctuations for starlight strictly pertains to polychromatic light and not to monochromatic light. This is true because rays of different wavelengths arriving at the same observation point traverse different paths in the atmosphere and suffer different atmospheric refraction. In fact for large zenith angles the total intensity of polychromatic light experiences smaller relative fluctuations than the intensity of monochromatic light. However, measurements of the star and laser beacon scintillation will only be attempted at relatively low zenith angles.

Feasibility of Scintillation Experiment - Further analysis is required to establish the precise set of system parameters (diameters of receiving apertures, signal-to-noise ratios, optical and electrical filter bandwidths, etc.) for this experiment and the compatibility of this experiment with the others. However, it is clear at this point in the analysis that the hardware for performing the experiment is within the "state of the art," and that the scientific and engineering benefits that would accrue from the execution of the experiment are of value.

4.2 ATMOSPHERIC EFFECTS ON POLARIZATION

This experiment has as its objective the detection and measurement of any effects the atmosphere may have on plane and circularly polarized light, with particular emphasis on depolarization, for both the up and down-looking directions. Attitude control of a vehicle and optical communications are two

problems which can possibly be solved by methods utilizing the 100 percent polarization of a laser source. The torsional alignment of a vehicle about the line of sight may be determined by locating the plane of polarization of the upgoing laser beam. A discussion of the difficulties and limitations in determining small rotations about the line of sight by polarization techniques at large ranges is discussed in Appendix B. Also, any optical communication system which depends on some form of polarization modulation may be affected by depolarization of the beam. As was pointed out in the Phase I Report, no large amounts of depolarization are anticipated from atmospheric sources; that is, not enough to seriously degrade the envisioned optical communications scheme. However, an RLOS polarization scheme may be sensitive to slight losses of polarization of the source.

Finally, any such loss of polarization or rotation of the plane of polarization might be related to the number of scattering particles in the atmosphere if they are aligned anisotropically by some preferred direction mechanisms such as wind or gravity. The existence of the effect would itself be of scientific interest.

The Experiment - Refer to Figures 4-9 and 4-10 for block diagrams of the polarization experiment. Figure 4-9 depicts the earth transmitter configuration. Figure 4-10 depicts the satellite receiver configuration. The earth transmitter system will send 8400Å plane polarized laser light to the satellite. The plane of polarization will be determined by the RLOS control system upon command from the ground computer. The computed rotation about the line of sight referenced to earth coordinates will then be recorded and used for non-real time data processing of polarization data.
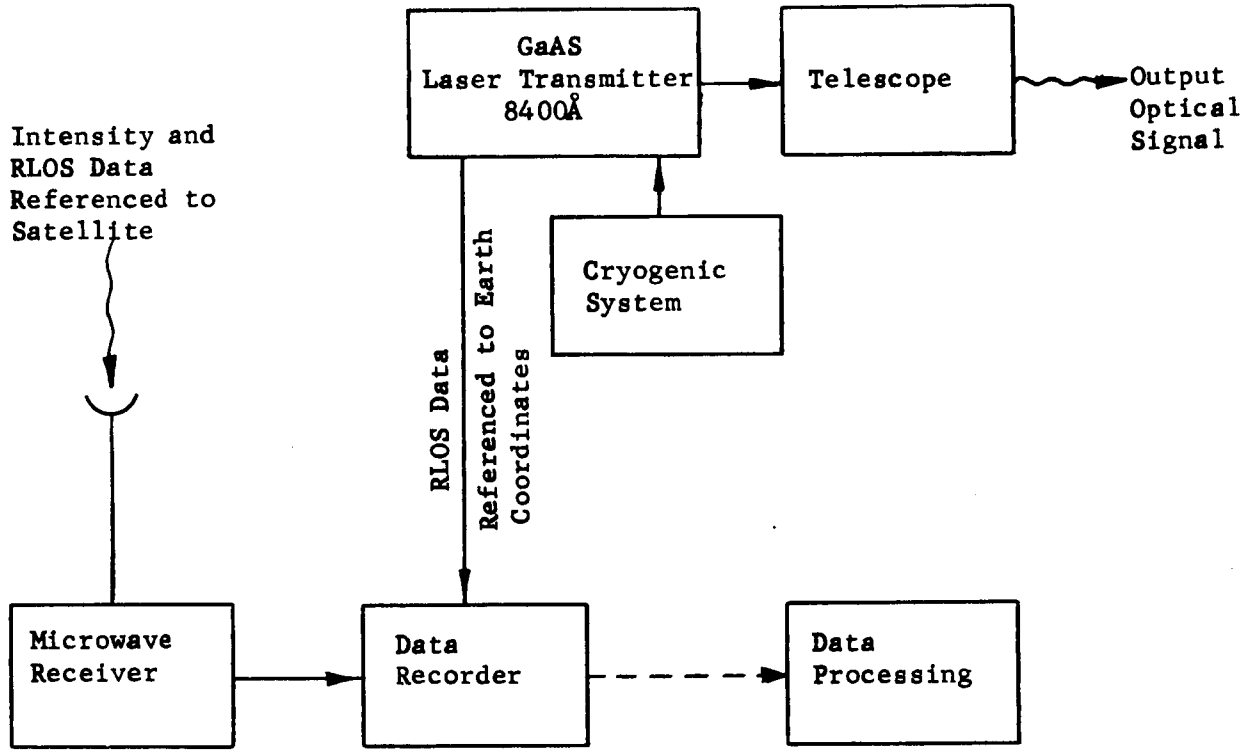
Earth Transmitter Configuration

Figure 4-9.   Block Diagram of Atmospheric Effects
on Polarization Experiment (Earth -
Satellite Link)
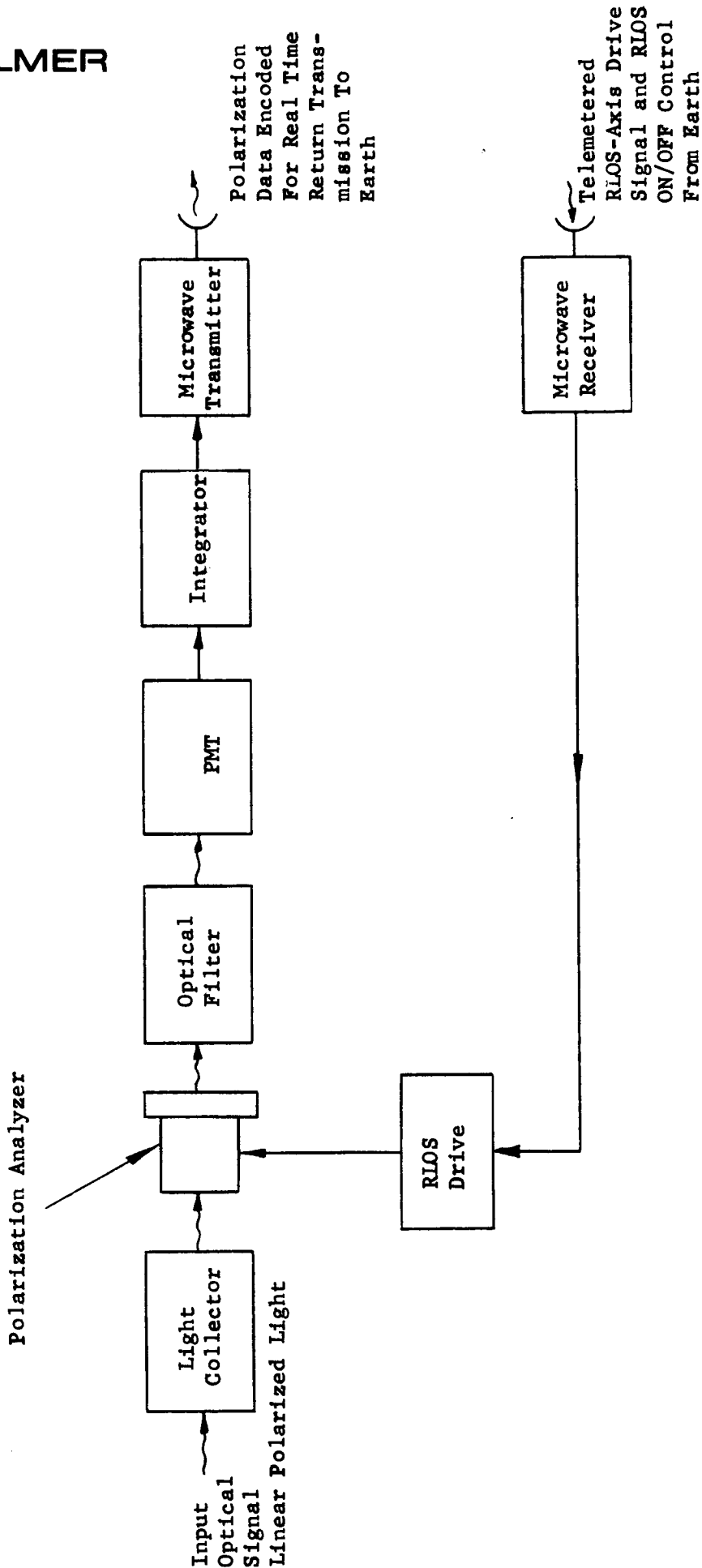
Figure 4-10. Block Diagram of Atmospheric Effects on Polarization Experiment (Earth-to-Satellite Link)

The satellite light collector receives the upgoing linear polarized light and passes it on to a rotating analyzer. The azimuth drive assembly which rotates the analyzer is commanded via the upgoing microwave telemetry link. The output of the polarization analyzer is then optically filtered and detected by a PMT. The transmitted intensity will be measured at several RLOS angles spaced at equal intervals, and then integrated to average out the effect of atmospheric scintillation. The integrated output and RLOS angles referenced to satellite coordinates are then encoded in a format suitable for real time microwave transmission back to earth. This method is sufficient to obtain for both totally and partially polarized light the rotation about the line of sight and the degree of polarization.

The intensity of scintillating linearly polarized light transmitted by the analyzer can be expressed as:

$$\overline{I} = 1/2 \; \overline{a^2(t)} \; \cos^2\alpha$$

where:

$\overline{a^2(t)}$ = time averaged scintillating intensity

α = angle between the plane of polarization and the transmitting plane of the analyzer.

By rotating the analyzer the transmitted intensity will be varied between maximum and minimum values, and the degree of polarization will be given by $\dfrac{I_{max} - I_{min}}{I_{max} + I_{min}}$ where the subscripts indicate maximum and minimum intensities. The direction of maximum intensity indicates the plane of polarization. Simultaneous measurements of the transmitted intensities through four stationary analyzers arranged in quadrature could also be employed to obtain this information.

If an RLOS attitude control polarization technique is utilized, then during the polarization experiment the RLOS attitude control channel must be disabled and another means must be sought to obtain rotation about the line of sight. A stellar tracking system might be utilized for this purpose. However, there remains at present some serious question about the utility of an RLOS polarization attitude control for deep space applications (refer to Appendix B). This then casts some doubt as to the utilization of RLOS polarization attitude control for the satellite case since the satellite is to simulate deep space conditions. If the inference is a valid one, then the engineering significance of the polarization experiment diminishes. This question requires further investigation in terms of probable advances in the state of the art of lasers, i.e., obtaining greater power levels to make RLOS polarimetry feasible.

At this point we will examine the satellite-to-earth link portion of the polarization experiment. Refer to Figures 4-11 and 4-12. The satellite transmitter is the same one used for 6328Å PCM-PL communications with provision for bypassing the quarter wave plate so as to enable the transmission of linearly polarized as well as right- and left-circularly polarized light. The earth receiver configuration consists of a light collector, polarization analyzer, predetection optical filter and PMT for intensity detection. RLOS control signals actuate the RLOS axis drive system to rotate the analyzer. The output of the PMT is integrated as before to eliminate the effect of intensity scintillation and then recorded. Recording of the output of the PMT directly should also be provided for non-real time data processing.

Gas Laser Transmitter
6328Å He-Ne

Output
From
Modulator
Driver of
PCM-PL
Communications
System

Polarization
Modulator

Quarter
Wave Plate

Telescope

Output
Optical
Signal

Linear Polarized
Light or Right Circular
Polarized Light or Left
Circular Polarized Light

Microwave
Receiver

Polarization
State Control Signal
From Earth
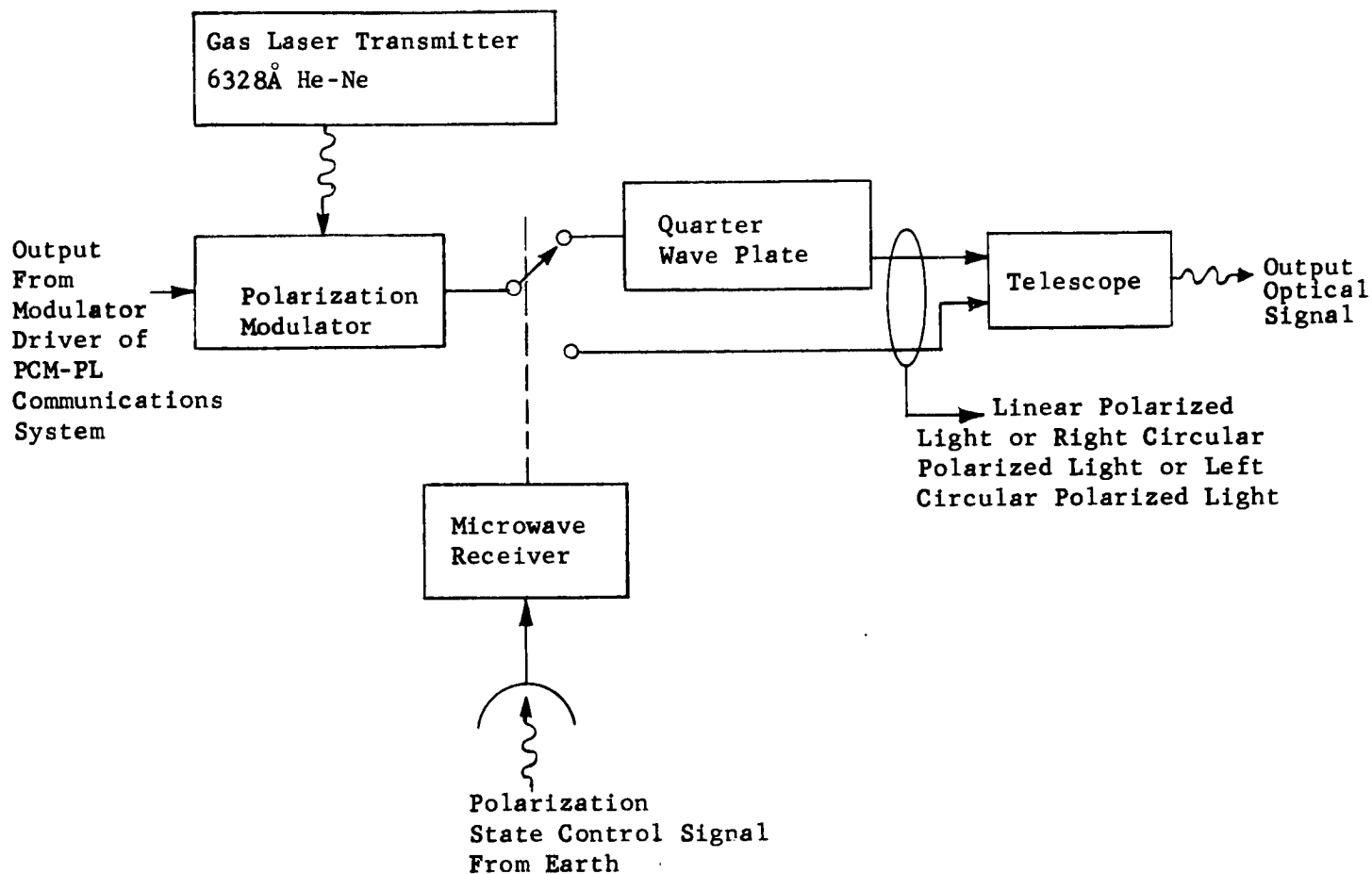
Satellite Transmitter Configuration

Figure 4-11.   Block Diagram of Atmospheric Effects on Polarization
Experiment (Satellite - to - Earth Link)

PERKIN ELMER
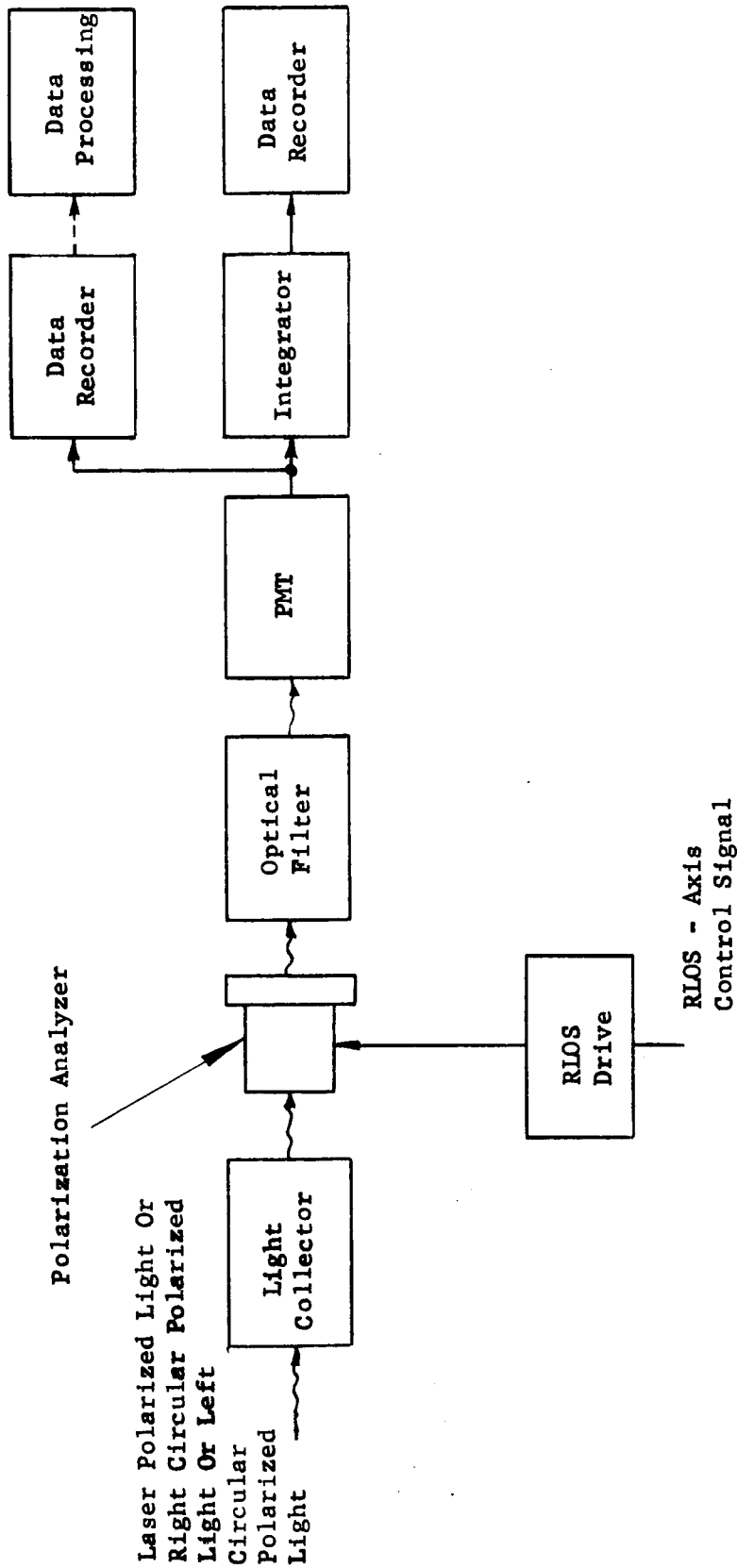
Figure 4-12. Block Diagram of Atmospheric Effects on
Polarization Experiment (Satellite To Earth Link)

4.3   REMOTE MANUAL OPTICAL ALIGNMENT

     The maintenance of an instrument's optical alignment is a diffi-
cult mechanical problem, especially when the alignment equipment must survive
a rugged launch. While in the hostile space environment, it is necessary to
provide for occasional, small realignment adjustments. Such adjustments are
usually made on terrestrial telescopes by a skilled optical technician, based
on his visual appraisal of some test image.

     The whole problem of maintaining optical alignment in large aper-
ture spaceborne telescopes is difficult to solve with feedback control systems for
several reasons:

(1) High positional accuracy is required. The
relative positions of mirrors, lenses, and
other elements must be closely controlled to
avoid aberrations and to maintain performance
to diffraction limits.

(2) Visual two-dimensional information is required.
The test image is usually found to be imperfect
from its proper shape in some way. Corrections
are then made until the image is improved.
Since the shape and disposition of an image is
the same as its spatial distribution, the in-
formation about distortions is conveyed by a
two-dimensional array. Any electronic data
system (digital or analog) holding time as the

(4) Physical parameters of the elements vary unpre-
dictably with age. If an attempt is made to
solve this problem with a stored program, the
number of possible contingencies which must be
anticipated and programmed for recognition and
correction will be found to be very large.

Partly for these reasons optical alignment of a large aperture
instrument is almost never undertaken without some amount of human interven-
tion. As larger aperture systems are lofted in the future, the need for a
method of remote manual optical alignment will become more urgent. The ex-
periment on remote manual optical alignment will be beneficial to both opti-
cal designers and astronomers. It will provide the hardware core of technology
so that man will be able to build the next generation of diffraction limited
telescopes in space. It will increase confidence in man's ability to project
his manipulatory powers over planetary distances via communications systems.

The Experiment - Two crucial alignment problems in the Optical Technology
Satellite might be aided by a redundant remote alignment system. Focusing
and positioning the secondary mirror with respect to the primary mirror could
be accomplished by human intervention as well as by some automatic system.
The boresighting of transmitter and receiver might also be adjusted remotely.
Also, other problems might appear during the subsequent design which can be
solved with remote adjustment. Of course, the diagnostic electronic adjust-
ments cannot be left out. The remote manual alignment system would handle
only small adjustments aimed at improving the performance of a working system
to diffraction limits. Obviously a non-working system cannot be used to improve

only independent variable is limited in its
ability to interpret two-dimensional informa-
tion automatically. Human eyesight, on the other
hand, does not suffer from this one-dimensional
limitation.

(3) Observed distortions may not correspond uniquely
to required adjustments. In an optical system
with many elements, each having many degrees of
freedom, it has often been found that alignment
itself is not unique. There may be several
possible ways to align a system, and it may perform
equally well no matter which way was followed.
Careful design which restricts the amount of
adjustment of each element will reduce the
problem.

Once an instrument is designed properly, as above,
it can be aligned according to a set, detailed
procedure; but even then there can be variations
in alignment from one instrument to the next
because of the inevitable variations in "identical"
mechanical and optical elements. Because of this
the observed image imperfections in two instruments
may be quite similar, but the corrective action
required may vary.

itself. If the adjustments required are <u>small</u>, they may be performed with the alignment system. If they are large they will have to be made "blindly" by the electronic equipment until the optical system begins to function. The satellite systems must be reliable enough so the probability is small that large adjustments will be required.

Experiment Procedure

(1) The optical technician will perform adjustments of focus and position of the telescope elements, and of the boresighting of transmitter and receiver, at a suitably equipped console. There may be a television camera* to monitor a test image at several different points in the optical path, as chosen by the technician. The technician will rely on the video display and his knowledge of the satellite optical system is making adjustments.

(2) During each trial as above there will be inserted in the communications loop a transport lag chosen by the experimenters, of up to fifteen minutes. This time lag will be constant during the course of an experimental run.

(3) It may be of interest to compare the performance of the system when a test source is used for alignment, with the performance when the test source is replaced by a suitable earth beacon which has passed through the whole atmosphere. The difference may be great enough to require reconsideration of the alignment procedure.

---

*The television camera tube may be constructed for sensitivity to an 8400Å source if a gallium arsenide ground beacon is used. If an argon laser were used as a ground beam, then a more common spectral sensitivity vidicon would be more suitable. In addition to the spectral sensitivity of the image tube, there are real problems of developing useful image tubes for this application. Blooming of the image and dynamic light range problems have not been solved for TV tubes.

4.4　OPTICAL HETERODYNE DETECTION IN THE SATELLITE

　　　This experiment has as its objective the development of sufficient engineering experience with design and operation of a spaceborne heterodyning system so that its feasibility, reliability, performance and cost can be evaluated relative to an alternate intensity detection scheme using predetection filtering.

　　　Another purpose of this experiment is to evaluate the utility of Doppler velocity measurements made using the Doppler shifts of the optical carrier.

　　　The experimental procedure that could be employed for optical heterodyne detection aboard the satellite consists of tracking of the earth beacon by the tracking receiver telescope, measurement of the signal-to-noise ratio, tracking performance and frequency shifts. These data would then be encoded for real time return transmission to the earth via the microwave telemetry link.

Bandwidth Considerations - Refer to Figure 4-13 for a sketch (not to scale) of the bandwidth requirements for satellite heterodyne reception.

　　　In order that the optical heterodyne system be competitive with a predetection intensity detection system, the post detection bandwidth of the heterodyne system must be less than that achievable with good narrow-band optical filters. It appears at the present state of the art that a 0.1Å Lyot filter is about the narrowest available. At laser transmitter wavelengths of 6328Å and 8400Å this amounts to a frequency band of 7.48 gigacycles and 4.25 gigacycles respectively. Typical system bandwidths would be of the order of a

4-28

Information
Bandwidth

Extent of
Tuning Range Set
By Doppler Shift

Heterodyne Detection
Limit Set By Tuning Uncertainty
And Random Rapid Disturbances

0

10 mc/s

50 gc/s

5 gc/s

Frequency

1 kc/s

Upper Cutoff
Frequency for
Noise

Intensity Detection
Limit Set By Predetection
Filter

Upper Cutoff
Frequency for
Information
Modulation
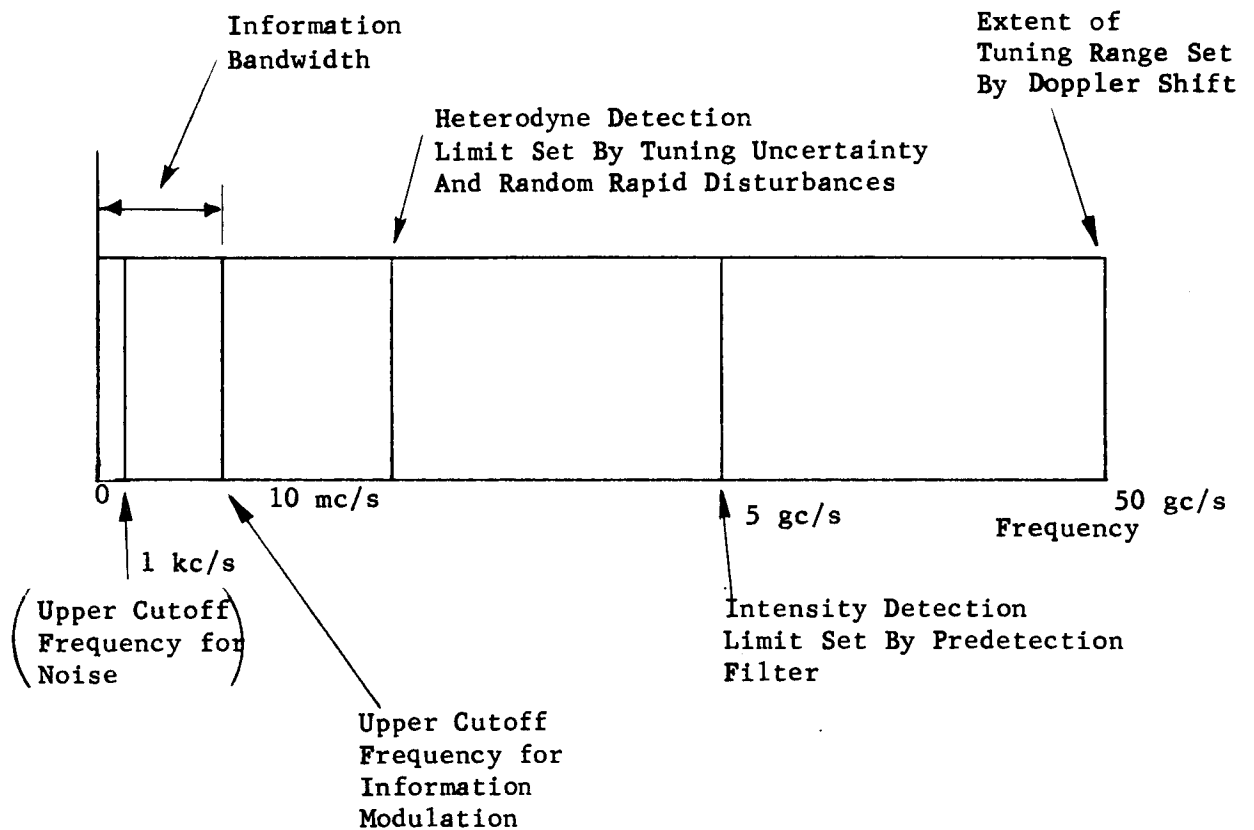
Figure 4-13. Bandwidth Requirements For Satellite
Heterodyne Reception

few gigacycles per second; this limit set by tuning uncertainty and random

rapid disturbances.

The frequency perturbations in the i.f. that must be contended with

are, transmitter and local oscillator instability, path refraction in the

atmosphere, vehicle motion with respect to the earth terminal, and vehicle and

receiver vibration. These perturbations can be classified as either slow or

rapid. The slow changes are due to vehicle motion and oscillator drift. The

rapid shifts are due to vibration, refraction, and oscillator noise.

The satellite receiver must have an optical bandwidth that takes

into account the range of Doppler shift anticipated. The Doppler shift at

optical carrier frequencies can mean microwave frequency shifts. The Doppler

shift is given by:

$$f_{Doppler} = f_L \frac{(c+V_r)}{(c-V_r)} \approx \frac{2V_r}{c} f_L$$

where: c   speed of light $= 3 \times 10^5$ kilometers/sec.

f_L = laser transmitter frequency in cps

V_r = radial component of velocity between the earth transmitter and

satellite receiver in units of kilometers per second.

The Doppler shift $f_{Doppler}$ is in cycles per second. In space

communications, where the radial velocities may be as high as 15 kilometers per

second, the Doppler shift may be as high as 50 GC or greater.

Since the heterodyne receiver must have an optical bandwidth that

takes into account the range of Doppler shift (the satellite is to simulate

deep space conditions), the aforementioned few GC optical bandwidth will have to

be wider, thereby increasing the noise from the background. An alternative to this wide bandwidth requirement is to tune or frequency track over the 50 GC range. This then dictates a requirement of either multiband local oscillator or transmitter, or very broadband photodetectors for a heterodyne application. In addition, mode and frequency control of the lasers would be necessary. For this experiment the tuning procedure would probably be accomplished on earth. The earth laser will have to be high powered and frequency stabilized.

The laser local oscillator tuning requirement for Doppler shift compensation may dictate the need for Zeeman splitting. This is true since, the Doppler width of a gas laser transition is typically about 1 GC and is inadequate for the range envisioned.

Vibration, path refraction, and oscillator instability will cause frequency deviations of much smaller magnitude than vehicle motion, but the shifts will be rapid and random. Reference 4 has suggested that these components of frequency shift could be compensated for by an AFC system employing an FM discriminator which detects the i.f. carrier average frequency. This compensation could be superimposed on the vehicle motion compensation.

The Experiment - Although it is felt that satellite optical heterodyne detection may be extremely difficult to accomplish, a tentative block diagram of such an experiment is presented to indicate the magnitude of the problem. Refer to Figure 4-14 for a block diagram of the earth equipment required for this experiment. A suitable low frequency tracking signature, as well as the information bearing signal will modulate the transmitted laser beam and be

Tracking Signature
Signal Generator

Frequency
Tuning
System

High Powered
Frequency
Stabilized
Laser

Optical
Modulator

Telescope

Output
Optical
Signal

Microwave
Transmitter

Microwave Output

Frequency Control
Signals

Data
Recorder

Microwave
Receiver

Microwave Input

Data
Porcessing

Earth Equipment
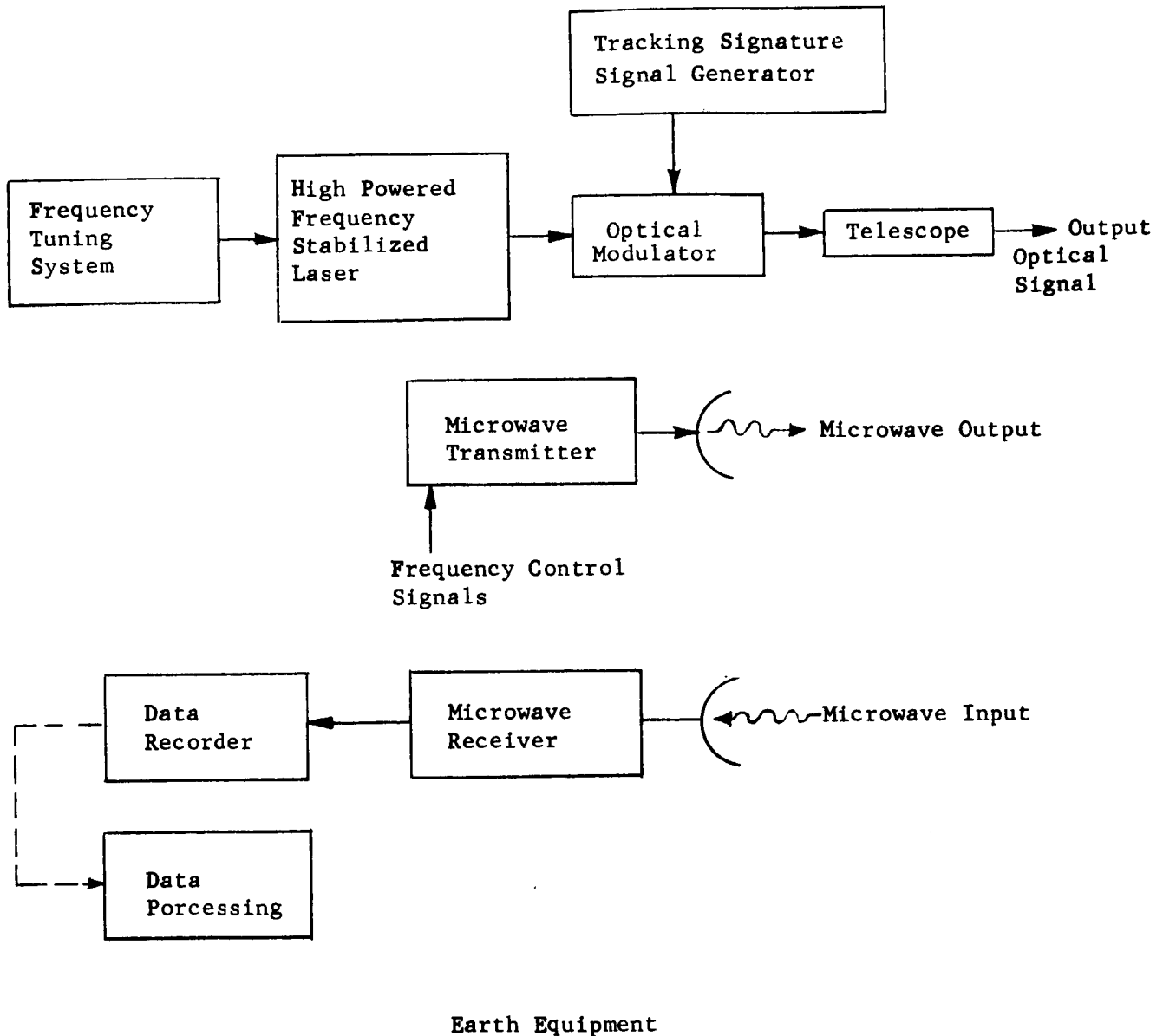
Figure 4-14. Block Diagram of Optical Heterodyne Detection
on Satellite Experiment

4-32

transmitted through a telescope for satellite reception. In addition control
signals for the microwave tuning requirements at the satellite will be
telemetered from earth to the satellite via the microwave link.

At the satellite receiver, (refer to block diagram of Figure 4-15),
a frequency stabilized laser local oscillator will be employed to beat with
the incoming signal photons on the detector photocathode and produce a desired
beat frequency. The possible large Doppler-shift at optical frequencies can
present serious problems in the heterodyne system. As the radial component
of vehicle velocity changes, the Doppler-shift frequency changes, causing a
change in difference frequency. In order to accept this change, the i.f.
must either be extremely broad or must be rapidly tunable over a broad range.
The latter alternative is shown in Figure 4-15. Both alternatives present
serious problems at the present state of the art, since microwave broadband
amplifiers are of one octave or less, and narrow-band microwave amplifiers
cannot be tuned over more than one octave.

A traveling wave phototube and amplifier combination consisting of
a standard TWT with a photocathode is shown as a possible detector candidate
having gigacycle capability. Although there is question at the present time
if the traveling wave phototubes can meet the gain requirements of detection
of a shot noise limited signal, the wide bandwidths of the microwave phototube
do afford a reduction in the stiff tolerances on local oscillator and signal
frequency stability and also give maximum useful bandwidth for heterodyning.[5]

A power and frequency stabilized microwave reference, oscillator
frequency multipliers, and microwave mixer will be required to demodulate the
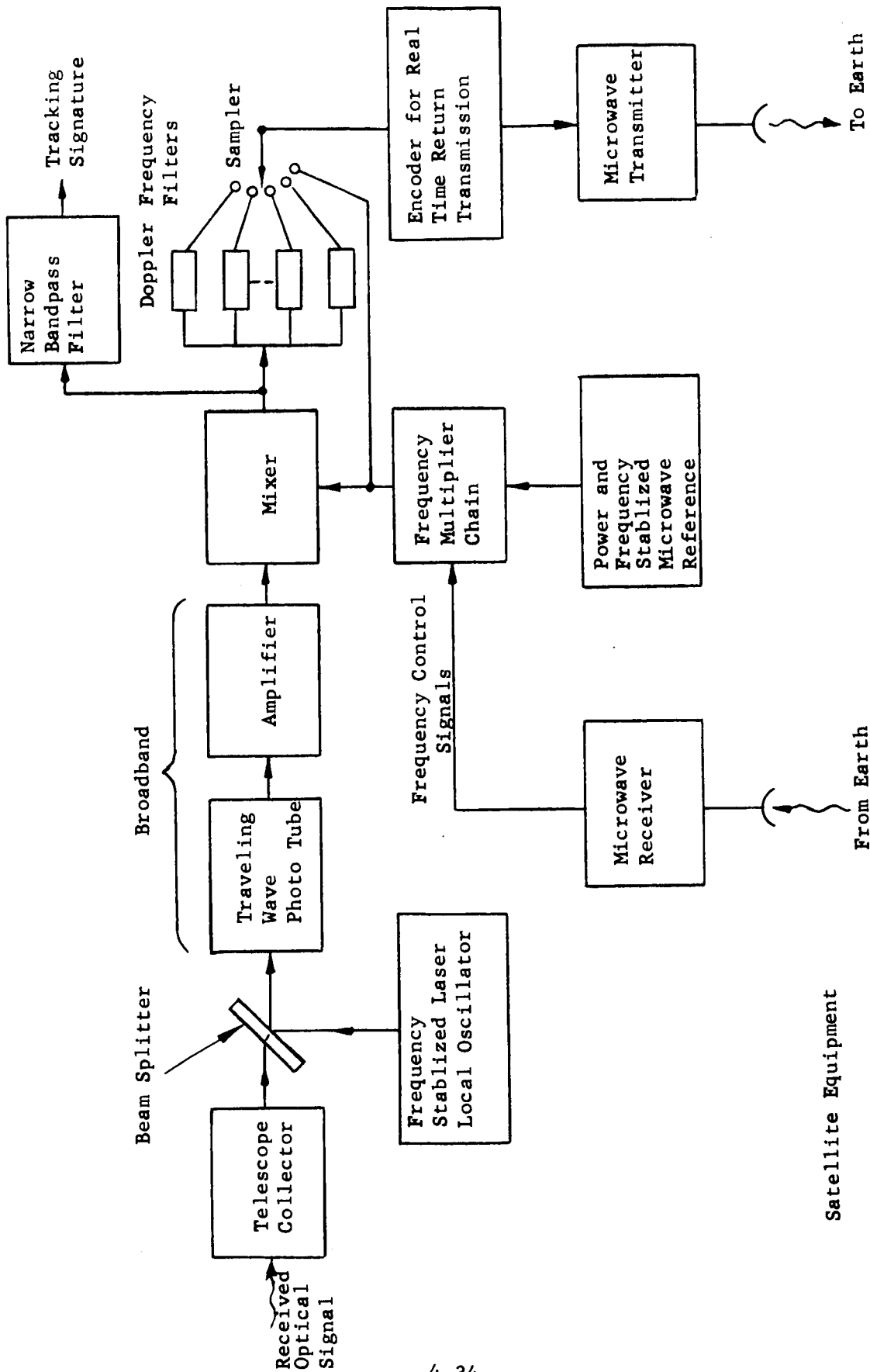
Figure 4-15. Block Diagram of Optical Heterodyne Detection on Satellite Experiment

microwave signal. The output of the microwave mixer would then be sent to a
bank of bandpass filters covering the Doppler frequency range of interest.
Also the tracking signature would be extracted by a narrow bandpass filter at
this point. The output of the Doppler bins could be sampled and encoded for
real time return transmission to earth via the microwave link. This data
will be recorded and processed on earth. Control signals from earth for
the satellite frequency multiplier system will be transmitted by the microwave
telemetry link.

Noise Analysis of Traveling Wave Phototubes - The information bearing optical
signal is mixed at the photocathode surface of the traveling wave tube with a
laser local oscillator reference. The light output causes the emission of a
current modulated photoelectron beam which contains the difference or beat
frequency signal between the local oscillator and signal light. The current
modulated beam is passed through a helical slow-wave structure, (broadband
microwave circuit). Power at the difference frequency is efficiently coupled
to the circuit if the electron beam velocity is roughly equal to that of the
electromagnetic wave on the circuit. This condition can be instantaneously
realized over an octave bandwidth.

McMurtry[6] has shown that the signal to noise ratio for an optical
heterodyne system employing traveling wave phototubes, operating against a
shot noise background caused by the direct beam current in the tube, can be
expressed as

$$\frac{S}{N} = \frac{\eta \, n_s}{B}$$

where: η is the quantum efficiency of the photocathode surface

n_s is the arrival rate of signal photons

B is the traveling wave tube amplifier bandwidth.

If the amplifier resolution time τ is defined as the reciprocal of the bandwidth B, then the minimum detectable number of signal photons per second is equal to:

$$n_s \text{ (min)} = \frac{B}{\eta} = \frac{1}{\eta \tau} = \frac{1}{\eta} \frac{\text{photons}}{\text{amplifier resolution time}}$$

Some interesting conclusions can be drawn from the above analysis. The signal-to-noise ratio is independent of local oscillator strength and of the magnitude of the direct current. Therefore, a strong local oscillator signal can be used and one obtains a large direct current to aid in the amplifying process, without degrading the signal-to-noise ratio. Also increased shot noise at large direct currents is balanced by increased conversion efficiency. It can also be seen that the larger the cathode quantum efficiency the better the sensitivity and performance against noise. Obviously for a quantum efficiency of unity, the minimum detectable signal arrival rate equals the ultimate detectable for any ideal linear receiver, namely, one photon per resolution time.

For a bandwidth of 5 gigacycles per second, laser wavelength equal to 6328Å, and a quantum efficiency of 0.05, the minimum detectable signal power is approximately equal to 3×10^{-8} watts.

<u>Feasibility of Optical Heterodyne Detection on Satellite</u> - Optical heterodyne detection has several advantages over intensity detection techniques. Optical heterodyne detection enjoys a three 3-db advantage over intensity detection, and background discrimination is provided without use of an optical

filter. Because of the directional requirement for heterodyning, only the
background energy that arrives parallel to the local oscillator energy will
generate difference frequency components that are amplified. Background noise
is further limited since only those noise components that fall within the i.f.
bandwidth will be amplified. However, in order to avoid the necessity for an
i.f. bandwidth large enough to accomodate the envisioned deep-space Doppler
shifts with the attendant background noise, frequency tuning is required
over wide bandwidths.

The advantages of optical heterodyne detection appear at present
to be substantially outweighed by several disadvantages; namely the requirement
for high power frequency-stabilized and mode-controlled lasers, severe tuning
requirements, and the necessity for broad-band photodetectors.

However, further examination of the Optical Technology Satellite
system parameters, as well as the ever advancing state of the art is required
before any clear cut decision can be made as to whether optical heterodyne
detection is a suitable technique for space applications.

4.5 OPTICAL HETERODYNING ON EARTH

The objective of this experiment is to verify the theoretical
prediction that the signal-to-noise ratio in heterodyne detection in the
atmosphere is limited by the transverse coherence diameter of the atmosphere.
A second objective is to measure this transverse coherence diameter.

Essentially the satellite laser tracks the earth beacon and also
transmits signals to the heterodyne receiver telescope. This receiver tracks
the vehicle, and the heterodyne signal-to-noise ratio is recorded for various
receiver aperture diameters.

The Experiment - Refer to Figures 4-16 and 4-17 for block diagrams of the satellite and ground equipment, respectively, required for this experiment. Ground commands are received by the satellite microwave telemetry system to disable the PCM-PL transmitter system, and turn on the heterodyne transmitter. A suitable tracking signature and information-bearing signal are impressed on the optical carrier and then sent through the telescope for transmission to earth. The ground receiver, similar to the system employed for the satellite receiver described previously, trackes the vehicle, and heterodyne signal-to-noise ratio is recorded for various aperture diameters.

Feasibility of Optical Heterodyne Detection on Earth - The problems of detection that are discussed in the section on space heterodyning are applicable to optical heterodyning on earth. In addition there is the severe problem of atmospheric turbulence and the attendant signal power loss caused by spatial amplitude and phase fluctuations over the receiving aperture. Signal power loss is defined as the ratio of received signal power to the power which would be measured if phase fluctuations were absent. Table 4-2 lists the signal power loss for several receiving aperture diameters. These figures are based on the case of vertical downward laser transmission at 6328Å through the atmosphere to an earth receiving station.[1]
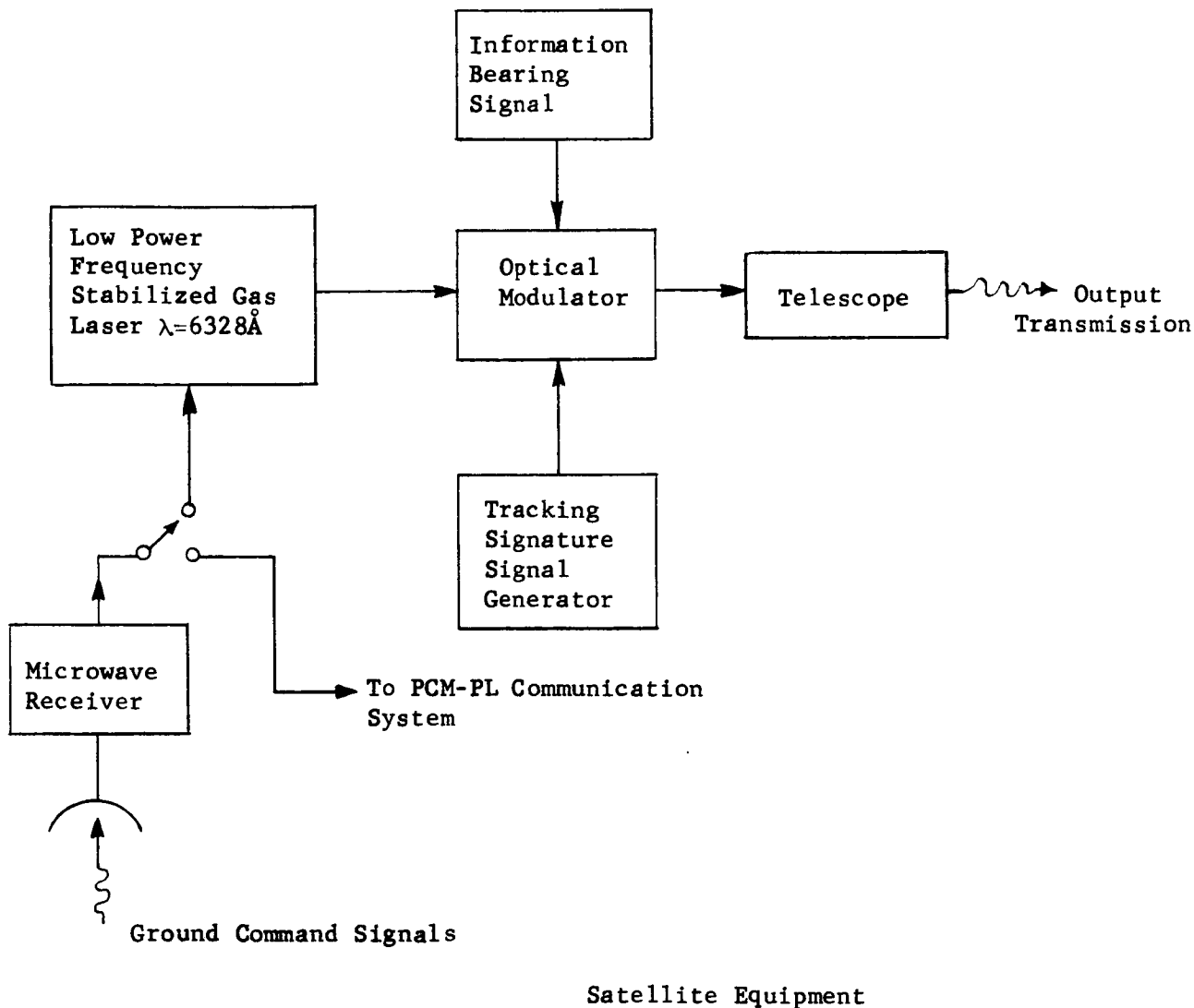
Figure 4-16. Block Diagram of Optical Heterodyne
Detection on Earth Experiment
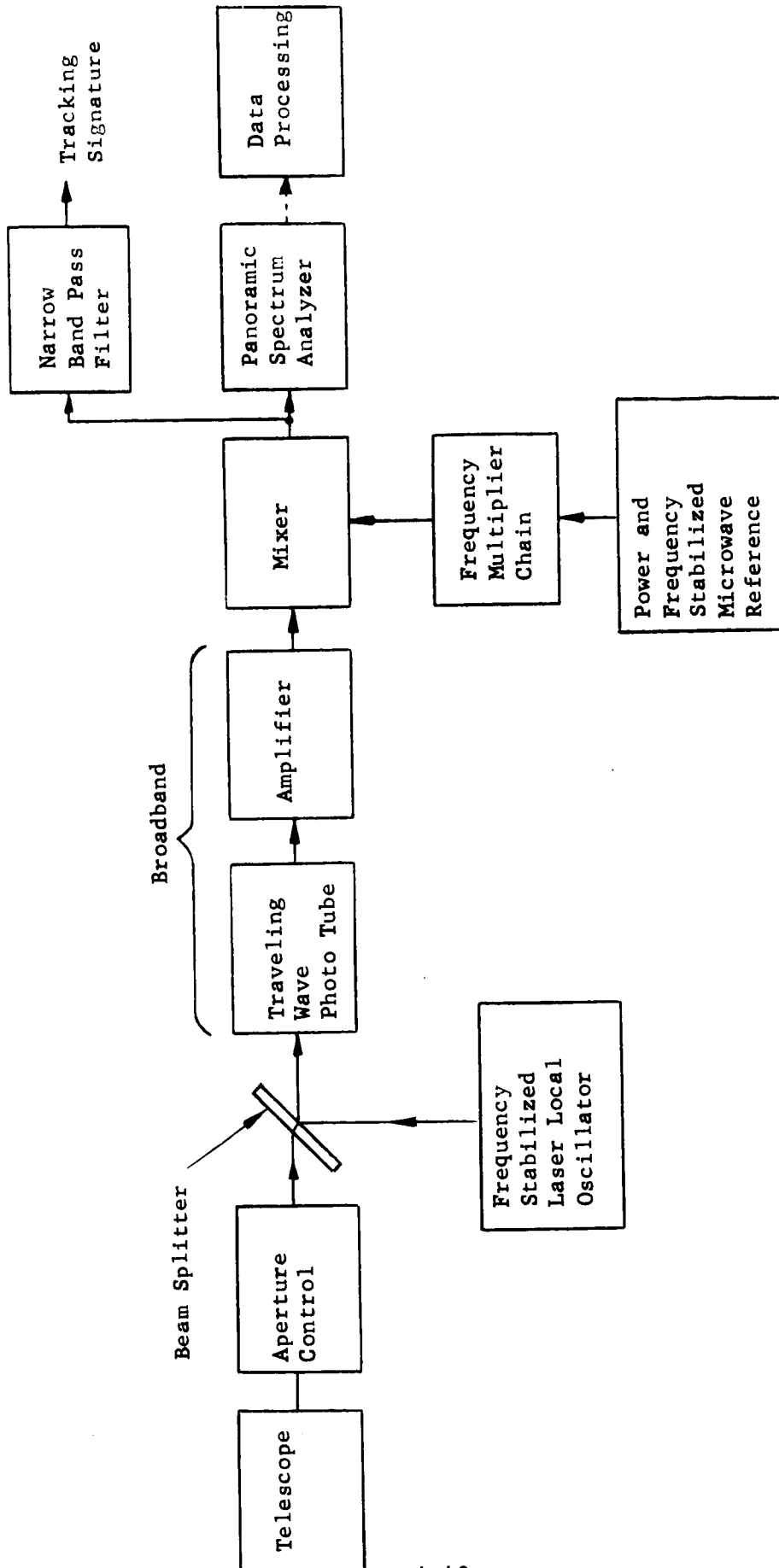
Figure 4-17. Block Diagram of Optical Heterodyne Detection on Earth Experiment

TABLE 4-2
SIGNAL POWER LOSS FOR SEVERAL RECEIVER APERTURE DIAMETERS

Signal Power Loss (db)	Diameter of Receiver Aperture (cm)
-1.5	6
-5.00	12
-9.75	24
-12.75	36
-15.38	48
-16.68	60

It appears from the above considerations that optical heterodyne detection on earth, although highly attractive, may be extremely difficult to accomplish on earth with large receiving apertures. An intensity detection system may be more efficient for ground operation.

It is suggested that more ground-to-ground experimental tests of optical heterodyne detection through long atmospheric paths be performed to gather further data on signal power loss. Also, phase correction and discrete demodulation techniques should be investigated for the correction of wavefront distortion theoretically before experiments as outlined in Figure 4-16 and 4-17 are performed.

4.6 0.1 ARC SECOND TRACKING DEMONSTRATION

The ability to communicate at high information rates over inter-planetary distances requires the use of narrow beams to avoid excessive transmitted power requirements. While small beamwidths require very large

antennae at microwave frequencies, much more practical antenna sizes are needed to accomplish the same ends at optical frequencies. Even if one ignores the transit time and aberration effects on pointing to be expected in a working system, a major problem arises with beamwidth reduction in that pointing accuracy becomes increasingly more stringent.

If one considers, for example, a diffraction limited optical system of aperture diameter D transmitting at wavelength λ to a distant receiver, the pointing error ϵ should be less than $1.22\ \lambda\ /D$, the value which results in essentially zero power density at the distant receiver. For the case of $6328\overset{o}{A}$ transmission and an 8-to 32-inch diameter, the pointing error should be less than 0.8 to 0.2 arc-seconds with errors of half these limits providing a twofold decrease in distant received power as compared to the case of zero error.

Experience with the balloon-borne Stratoscope II astronomical telescope, which utilizes stellar guidance techniques, indicates that the three-ton gimbaled structure was stabilized to 1 or 2 arc-seconds rms while its optical line of sight is directable by transfer lens action towards distant stars with pointing errors well within the 0.15 arc-second diffraction limit of the instrument. Preflight measurements with the equipment tracking simulated stars indicated that expected LOS errors are in the order of 0.02 arc-second.[*] Although these facts tend to indicate that the practicality of high pointing accuracy has already been demonstrated by Stratoscope II, it is important to realize that a deep-space communication telescope will not be

---

[*] For 9th magnitude stars; even better performance is expected on brighter stars for the 36-inch aperture instrument with an optical efficiency of about 30% from the aperture to the S20 detectors.

analogous to Stratoscope II. The latter instrument operates at a nominal

80,000 feet altitude and guides on stars viewed through only two or three

percent of the earth's atmosphere and so avoids most of the optical degradations

caused by air turbulence and refractive index inhomogeneities. Moreover, the

equipment is subjected to the soft launch environment of a balloon. Pointing

disturbances during tracking arise from very small fluctuating wind com-

ponents acting directly on the structure and, in addition, from torques due

to suspension axis bearing imperfections which allow coupling of the in-

strument to the very low frequency (1/15 cps) and amplitude ($< \pm$ 1/4 degree)

pendulous motions of the balloon suspension.

A deep space telescope guiding on an earth ground laser beacon,

however, not only experiences the optical effects of the whole earth's

atmosphere (mostly scintillation) but also the degradations induced by signi-

ficant amounts of background light (reflected sunlight which may even contain

appreciable modulation components). Input disturbances in a practical space

instrument, moreover, could greatly exceed those experienced with Stratoscope,

being generated for example by rotation of the vehicle's momentum wheels or

by an astronaut.

This engineering experiment shall be conducted to demonstrate with

earth satellite equipment the practicality of 0.1 arc-second tracking for a

deep space telescope whose expected angular tracking rates will be simulated

by an appropriately inclined synchronous orbit. The approach involves the use

of the two-axis telescope which directs its LOS toward a laser ground beacon

while transmitting laser energy back along this line of sight. Measurements

of the transmitted beam pattern, as received on earth from the diffraction

limited optical system in space, will be made to assess tracking accuracy and
to provide some measure of the diffraction limit capability of a space optical
system.

The Experiment - The recommended implementation for this experiment as shown in
Figure 4-18, was chosen to minimize the satellite equipment complexity. A
microwave system serves as a telemetry and command link for required remote
controls such as power on-off, temperature monitoring, status indication, etc.
The vehicle equipment generally consists of an acquisition subsystem, satellite
orientation subsystem, telescope orientation control subsystem, wide and narrow
field of view beacon sensing channels, and an optical system which features a
pointing error correcting transfer lens loop and whose elements are shared by
both the receiving and transmitting channels. The functions of these equipments,
as described in the Phase I Report,* is to locate the ground beacon by scanning
with a wide (1°) field of view at a known offset angle from the sun-vehicle
reference direction. For deep space operation, the offset angle θ_o would be
derived from an on-board stored program, but for the satellite simulation θ_o is
supplied via the microwave link from the ground computer. During the "scan
operation", the telescope is caged to the vehicle or forced to track the vehicle
by controlling the gimbal axis torquers to maintain the associated position pick-
offs at zero. This mode of operation, positional hold mode, continues (as the
vehicle is forced by the acquisition subsystem action to execute its circular
scan pattern) until the beacon is sensed by the wide FOV error sensor. At this
time the telescope is controlled by this sensor and vehicle orientation control is
such as to null the gimbal axis pickoffs, or equivalently, to follow the telescope.

---

*Pages 5-12 through 5-25

When the telescope is so pointed within one arc minute, the beacon image passes through the reflecting field stop to the fine (or narrow FOV) sensor which controls the transfer lens (and, therefore, the optical line of sight) to capture the beacon image. Until the beacon is sensed by the fine sensor, the transfer lens is held centered by positional hold mode operation similar to that described above for the telescope, and, subsequent to this, the transfer lens position sensors (rather than the wide FOV sensor) supply pointing error information to the telescope torquer electronics. Telemetry data received by the beacon personnel continually presents information relative to the state of the satellite, equipment conditions, and operations and allows, for example, turning on of the vehicle's laser and modulator after the beacon is acquired.

The use of a 32-inch diameter aperture and a 6328Å laser beam results in a diffraction limited resolution of 0.196 arc-second and, at the ground station range of approximately 20,000 miles, the beam's diffraction pattern dark ring will be in the order of 200 feet in diameter. Several moderate sized ground receiving telescopes can, therefore, be arrayed, as in Figure 4-19 for example, to sense the position of the vehicle transmitted laser beam. A comparison of this actually sensed position with that computed from ephemeris data will yield the desired pointing error information. Some appreciation for the measurement sensitivity can be obtained by considering the magnitude of difference signal generated between collectors A and B by a beam shift in the X direction. With the beam symmetrically positioned, the energy at collector A or B is equal to X and that at C is nearly 2X.[*]

---

[*]
Refer to Phase I Report Figure 6-2 which shows the light intensity distribution expected at the ground for diffraction limited optical conditions.
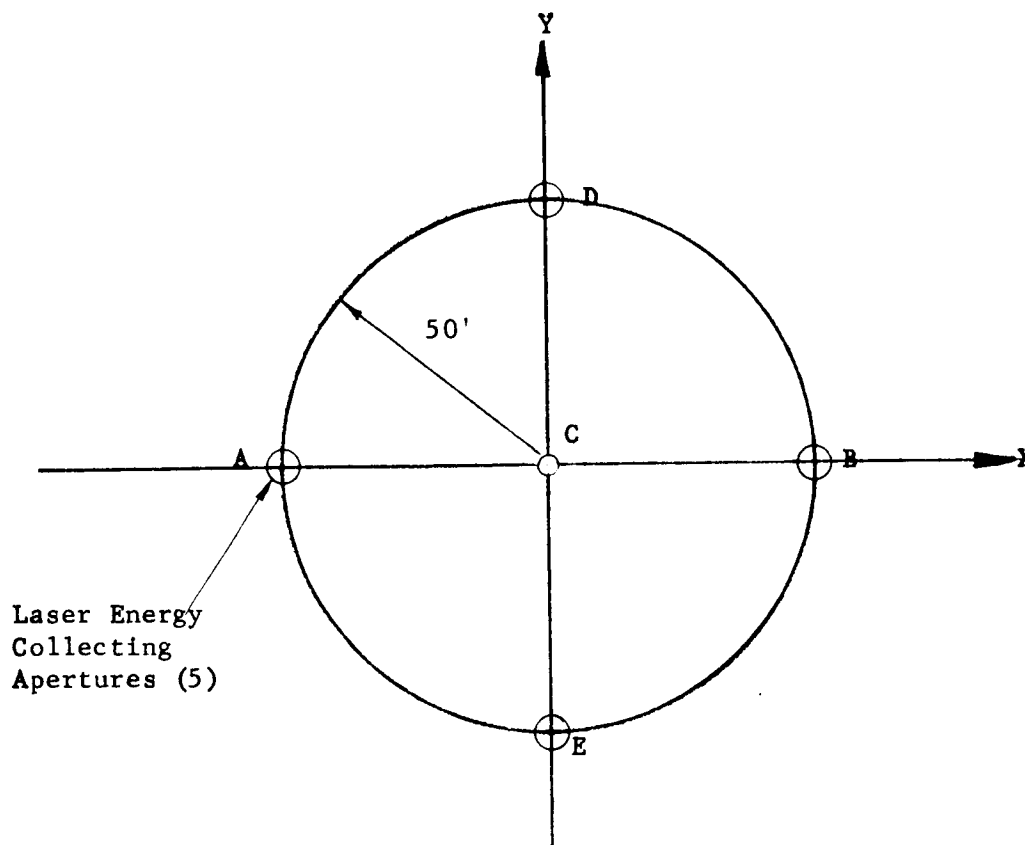
Figure 4-19. A Possible Ground Beam Position
             Monitoring Equipment Array

PERKIN-ELMER
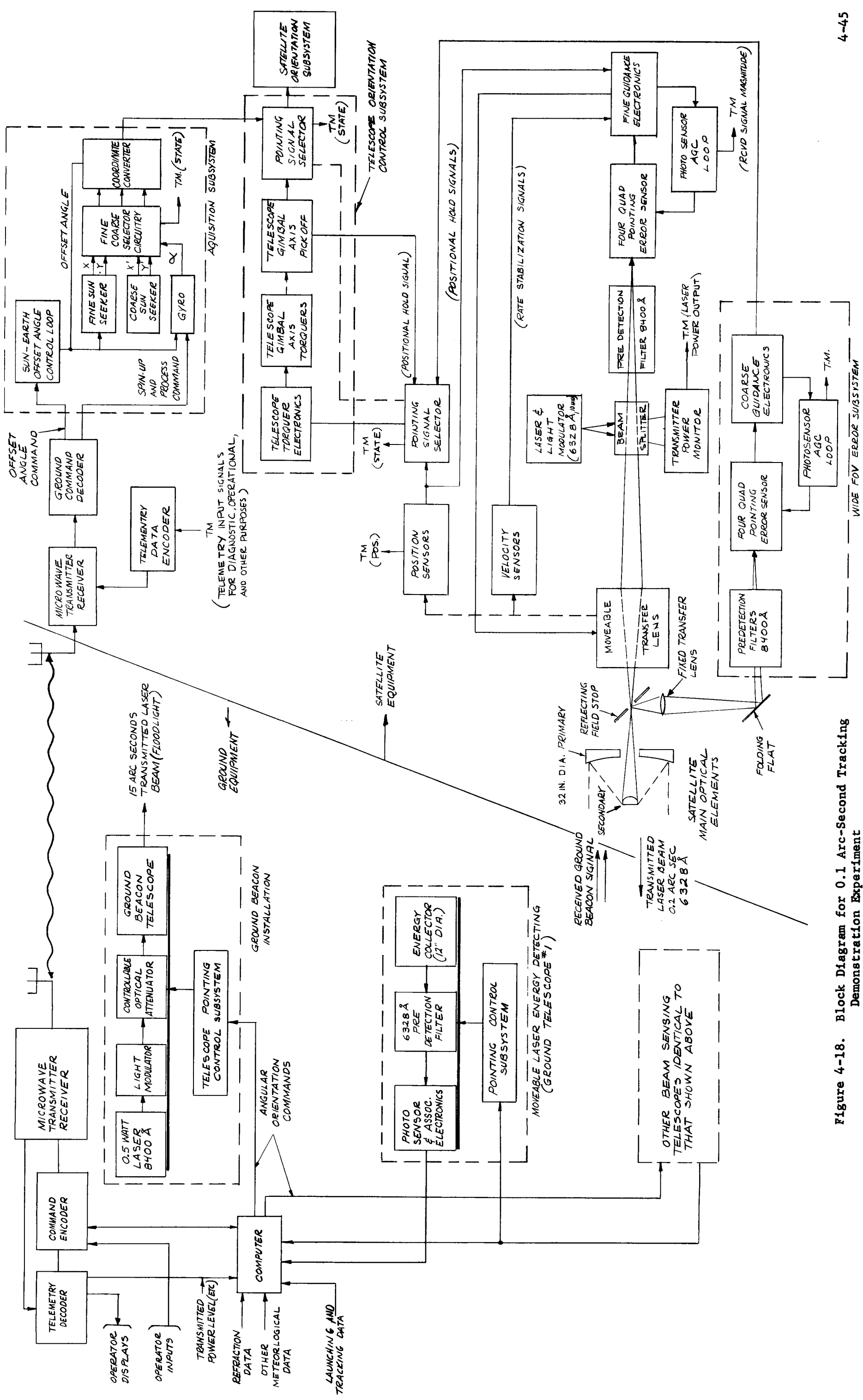
Figure 4-18. Block Diagram for 0.1 Arc-Second Tracking Demonstration Experiment

For a beam shift of 50 feet along the X axis corresponding to 0.10 arc-second telescope pointing error, the energy at apertures A, C, and B becomes 2X, X, and zero, respectively indicating a difference signal magnitude of approximately 2X per 0.1 arc-second. The aperture size of the ground telescopes used in the array has been tentatively chosen as 12 inches diameter in order that atmospherically induced scintillation fluctuations shall introduce only small beam position measurement errors.

Since the pointing error is not expected to contain components above, say 10 cps, signal filtering can remove higher frequency scintillation components and reduce scintillation-induced fluctuations to approximately 15 percent[7] of the nominal signal intensity magnitude for each of the selected 12-inch apertures.[8] This represents only a small equivalent pointing error (approximately 0.015 arc-second) and is therefore acceptable.

Selection of the aperture size also allows use of uncooled ground telescope detectors. The RCA 7265 S20 photomultiplier operating at 25°C, for example, has a dark current equivalent input power of 7×10^{-14} watts at 6328Å while the input laser power to the aperture will nominally be about 10^{-6} watts assuming no optical transmission losses. The statistical noise fluctuations for this dark current level will certainly be negligible, as will be seen below, for any reasonably expected optical attenuations and can be ignored compared to that in the temporally coded signal itself.

The relatively large amount of signal power expected at each aperture is significant in that the signal-to-noise ratio (S/N) of each detector will be

substantial even with wide sensor field of view. Quantitatively, the (S/N) can

be expressed as

$$S/N = \frac{Q\,N_g\,N_v\,\dfrac{P_s}{8}\,\left(\dfrac{D_g}{B_s R}\right)^2\,AC}{\left[2\,\Delta F\,C\,Q\,\left(\underbrace{N_v\,N_g\,\dfrac{P_s}{8}\,\left(\dfrac{D_g}{B_s R}\right)^2\,A}_{\text{Signal Pwr at Detector}} + \underbrace{N_g\,\left(\dfrac{D_g}{2}\right)^2\,\pi F N_r\,\Delta\lambda}_{\substack{\text{Sky Background}\\\text{Power at Detector}}} + \underbrace{P_t}_{\substack{\text{Dark}\\\text{Current}\\\text{Equivalent}\\\text{Pwr of}\\\text{Detector}}}\right)\right]^{1/2}}$$

where the following definitions apply and the indicated values are considered

either reasonable or pessimistic.

Q = S20 phototube quantum efficiency = .05 electrons/photon

N_g = ground telescope optical efficiency = 0.2

N_v = vehicle telescope optical efficiency = 0.2

P_s = satellite laser power output = 10^{-2} watts

D_g = ground telescope collector diameter = 12 inches

B_s = satellite telescope resolution = 0.2 arc-second

R = satellite range = 20,000 miles

A = atmospheric transmission at 6328$\overset{\circ}{A}$ = 0.7

C = conversion factor from watts to photon/sec at 6328$\overset{\circ}{A}$ = 3.2×10^{18}

F = ground detector FOV = 2 min radius = 10^{-6} steradians

N_r = day sky background = 0.017×10^{-5} watts/cm^2/steradian/$\overset{\circ}{A}$

P_t = phototube (S20) dark current equivalent power = 7×10^{-14}

watts

ΔF = detector frequency response = 10 cps

$\Delta\lambda$ = predetection filtering bandwidth = 10 Å

Substitution of the indicated values into the foregoing expression yields

$$S/N = \frac{6 \times 10^8}{\left[3.2\times10^{18}\left(\underbrace{3.32\times10^{-9}}_{\substack{\text{Signal}\\\text{Power}}} + \underbrace{0.2625\times10^{-9}}_{\substack{\text{Sky Back-}\\\text{ground Pwr}}} + \underbrace{7\times10^{-14}}_{\substack{\text{PMT}\\\text{Equivalent Power}}}\right)\right]^{1/2}}$$

The high ratio obtained above indicated that acceptable S/N will also result with substantially larger ground collector fields of view (see Figure 4-20) and/or with protection filters wider that the assumed 10Å.

The proposed scheme would utilize collectors of about one to four degree diameter fields to minimize pointing accuracy requirements while maintaining S/N ≥ 100. This is especially important when one considers the experimental contraints imposed by transit time and aberration effects.

Both these effects prevent the vehicle's transmitted beam from being received at the ground beacon when perfect tracking and vehicle transmit receive alignment conditions prevail. In effect, this is because no point ahead mechanism is included in the satellite telescope No. 1. Hence, the ground facilities must provide a variable positional separation between the ground beacon and the ground receiving array as well as some means of pointing each of the separate optical lines of sight. As proposed, the ground beacon will be a fixed installation, controlled by ground computer with ephemeris and
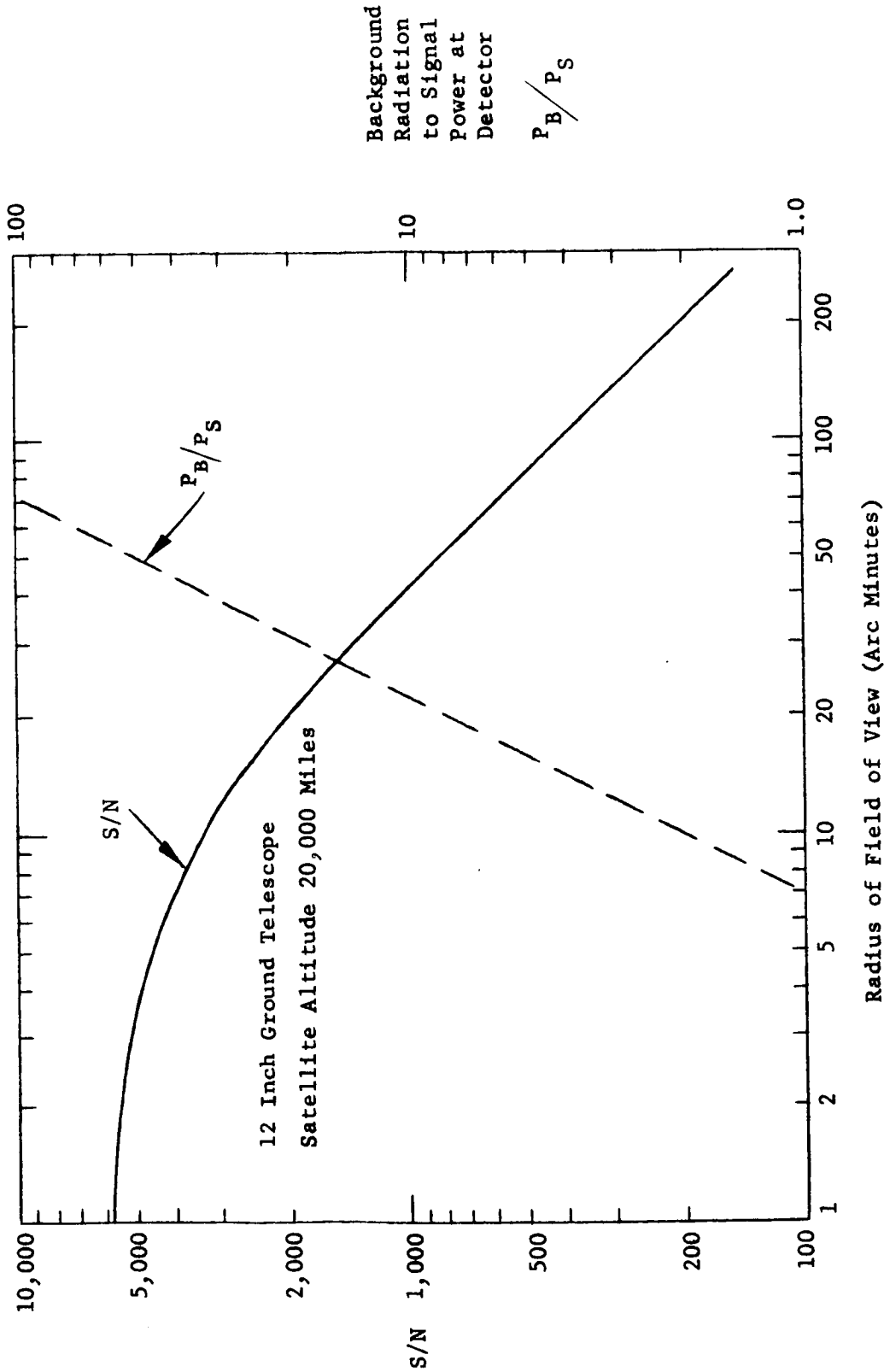
Figure 4-20. Signal to Noise Ratio Dependency on Field of View

meteorological data to direct a laser beam towards the predicted vehicle position with necessary precision.

Table 5-6 of the Phase I Report indicates that a S/N ratio and bandwidth (6 at 20 cps) adequate for tracking purposed will be achieved with one square degree of earthshine from 66 mw of GaAs beacon power and a 5 arc-second beamwidth. Hence, with a 0.5 watt ground transmitter power the beacon beamwidth could be made as wide as 15-arc-seconds, and beacon pointing requirements could be broadened to ± 5 arc-second. It should be noted that even higher beacon powers are readily available to permit further relaxation of beacon pointing requirements.

Ground receiver array motions shall be used to compensate for point ahead effects, which result in large but not impractical receiver array-to-beacon displacements. Transit time effect due to earth spin will cause a displacement d_T equal to the positional change of the beacon during the round trip time at the speed of light. The earth beacon velocity (see Figure 4-21) is nominally directed tangentially eastward with magnitude $\omega_e r_e$ cos (latitude) and the vehicle-beacon separation range, corresponding to zeniths from 0 to 90°, can vary between a minimum of $r_s - r_e$ and a maximum of $\left(r_s^2 - r_e^2 \right)^{1/2}$. Assuming that r_s = 19,752 nautical miles, r_e = 3,444 nautical miles, and beacon latitude = 30°, values for d_T range from 262 to 312 feet. This, in itself, would call for a receiver array located 287 feet to the west of the beacon with computer corrections equivalent to ± .050 arc-seconds to account for the ± 25 foot errors. Such an approach has practical limitations due to the additional effects of aberrations (Bradley Effects).
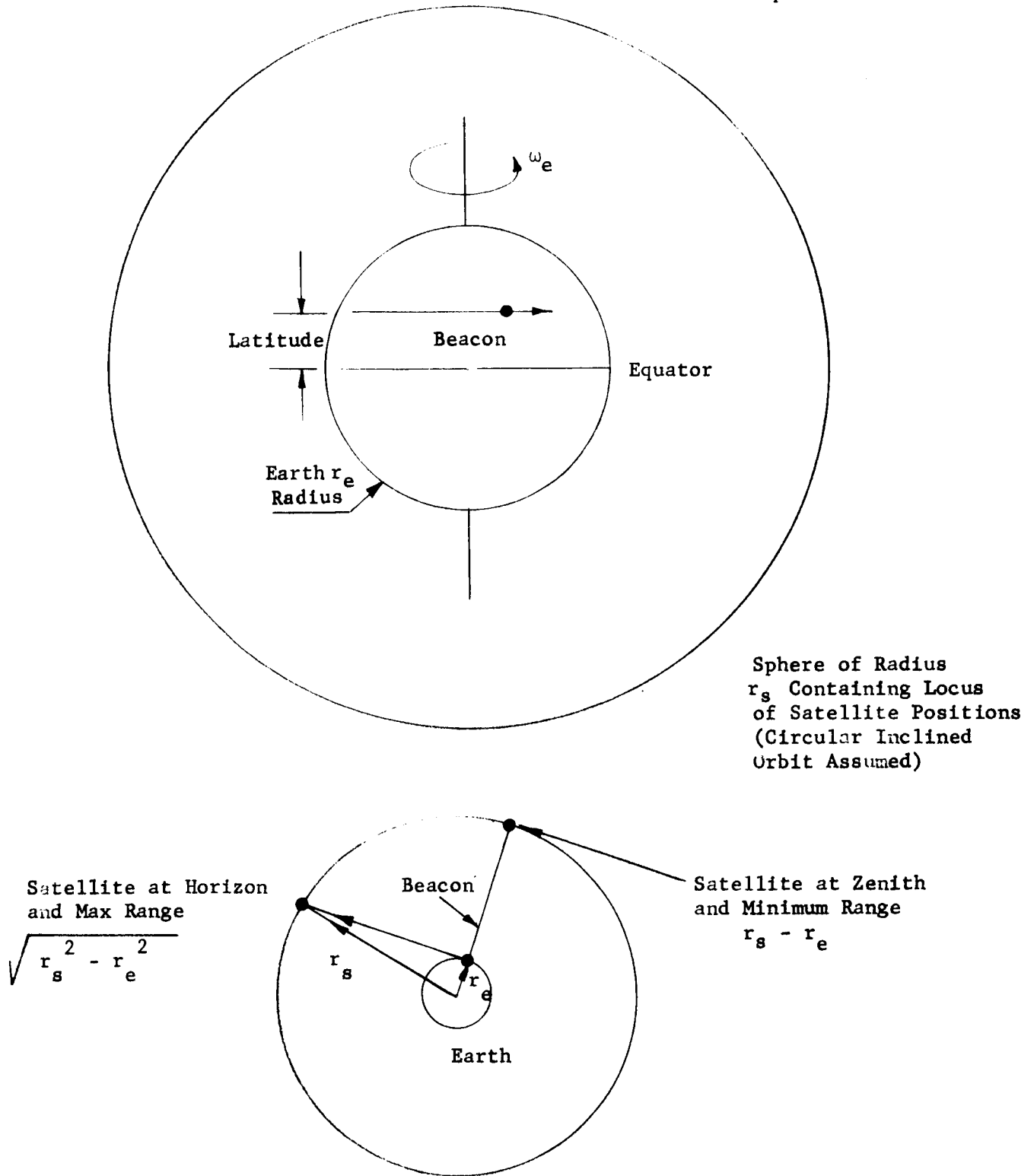
Figure 4-21.   Geometry for Transit Time Calculations

The displacements from this cause can be roughly estimated by assuming a constant satellite-to-beacon range of say 18,000 nautical miles and the satellite angular rates as seen at the beacon given by the Phase I Report, pages B-14 and B-16.

For a 60° orbital inclination, the maximum angular velocities in the east-west and north-south directions are given as 3.8×10^{-5} and 7.5×10^{-5} rad/sec, respectively, corresponding to an eastward displacement varying from 420 to 1330 feet and north-south maximum displacements of ± 900 feet. The time variation of these displacements is such that the locus of vehicle transmitted laser beam positions describes a "figure 8" pattern on the ground once per day.

The relatively small pattern dimensions and the slow rate of beam motion along the locus makes it practical to accurately place the ground array at points along this locus with unbalance signals from the individual receiving collectors indicating vehicle pointing errors. Since each of the collectors has wide field of view, relatively crude angular pointing mechanisms on each collector will suffice for vehicle tracking purposes.

It is important that relatively large atmospheric refraction errors will introduce very small vehicle tracking measurement errors. If one considers a random refraction angle effect as large as 15 arc-seconds occurring at a slant range of 15 miles in the earth's atmospheric layer, for example, the beam displacement error at earth would be in the order of seven feet which is equivalent to only 0.014 arc-second mispointing.

4.7   POINT AHEAD DEMONSTRATION

One of the keys to a successful deep space communications link is the ability both to receive or track a distant transmitter and, in addition, to accurately point the local transmitter in the correct direction. Since the transmitted beam should be narrow in width to achieve high communication rates with reasonable power, the pointing accuracy requirements can be stringent. In the case of a 0.1 arc-second resolution diffraction limited transmitting telescope, pointing errors exceeding about 0.05 arc-second result in substantial reductions of field intensity at the distant receiver. A rather practical approach for obtaining high angular pointing accuracy is to use the receiving line of sight towards the apparent position of the distant transmitter or beacon as a reference direction from which to base the transmitter LOS. The maximum displacement from this reference, for the case of the deep space vehicles transmitting to earth, is in the order of only 36 arc-second which makes possible, for example, the attainment of 0.036 arc-second precision with a 0.1 percent mechanism. While offset angular magnitude could thus be accurately implemented, some way of deflecting the transmitted beam in the correct direction must also be provided. The precision necessary is in the order of one half the beamwidth divided by the offset magnitude, which in the case of 0.1 arc-seconds beamwidth and 36 arc-second point ahead is within 0.05 degrees. (See Appendix B.)

While the pointing accuracy requirements are precise in the conventional sense, based on Perkin-Elmer experience they are considered practical to achieve in a deep space communication system. It would be desirable, however, in any such system to minimize the vehicle equipment complexity and therefore achieve the highest possible reliability. The implicit

operations required to establish the offset magnitude and direction data are

thus best computed on the ground and telemetered to the vehicle. The slowly

varying magnitude data could be conveniently transmitted in the ground beacon

signal, but a problem exists in similar transmission of the direction information

since the vehicle does not have a rotation reference about its receiver's line

of sight. Four system approaches are considered in the following paragraphs.

The polarization approach is the method presented in the Phase I Report, but

analysis during the Phase II portion of the project has indicated S/N difficult-

ies in this approach (see Appendix B).

Polarization Approach - The E vector orientation of the ground beacon laser

could be oriented by controlled laser rotation, to indicate the direction of

point ahead required. A polarization analyzer on the vehicle could sense this

vector orientation and supply signals to properly control point ahead direction.

For example, the vehicle itself could be rotated about RLOS into a position

allowing the use of a single axis point ahead mechanism to then introduce offset

magnitude. Essentially the same technique could be used wherein the same single

axis point ahead mechanism (and the analyzer), rather than the whole vehicle,

is rotated about the line of sight. The former approach is recommended, as noted

in the Phase I Report, because of its inherent equipment simplicity.

The analyzer itself could take several forms such as illustrated in

Figure 4-22. The incoming beam could be split in two and fed through crossed

polaroids to separate photosensors whose difference signal indicates direction
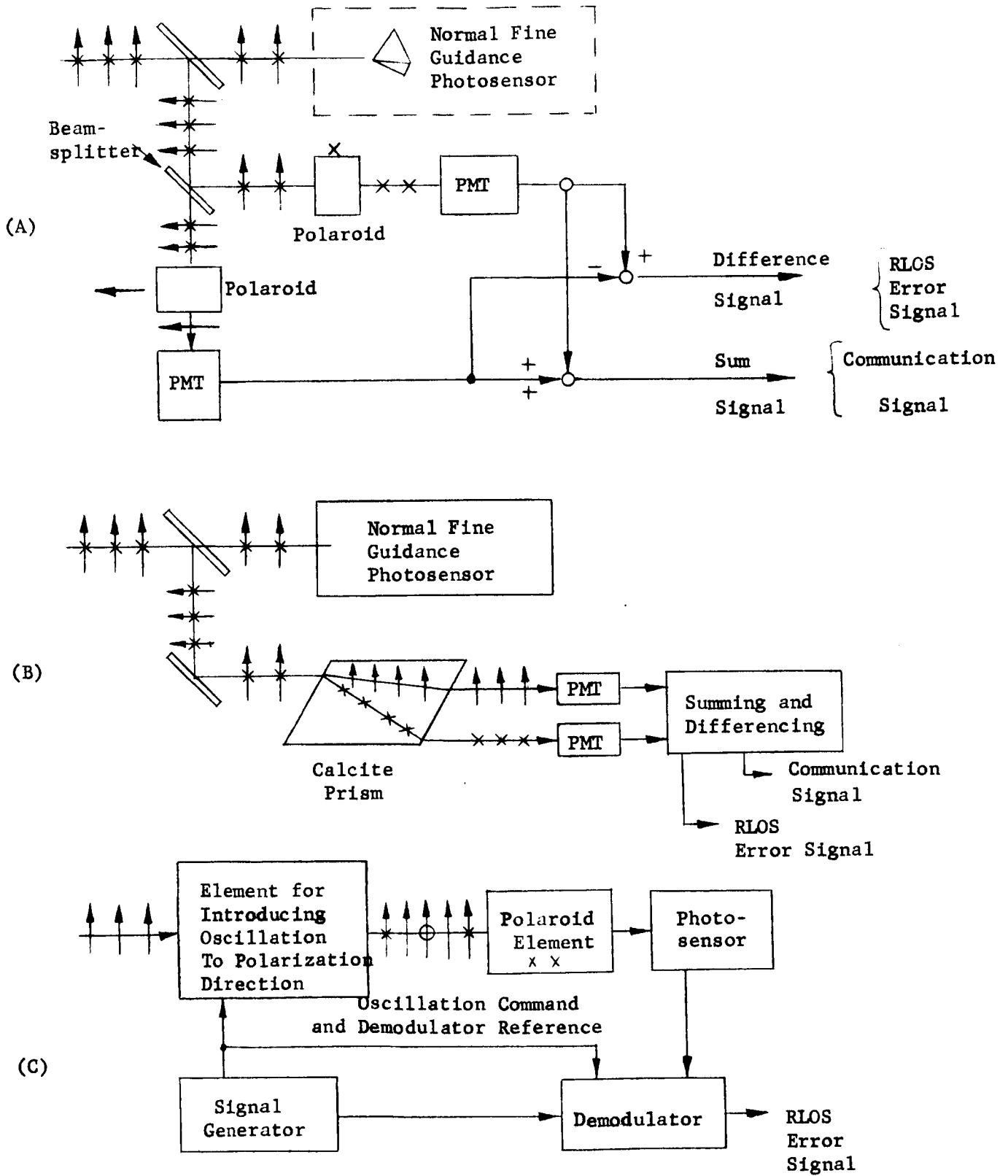
of received polarization.

Figure 4-22. Polarization Sensing Methods

A calcite prism, which performs the functions of the beamsplitter and crossed polaroids, is an alternate way employing the same concept.

A third approach basically involves the use of a polaroid (or calcite) element oscillated about a nominal center position. Here the output of the associated photosenser contains no components at the oscillation frequency only when the center position of the polaroid element corresponds to least light transmission.

Second Ground Beacon Approach - Establishing the correct pointing direction could involve the use of a second ground beacon whose angular position relative to the LOS to the first beacon is sensed by the vehicle and used as a reference direction.* The correct pointing direction relative to this reference direction can be supplied in the beacon signal along with offset magnitude information. However, this does not appear practical for the deep space range of 100 million miles. This is because a tracking error of 0.05 arc second is equivalent to a 5 min rotation reference error if the two beacons are separated 36 arc second, a value greater than the earth's 16 arc second angular subtense at 10^8 miles. While errors smaller than 0.05 arc second are possible, the approach is presently considered inadquate for practical beacon separation.

Star Tracker Approach - A third method of roll reference stablization involves star tracking equipment operating to keep the vehicle roll angle at a computable position as in the Second Ground Beacon Approach above. While the extra hardware is not desired, it may be acceptable. One possibility involving the use of the sun as a conveniently bright star bears investigation to determine whether the

---

*In principle this is the approach used in the Stratoscope II program. Stratoscope II stablizes RLOS by guiding on two stars.

ground beacon-sun angular separation must be excessively large in view of the sun's 32 minute diameter (and therefore larger errors in establishing the sun's center).

Arbitrary Reference Approach - This, at present, is the most promising approach for roll stabilization following acquisition. It would involve the star tracker principle as described above but would differ in that any convenient and even unknown star could be used. A fixed sidelooking telescope attached to the vehicle would seek out and lock on a bright star immediately following beacon acquisition. The vehicle point ahead equipment would then execute a circular scan at the off-set magnitude while transmitting a unique code (i.e. satellite clock time). This code indicates instantaneous scan position relative to the scan start position. The number of scan elements (or code symbols) corresponding to a search at 36-arc-seconds offset angle (with a 0.1 arc-second beam) is only about 2300. The code signal received at the earth receiver can be translated by the earth station into the correct point ahead angle for the spacecraft. This point ahead information is telemetered to the spacecraft.

The last three methods would require on-board vehicle complexities such as a computer and a two axis point ahead mechanism while the polarization technique avoids these complexities by simply establishing a reference direction which is precisely the point ahead direction. Although the polariza-tion sensing method initially appeared superior to other alternates, further S/N study (refer to Appendix B) indicated intolerably high errors beyond 10^6 to 10^7 miles range (when reasonable assumptions for ground beacon power, beam-width, vehicle receiver aperture, etc., were made). This basically is due to the fact that sensor S/N is based upon only a small fraction of the total received

signal; for a one minute sensing accuracy, the S/N is about 1/3600 of that based upon the total signal itself. Unfortunately, this limitation cannot be overcome by resorting to high peak power pulse beacons which, as is shown in Appendix F, offer S/N improvement only through better discrimination against background light. Hence without drastic breakthroughs in laser efficiency, laser power output, and photo-emissive quantum efficiency, an alternate to the polarization approach is required for a deep space link. Further evaluation and analysis will be necessary to select the optimum arrangement

But, even with this selection, some difficulty will arise in close simulation of the deep space conditions with the Optical Technology Satellite due the difference in geometry of the trajectories. In deep space, the angular rates for the beacon-sun angle are much lower than the rates for the satellite.

Although alternate RLOS approaches have been presented, and the Arbitrary Reference Approach seems more promising than the Polarization Approach; the Polarization Approach has adequate S/N at 20,000 miles and the experiment discussion which follows is based on that approach.

The Experiment - The experimental equipment block diagram shown in Figure 4-23 contains many components (asterisked) which are essentially identical to those shown previously for the tracking experiment block diagram. The major exceptions to this are:

    (1)   the ground beacon installation which includes a polarization control element to rotate the laser light E-vector (in response to computed commands),

    (2)   the inclusion of a beacon light modulator not only to perform temporal coding useful for background light discrimination purposes, but also to transmit offset magnitude data,

(3) use of a point ahead mechanism for use as described in the Phase I Report,

(4) inclusion of a polarization subsystem utilizing one of the previously described sensing techniques that controls the satelitte and/or the beam deflection mechanism roll orientation and, so, point ahead direction.

(5) a fixed rather than movable ground station array located about 3.6 miles from the beacon or, equivalently, 36 arc-seconds away.

Also shown but possibly not required is a tracking sensor channel in the ground beacon telescope which includes a transmit receive transfer lens to compensate for instananeous tracking errors. Transfer lens position signals being proportional to telescope structure mispointing are fed to the computer for pointing command signal refinement.

The experimental procedure would closely parallel that for the 0.1 arc-second tracking experiment in that the ground beacon would be computer controlled to floodlight the predicted vehicle position and the vehicle receiver would acquire and commence tracking of the beacon. Either the microwave link or beacon coding could be used to transmit point ahead magnitude data while the directional information is supplied from the computer via beacon laser polarization direction control. A point ahead mechanism would be used for vehicle transmit beam deflection while the whole vehicle is controlled about the LOS to obtain directional control for the deflected beam. The point ahead commands thus introduced can allow transmission directly back to the ground beacon telescope if it is desired to close this communication loop. The magnitude of point ahead for this purpose will be in the order of a few arc-seconds with an accuracy of about

Figure 4-23. Block Diagram of Equipment for Point Ahead Experiment

4-63
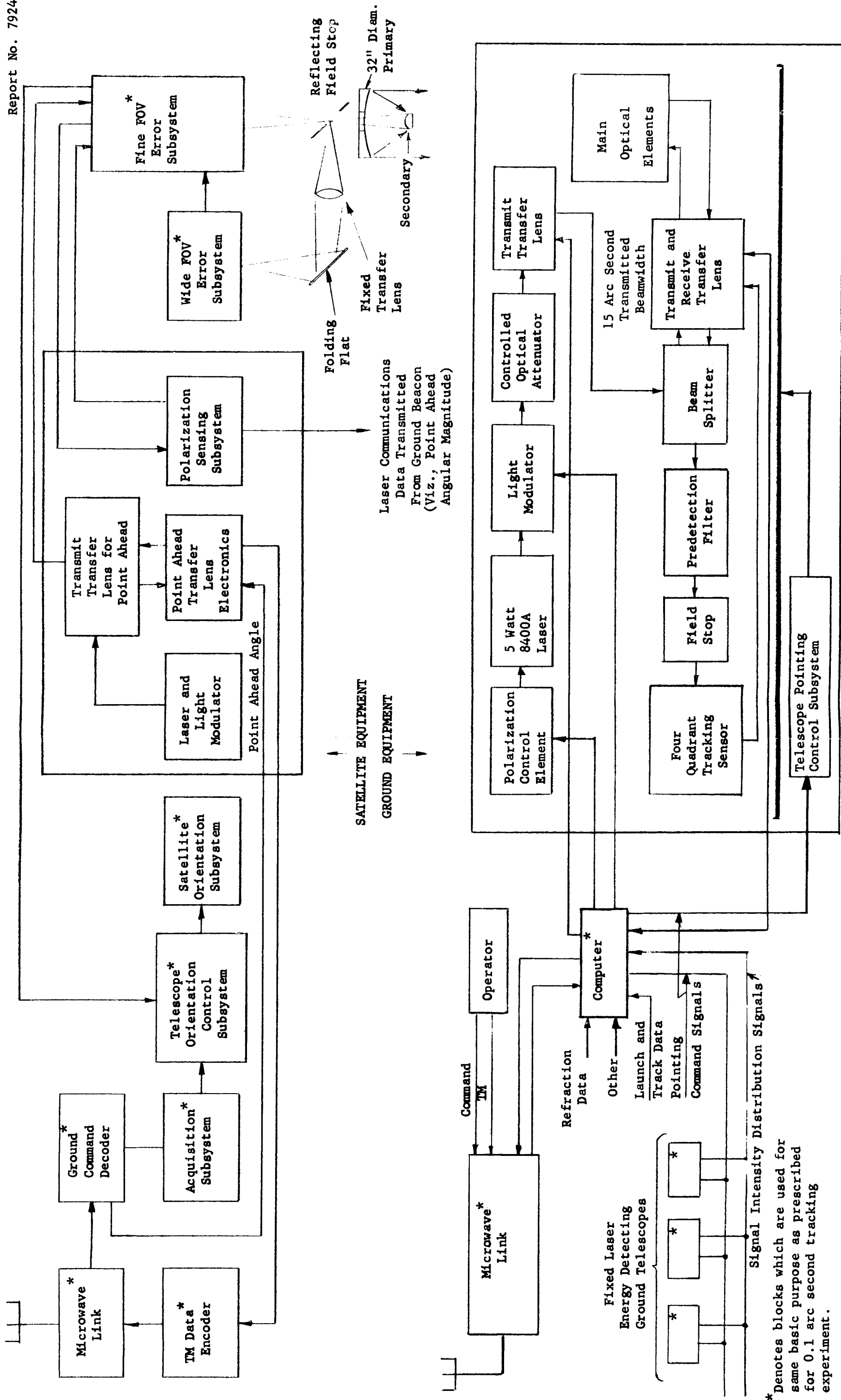
*Denotes blocks which are used for same basic purpose as prescribed for 0.1 arc second tracking experiment.

0.05 arc-second. The direction error due to the small point ahead magnitude will be greatly relaxed compared to that required for 36 arc-second point ahead. Use of the fixed energy detecting collectors arrayed around the beacon will provide information relative to vehicle transmitter line of sight errors. The signals from these auxiliary sensors are fed to the computer which monitors the errors or modifies the point ahead commands to remove the errors. In this mode of operation, the point ahead commands could be purposely perturbated to cause relative motion of the beam with respect to the receiving array and so obtain data relative to the received beam intensity distributions. This would provide some measure of the quality actually achieved by the optics in space.

With either this ground arrangement or when transmitting to the auxiliary sensors positioned 3.6 miles away, "static or bias errors" introduced into the satellite, for example, by launch environmental conditions can be detected and, if desired, compensated out by computer corrections.* Moreover, the performance of the system can be assessed as a function of naturally occuring daily and seasonal changes of background light level and/or manually adjusted beacon transmitted power level. Evaluations of the ability to maintain simultaneous communications in both directions as a function of artificially introduced (transit time simulating) time lags can also be carried out. The basic technique of evaluating point ahead errors is identical with that described for the 0.1 arc second tracking experiment.

---

* A focal length change of the vehicle's optics can change the scale factor of the transmit beam deflection mechanism. This can be assessed by noting the multiplying constant required by the otherwise correct computed point ahead angles to obtain minimum tracking errors.

4.8 SPACE-TO-GROUND-TO-SPACE LOOP CLOSURE

The sequential steps and block diagrams are provided to describe the experiment planned for each telescope aboard the OTS for this instrument loop. The Telescope 2 sequential steps for this experiment are different from the steps for Telescope 1. Since Telescope 2 is easier to understand, it is discussed first in the following material.

<u>The Telescope 2 Experiment Procedure</u> (see Figure 4-24)

(1) Complete the acquisition operation on the satellite.

(2) Complete the acquisition operation on the ground.

(3) Satellite tracks ground laser beam.

(4) Point ahead subsystem on satellite shifts down-going beam to ground receiver location (information for the point ahead angle sent up to satellite via microwave link).

(5) Ground station locks on down-going beam from satellite and precisely guides up-going beam (with appropriate point ahead angle computed from ephemeris data).

(6) Pattern Scan Bias Electronics (as shown in Figure 6-7 of the Phase I Report p. 6-11) is turned on and the angle for the down-going beam is programmed off axis in a conical scan pattern.

(7) Simultaneous with this departure of the transmit beam off the line of sight (LOS), the amount of departure off the LOS is telemetered to the ground station via the microwave link.
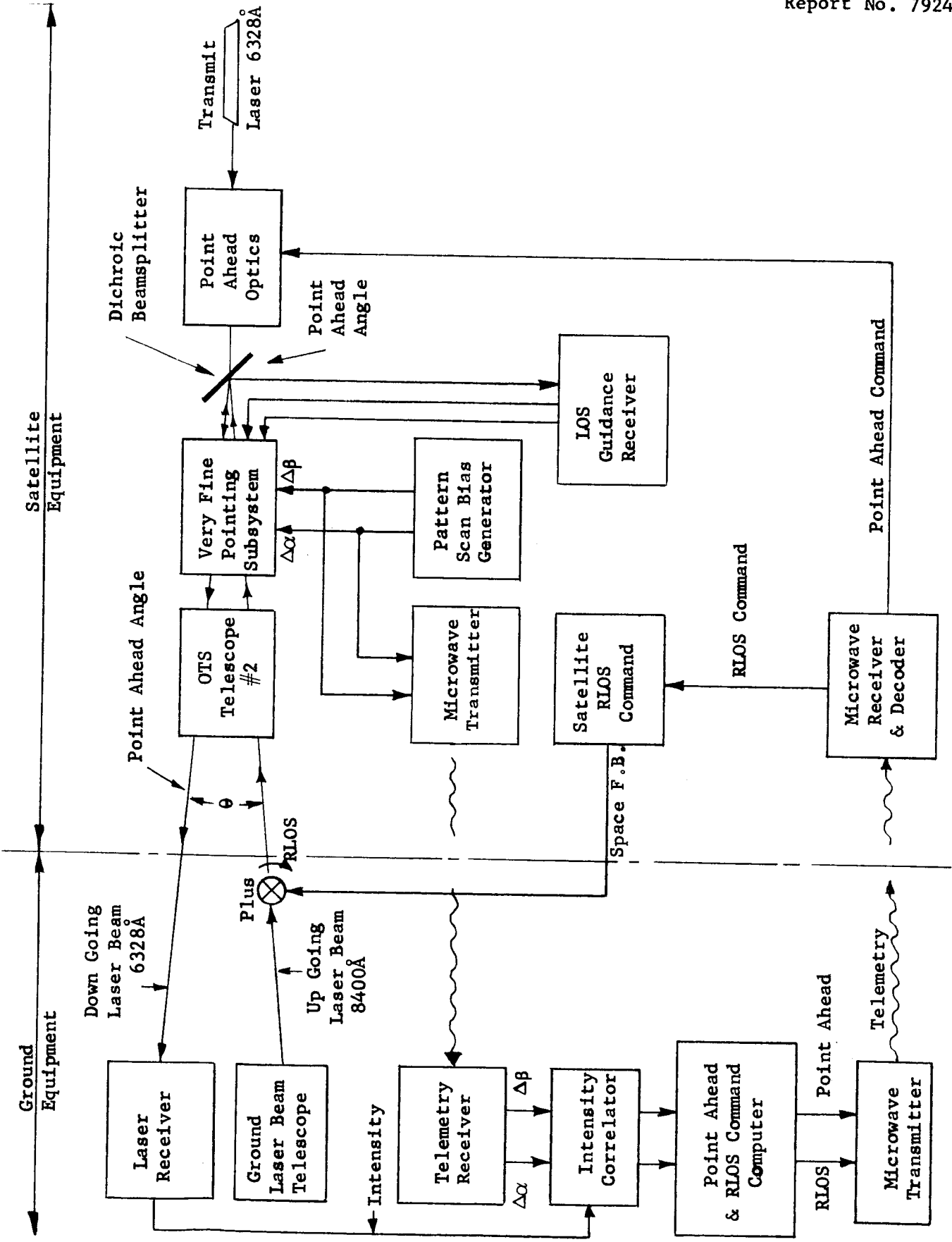
Figure 4-24. Space-to-Ground-to-Space Loop Closure (Telescope No. 2)

(8) The bias angles as received are correlated with the intensity received from the down going laser beam.

(9) The center of gravity of the intensity distribution as a function of the satellite bias angles which is computed on the ground is converted into point ahead commands on the ground to reduce the intensity center of gravity offset to zero.

(10) The new point ahead commands are transmitted to satellite from ground station via microwave link.

(11) Satellite receives new point ahead command and executes new point ahead angle as commanded by ground station.

(12) Control loop process continues until the intensity center of gravity of down-going beam is located at the receiving station on the earth.

(13) Point ahead commands are computed and telemetered to the satellite via the microwave link. This is a repeat of Step 10 above and the process continues until the error approaches zero.

The Telescope 1 Experiment Procedure (see Figure 4-25)

(1)   Complete the acquisition operation on the satellite.

(2)   Satellite tracks ground lasers beam.

(3)   The ground laser transmitter is moved away from
      the ground receiver in the direction necessary to
      locate the down-going beam from the satellite on
      the ground telescope. (This can also be accom-
      plished by having a number of ground laser trans-
      mitters located at the ground site, and one laser
      transmitter is turned on at a time until the down-
      going beam is impinging on the ground telescope.
      This is economically feasible since the laser
      powers are low (less than 1/2 watt is adequate)
      and the ground telescope optics are small (2 inches
      diameter). These steps are necessary for accom-
      plishing ground acquisition with telescope 1 on
      the OTS since this telescope does not have a point
      ahead capability).

(4)   Once the down going beam is being received by
      the ground telescope while tracking the dis-
      placed laser transmitter beacon, the next step
      is to make quantitative measurements of the
      intensity of the beam in real time as a function
      of distance coordinates on the earth's surface.
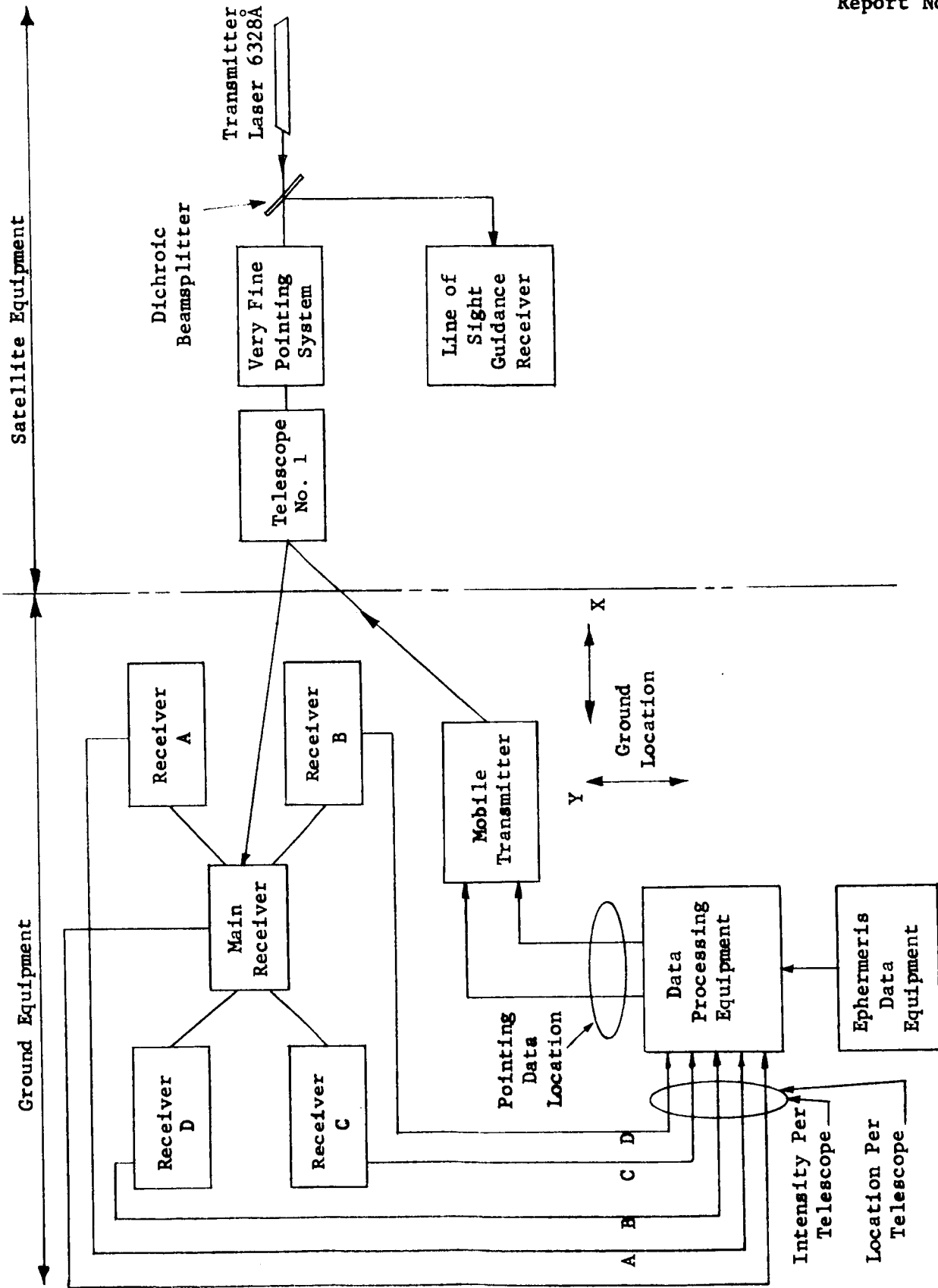
Figure 4-25. Space-to-Ground-to-Space Loop Closure (Telescope No. 1)

In order to make these intensity measurements,
a number of receiving telescopes are required at
the site. Each telescope is equipped with a prede-
tection filter (a dielectric filter for example
to reject skylight but with a pass band at 6328Å)
and a S-20 photomultiplier tube. The intensity
from each of these receiving systems along with
the receiving system location coordinates is fed
to the on-site data processing subsystem.

(5) The data processing center computes the intensity
center of gravity of the received down-going beam
and calculates an improved value of point ahead
angle and RLOS.

(6) The improved point ahead angle and RLOS value
are put to use in the system by displacing the
earth laser beacon transmitter accordingly until
the beam is accurately centered on the main
receiving telescope.

4.9 TRACKING TRANSFER DEMONSTRATION

One of the operations which must be performed by a deep space
communication telescope is a transfer of the link with one ground communication
station to another station. This requirement arises since communications down time
must be minimized. The transfer operation at 10^8 miles would involve a shift of
the vehicle receiver's line of sight by about 4000 miles on earth or equivalently,

8 arc seconds. This could be accomplished if the vehicle field of view is large enough to include two earth station beacons, which it is by simply turning off one beacon and turning on its replacement.* The vehicle receiving-line-of-sight will then lock onto the second beacon which sends its own point ahead data (offset magnitude and direction) so that the vehicle can properly transmit back.

Figure 4-26 indicates that the point ahead data for the two stations can differ sufficiently to require change at the start of station transfer. In principal, the time during which data cannot be transmitted to the vehicle can be zero since communication link breakage due to the earth's rotation or cloud cover, should be immediately known at the ground stations. Communication to earth, however, will be broken for at least the interval required to shift stations and accurately redirect the space laser transmitter beam. In the event of sudden beacon failure or cloud cover, the lost time can be at least as large as the radiation transit time from the vehicle. The operation of station transfer as outlined above is seen to present the same type of problem expected during the last stages of acquisition (where the beacon is seen by the tracking error sensor whose output signals act to correct the receiving line of sight) and with point ahead operations.

An alternate approach would involve the use of two ground beacon temporal coding frequencies and additional vehicle electronics to minimize, in effect, the possibility of ground beacon loss. The implementation (see Figure 4-27) is almost identical to that required for the point ahead experiment except

---

*It should be noted that the calculations indicate that it should be feasible to detect the earth beacon at ranges up to 10^8 miles in the presence of full earth-shine.
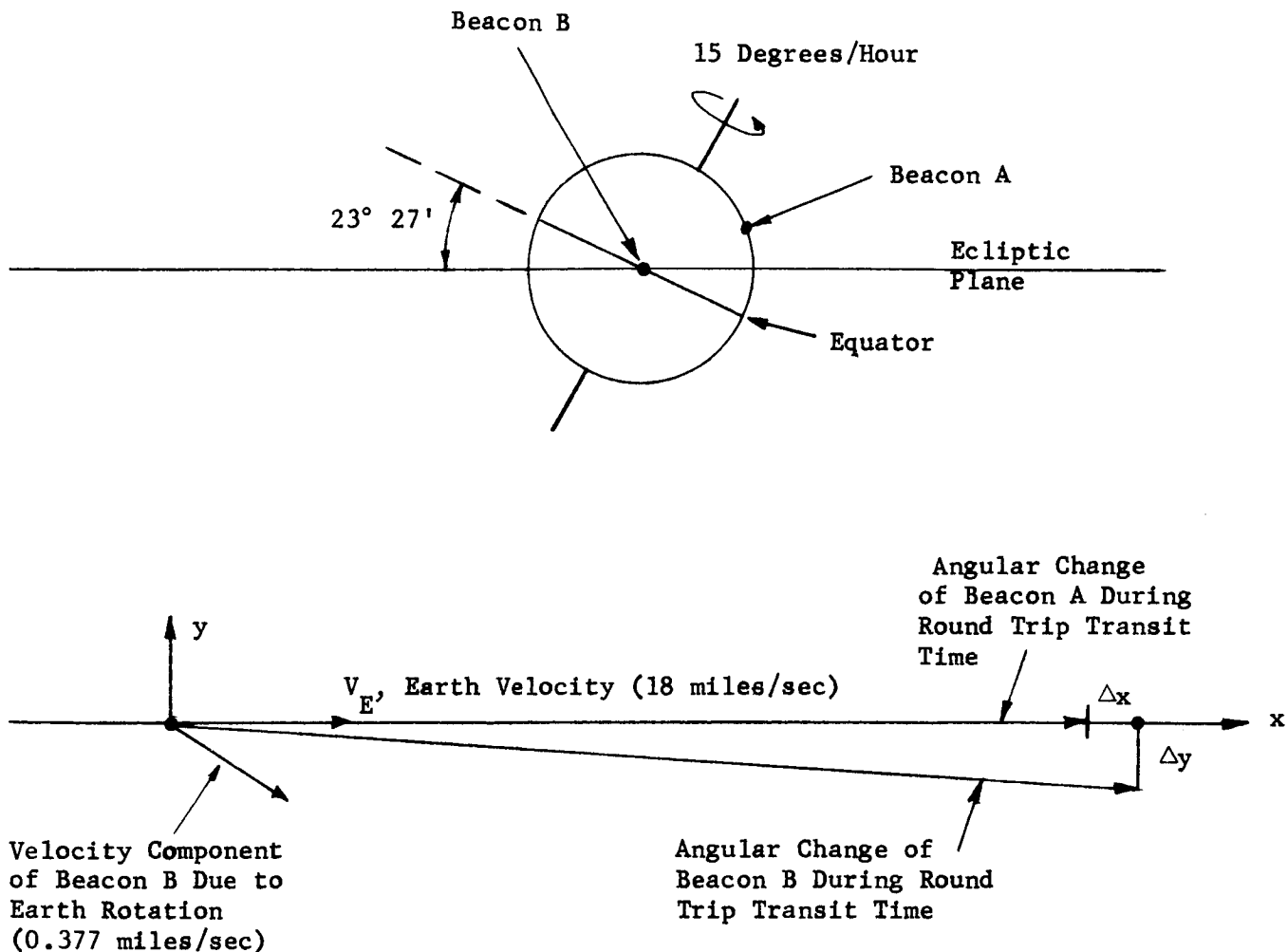
Figure 4-26.   Point Ahead Data Differences Possible for Two Ground
Stations Due to Transit Time Effects

that two complete ground stations are required and, the tracking control electronics would be similar to that given on page 5-22 of the **Phase I Report** Operation of station transfer would be initiated by a ground command from beacon A, operating with temporal coding f_1, for the vehicle to transfer to beacon B operating with coding f_2. Upon receipt of this command, the vehicle would (open its field of view if restricted and) make the transfer only if beacon B is detectable. Knowledge of the transfer at earth is deduced from a transfer of vehicle communication to station B.

The vehicle logic cirucitry can be arranged such that station transfer will also accur without ground command in the event the beacon being tracked disappears when an alternate beacon is in view. The beacon to be tracked is selected by switching based upon which beacon is viewed. Only if both beacons are viewed will ground commands carried by either or both earth beams govern the selection. After track is commenced, appearance of the selected beacon in the wide field of view (or acquisition) sensor generates a signal to accept tracking error signals from this sensor. Moreover, disappearance of beacon A during tracking will be accompanied by automatic transfer to beacon B if visible. Similar actions occur when transferring to subsequent beacons.

The satellite experiment itself would be an assessment of the equipment performance required for station transfer operation for station separations of 8 arc-second to 16 arc-second (equivalent to one half to one earth diameter at 10^8 miles). At shorter ranges, transfer can take place for angles up to 0.5 degree (one half of the wide field of view).
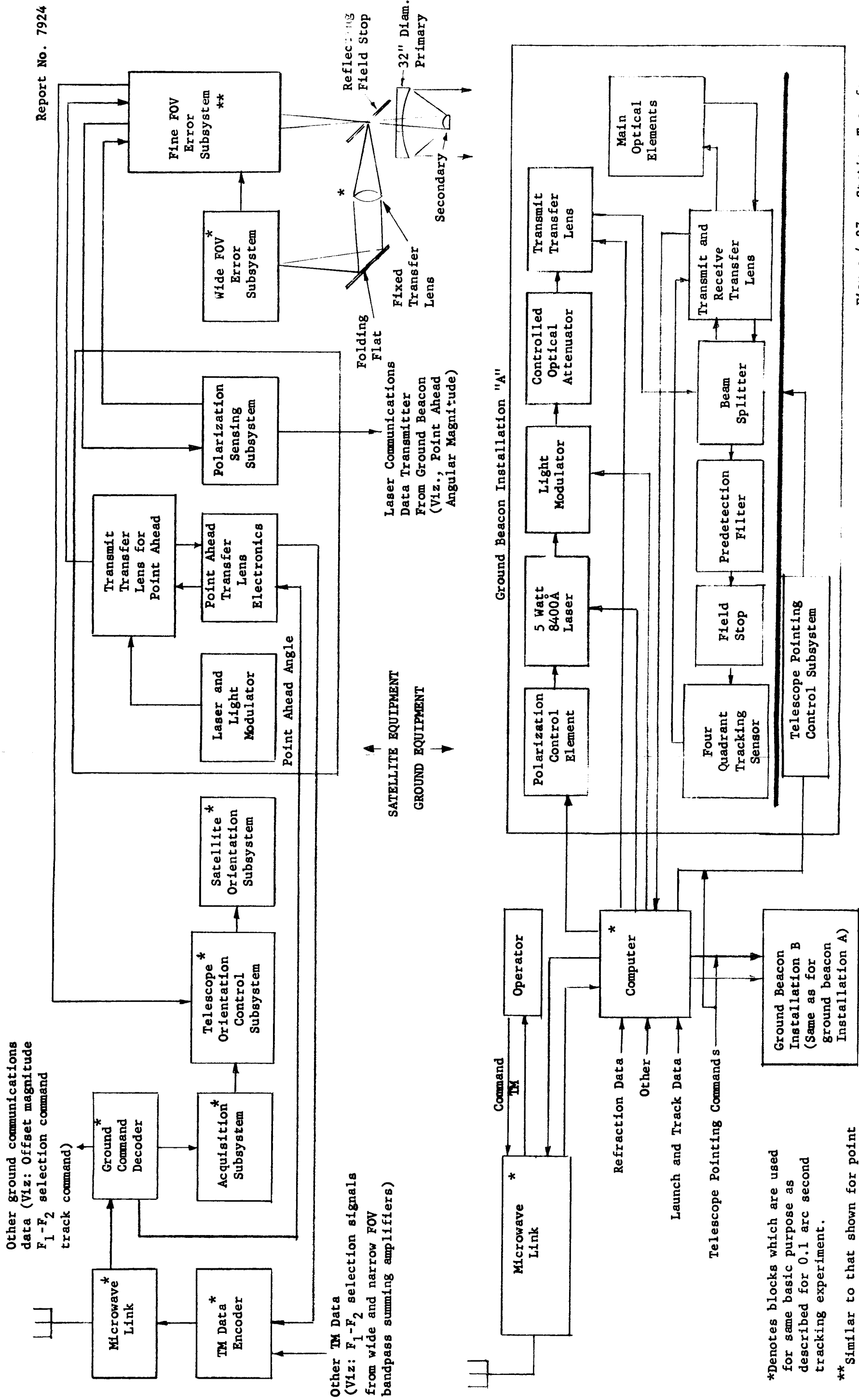
Figure 4-27. Station Transfer Block Diagram

*Denotes blocks which are used for same basic purpose as described for 0.1 arc second tracking experiment.

**Similar to that shown for point ahead experiment except for control electronics which are described in the OTS Phase I Report, pages 5-20 through 5-22

4.10 COMMUNICATIONS AT 10^7 CPS

This experiment has as its objective the engineering demonstration of an optical communication system that can operate reliably over a range up to 10^8 miles, with a bandwidth capability of 10 Mc/s. A pulse code modulation system employing polarization to mark the binary ones and zeros utilizing a 6328Å He-Ne gas laser has been selected as a representative and near optimum candidate for deep-space to earth communications. Refer to the Phase I Report for a discussion of the merits of this communication system over other candidates. The earth to spacecraft communication link will not be discussed in detail here, since candidates such as a double sideband supressed subcarrier system have been covered in the Phase I Report. Also, the data requirements for this link are much lower than those for the deep-space to earth link, as they consist only of low bandwidth command and control signals to the spacecraft for attitude control and low bandwidth instructions for the implementation of the various experiments. There is no known requirement for large bandwidth capability for the earth to deep-space link, which is fortunate, since this permits room for simplification and increased reliability of the vehicle receiver system.

The Experiment - Refer to Figure 4-28 for block diagrams of the satellite transmitter and earth receiver configuration. Continuous or pulsed data sources, as well as diagnostic data sources, can be accommodated in the satellite transmitter configuration. Continuous signals are sampled, quantized, encoded, and transmitted. Pulsed data may or may not need to be quantized, depending on its nature. Periodically, after a suitable number of clock pulses have been counted, a time code is generated and transmitted for synchronization purposes.
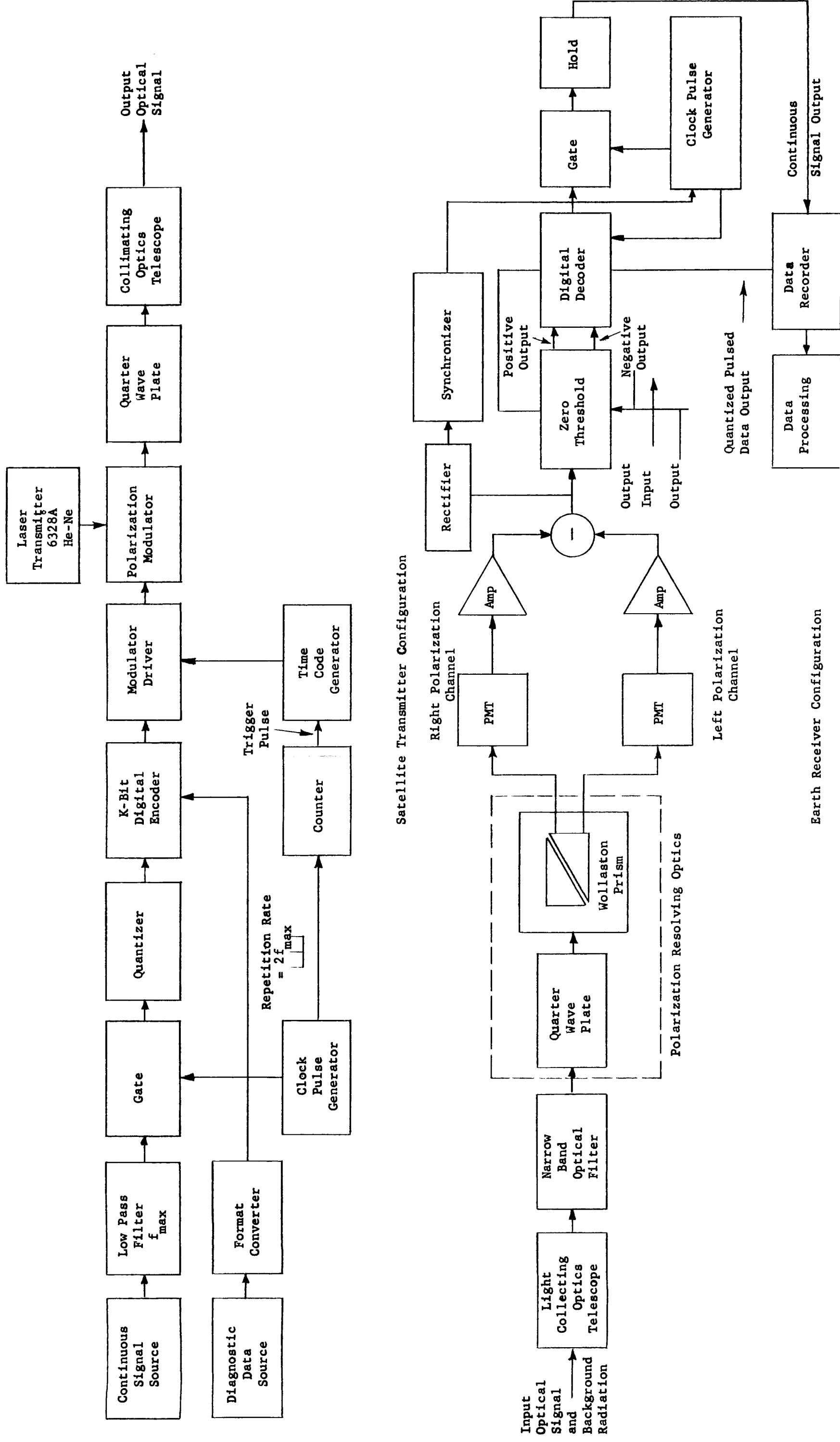
PERKIN-ELMER

Figure 4-28. Communications at 10^7 cps

The Kerr or Pockel cell type polarization modulator can be used. The output of the polarization modulator is then transmitted through a quarter wave plate to provide either left- or right-circular polarization. The optical signal is transmitted through a telescope for ultimate reception at earth. The earth receiver telescope accepts the incoming optical signal and background radiation, and passes it to the polarization resolving optical subsystem. The polarization resolving optics consists of a narrow band optical filter, quarter wave plate, and Wollaston prism. All signal photons received during the transmission of a particular code bit will have the same polarization, but the background photons will, in general, have either polarization with equal probability. The prism separates the incoming beam according to polarization, and the two outputs of the prism are detected by two separate photomultipliers. The photomultiplier outputs are amplified and differenced. If the difference signal is positive, it is assumed that the signal photons were so polarized that they entered the left channel. If the difference signal is negative, it is assumed that the signal was meant for the right channel. The selection of right or left channel will correspond to the binary digit being transmitted, provided that the number of received signal photons plus the number of received background photons polarized the same way is at least one greater than the number of received background photons that are polarized in the opposite way.

The output of the zero threshold system is sent to the digital decoder, then sampled and held to obtain a continuous signal output which is recorded for non-real time data processing. The quantized pulse data output from the digital decoder would also be recorded for data processing.

Bit-time synchronization is accomplished by sensing the "quiet" time between reception of pulses. The output of the differencer is rectified. The synchronizer responds to inputs below threshold and adjusts the clock pulse generator rate. Frame synchronization is accomplished by either detecting the time code periodically and resetting the frame clock if necessary, or by choosing a coding system with a non-prefixing property, or by inserting a greater dead time between frames than between pulses.

Selection of a coding scheme awaits a decision on the type of data to be sent, and the final error rate required for it. Certain telemetered data may require far more accuracy than television picture data. In other applications, a very high error rate may be acceptable. The optimal coding is different for different desired error rates. Thus, simple coding may be best if a high error rate is acceptable. The system will require error correcting codes if low error rates are required from deep space. Thus, the code selection depends on the deep space experimenter needs.

The space experiments will produce communication data to verify signal-to-noise ratios and data error rates over the gamut of ranges from synchronous-satellite altitude to 10^8 miles, for various background conditions. This is accomplished by appropriate attenuation of received signals (at the transmitter) without attenuation of background.

SECTION V

PCM-PL OPTICAL COMMUNICATION
SYSTEM PERFORMANCE

The PCM-PL* modulation system described in Section 4.9 has been evaluated as a function of range and particularly as a function of the diameter of the transmitting aperture. Channel capacity has been calculated for both fixed error rate per bit and for fixed information bandwidth. Diameters of the diffraction limited transmitting space telescope were purposely chosen to span a wide range in order to determine the relationship between aperture and communications performance. The diameters chosen were 8, 16, 32 and 64 inches.

The quantum efficiency of the signal photodetector is of central importance since performance depends directly upon the signal photoelectrons from the detector. Bit rates have been calculated using a quantum efficiency of 8 percent representing selected S-20 surface photomultiplier tubes. In order to form a basis for comparison, unit quantum efficiency calculations were made and plotted.

Of equal interest is the comparative performance for local day or night conditions. When the ground receiver operates at night, background noise due to sky light is minimized while daytime operation is characterized by the presence of considerable background noise from the sky even after the utilization of narrow band filters.

---

*Pulse Code Modulation - Polarization

Except for the variation in transmitting diameters and the variation of quantum efficiencies, the design parameters employed in the calculations are the same as those used in the Phase I Report. These are repeated in Table 5-1. A five bit per word system was again chosen for evaluation although other PCM word lengths are possible as well as the error correcting codes described in the Phase I Report.

5.1 CHANNEL CAPACITY FOR FIXED ERROR RATE

It is of interest to examine a relationship between PCM-PL channel capacity and range at some fixed acceptable error rate per bit. It will be recalled from the Phase I Report that channel capacity for a five bit PCM-PL system may be expressed as the following function of error rate, R:

$$C = \frac{5}{T} + \frac{5}{T} \log_2 \left(R^R (1-R)^{(1-R)} \right) \tag{1}$$

where C = channel capacity, (bits per second)

   T = sample period per word (seconds).

   R = error rate per bit

The number of quanta, either signal or noise photoelectrons, which occur in the sample period T is given as

$$S = n_{es} T \tag{2}$$

$$B = n_{en} T \tag{3}$$

$$B = \frac{n_{er}}{n_{es}} S \tag{4}$$

where S = the number of signal quanta per sample period

   n_{es} = the generation rate of signal photoelectrons, (number/sec)

   B = the number of noise quanta per sample period

   n_{en} = the generation rate of noise photoelectrons, (number/sec)

TABLE 5-1

DESIGN PARAMETERS FOR LASER COMMUNICATIONS BETWEEN A DEEP-SPACE PROBE AND EARTH			
Input Parameters	**Symbol**	Reception On Earth of Space Transmission	
		Day	**Night**
Range (Statute Miles)	R	Variable	Variable
Wavelength Received (Å)	λ	6328	
Transmitted Power (Watts)	P	0.1	
Transmitted Beam Divergence (Radians)	α_t	$1.22 \frac{\lambda}{D_t}$	
Diameter of Transmitting Aperture (CM)	D_t	Variable	
Diameter of Receiving Aperture (CM)	D_R	1000	
Receiver Field of View (Radians)	α_R	9.7×10^{-5} (20 Arc-Sec)	
Atmospheric Transmission (60° From the Zenith) (%)	τ_A	70	
Optical System Transmission (%)	τ_o	50	
Pre-Detection Filter Transmission (%)	τ_f	15	
Pre-Detection Filter Bandpass (Å)	Δ_λ	0.5	
Background Brightness Blue Sky at 6328Å $\frac{\text{Watts}}{\text{CM}^2\text{-Ster-}\mu}$	$N_{\lambda B}$	5.0×10^{-3}	0
Background Brightness Earthshine at 8400Å $\frac{\text{Watts}}{\text{CM}^2\text{-Ster-}\mu}$	$N_{\lambda E}$	—	
Background Brightness Average Starfield Toward Ecliptic Plane $\frac{\text{Watts}}{\text{CM}^2\text{-Ster-}\mu}$	$N_{\lambda S}$	3.3×10^{-10}	
Receiving Photomultiplier Tube		RCA 7265	
Dark Current Radiant Input Power Equiv. at -70°C (Watts)	$P_{d_{-70°C}}$	2.0×10^{-15}	
PMT Quantum Efficiency (%)	ϵ	Variable	

A PCM-PL system operating at a particular fixed error rate, R, is character-
ized by a single value of B corresponding to each value of S. Therefore,
when values of n_{es} and n_{en} are given, a particular sample period T exists
which leads to simultaneous values of S and B corresponding to the desired
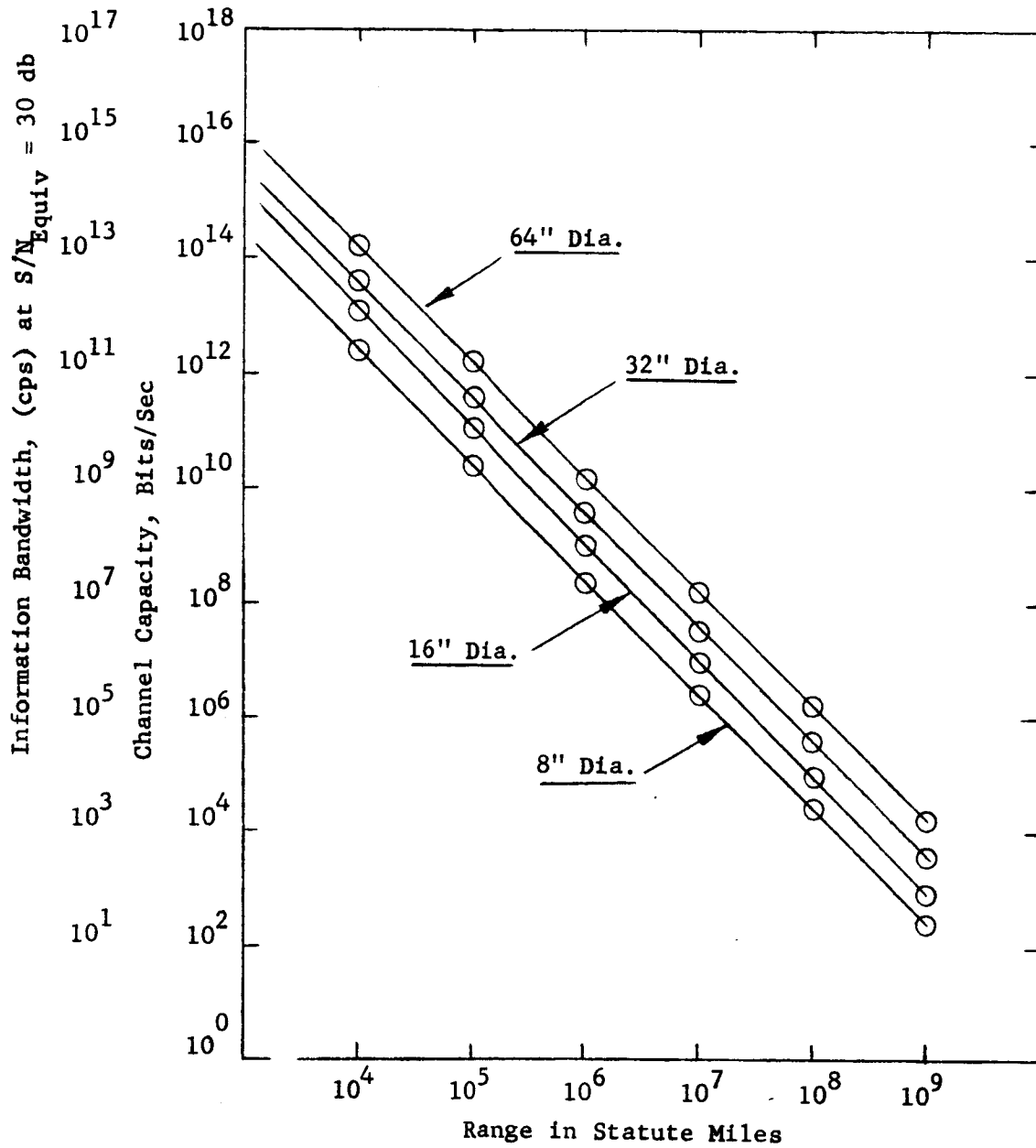error rate.

An error rate of 10^{-3} has been chosen for these calculations.
The basis used in arriving at this value was the examination of simulated
space photographs which had been transmitted utilizing a PCM system.   Var-
ious bit error rates had been artificially created in order to determine the
effect on TV image quality. Judging from these JPL photographs an error rate
of 1 in 300 lead to an acceptable image. In order to be conservative, an er-
ror rate better than this or equal to 1 in 1000 was chosen for the computer
runs. Necessarily, any judgment of acceptable pictorial quality with video
reproduction must be somewhat subjective.

Figure 5-1 and 5-2 show nighttime performance (quantum efficiency =8%
and 100% respectively). Channel capacity falls off linearly with range when both
are plotted logarithmically. This behavior is clear when one considers that
Equation 1 reduces to:

$$C = 5/T \tag{5}$$

when $R = 10^{-3}$

Parametric families of curves relating S, B and error rate R, were presented
as Figure 8-6 in the Phase I Report for a 5 bit system. From these curves,
S equals 31 and B equals 0 for $R = 10^{-3}$. At night, calculations show that
$n_{eb} \ll n_{es}$. Thus, from Equation 4 , B is approximately 0 for S equals 31, sat-
isfying the conditions for $R = 10^{-3}$. Equation 5 may be written therefore as

5-4

Figure 5-1.   Earth Reception of Space Transmission

Notes: Photomultiplier Quantum Efficiency = 8%

Error Rate Per Bit = 10^{-3}

Nighttime On Earth

See Table 5-1 for System Parameters.

Figure 5-2.   Earth Reception of Space Transmission
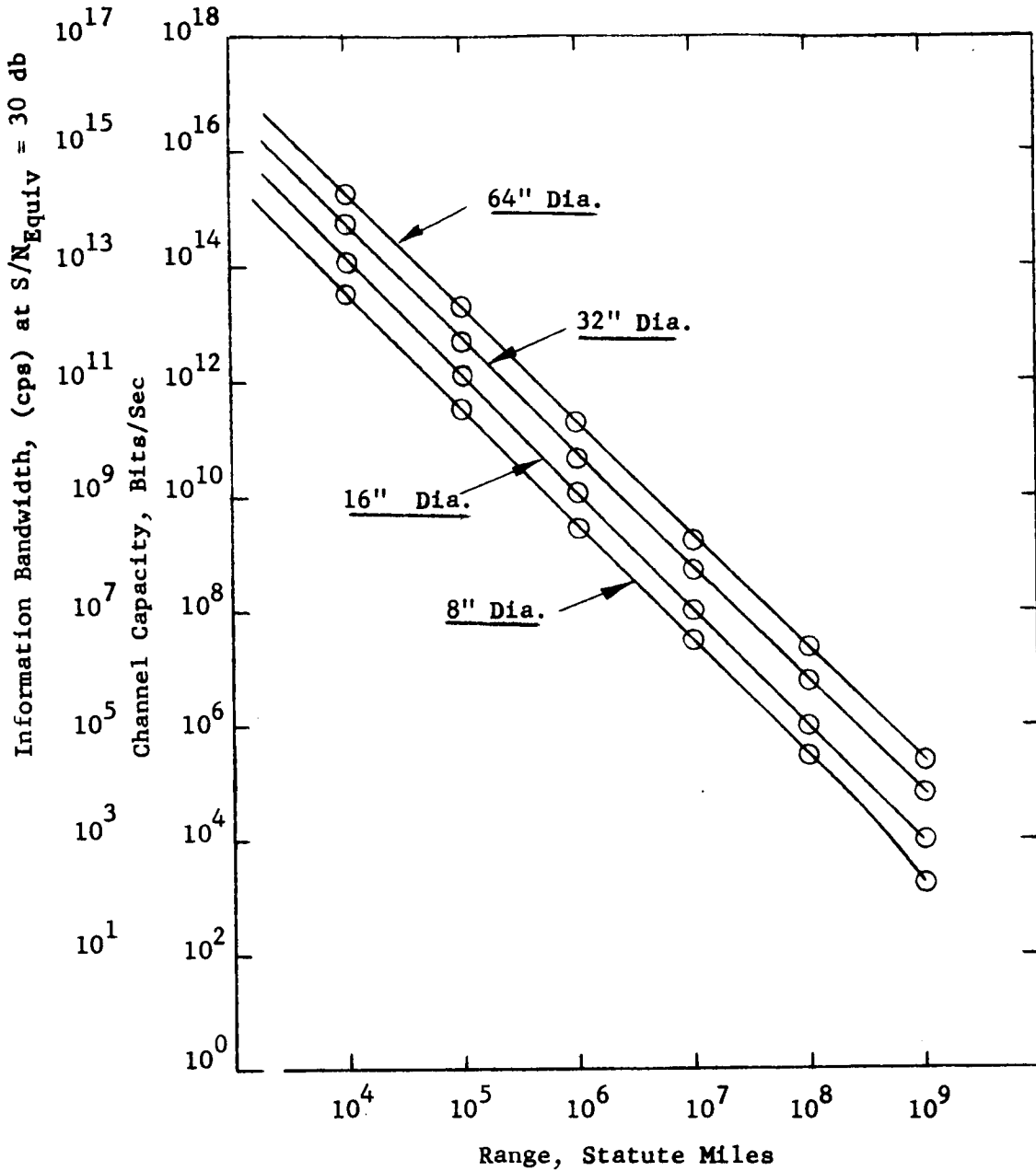
Notes: Photomultiplier Quantum Efficiency = 100%

Error Rate Per Bit = 10^{-3}

Nighttime On Earth

See Table 5-1 for System Parameters.

$$C \cong \frac{5}{31} \times n_{es} \qquad (6)$$

Since n_{es} varies inversely with the second power of range, it follows that channel capacity does also, as long as the signal is considerably greater than the noise which is the case at night. Each diameter considered is just twice the smaller one. Therefore, at each particular range the channel capacity for each diameter is four times as great as for the next smaller diameter since n_{es} is proportional to the aperture area. Under these conditions, channel capacity is simply related to information bandwidth since

$$T = 1/2F \max \qquad (7)$$

and therefore since

$$C \cong 5/T, \qquad (5)$$

$$F \max = C/10. \qquad (8)$$

Based on these simplifications, bandwidth in CPS is numerically ~10 percent of the channel capacity in bits/second.

The numerical results show that a synchronous satellite transmitting a 0.1 watt diffraction limited beam with an 8 inch aperture would be capable of sending about 10^{12} bits per second at the assumed error rate of 10^{-3} per bit. A 64-inch system would be capable of 6.4×10^{13} bits per second. It is clear that at the synchronous satellite distance equal to 2.2×10^{4} miles even an 8 inch diameter system leads to the channel capacity and information value far in excess of present communications requirements. Clearly, large aperture systems would be unnecessary for close range communications requirements.

However, at 10^{8} miles, an 8 inch diameter transmitting aperture would

permit a channel capacity of only 25,000 bits per second which is clearly in-
adequate for the high channel capacity requirements of real time planetary
reconnaissance. The 64-inch aperture system would be characterized by a
channel capacity equal to 1.6×10^6 bits/sec. This would permit the direct
transmission of slow scan TV or data compressed real time TV.

The daytime performance is identical to that shown in Figures 5-1
and 5-2 out to a range of 10^7 miles. At ranges greater than 10^7, the ratio,
n_{en}/n_{es}, is no longer small since n_{en} is constant and several orders of magni-
tude larger than at night. At ranges beyond 10^7 miles, the computer must be
used to determine the sample period which will produce an error rate of 10^{-3}.
A double series is very slowly convergent in the region of low signal to noise
ratio, and extensive computer time is required to calculate the daytime per-
formance curves. Thus daytime performance curves are not included for these
parameters.

5.2 CHANNEL CAPACITY FOR FIXED BANDWIDTH (See Figures 5-3 through 5-8).

The error rate per bit and the channel capacity change as the
range increases for different aperture systems. A fixed information bandwidth
of 1 megacycle was assumed. Referring to Figure 5-3, for the nighttime case
when the quantum efficiency equals unity, the channel capacity is equal to
10^7 bits per second out to some critical range, after which it drops rapidly.
The error rate (labeled next to each plotted point) increases rapidly after the
channel capacity begins to decrease.
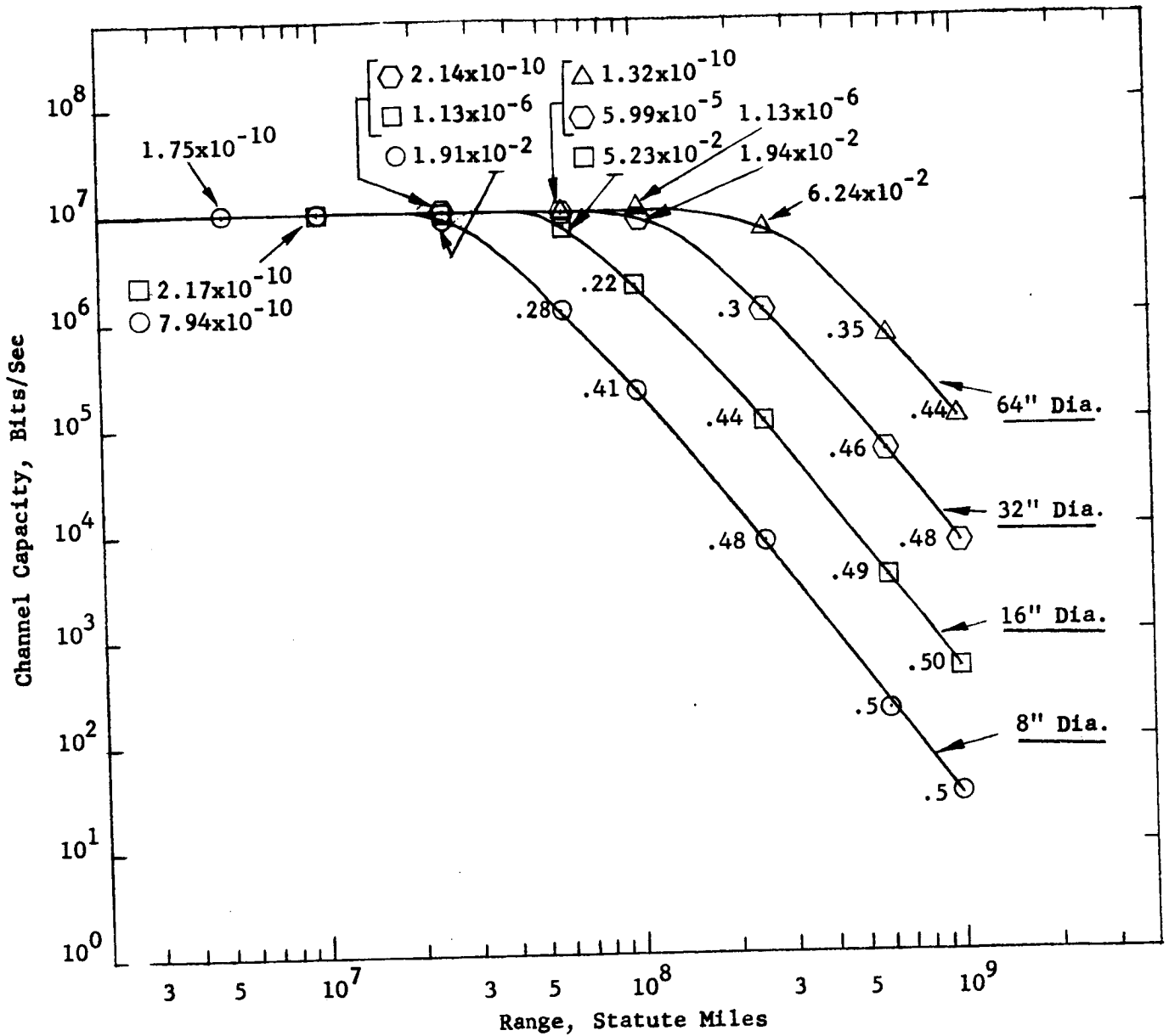
Figure 5-3. Earth Reception of Space Transmission
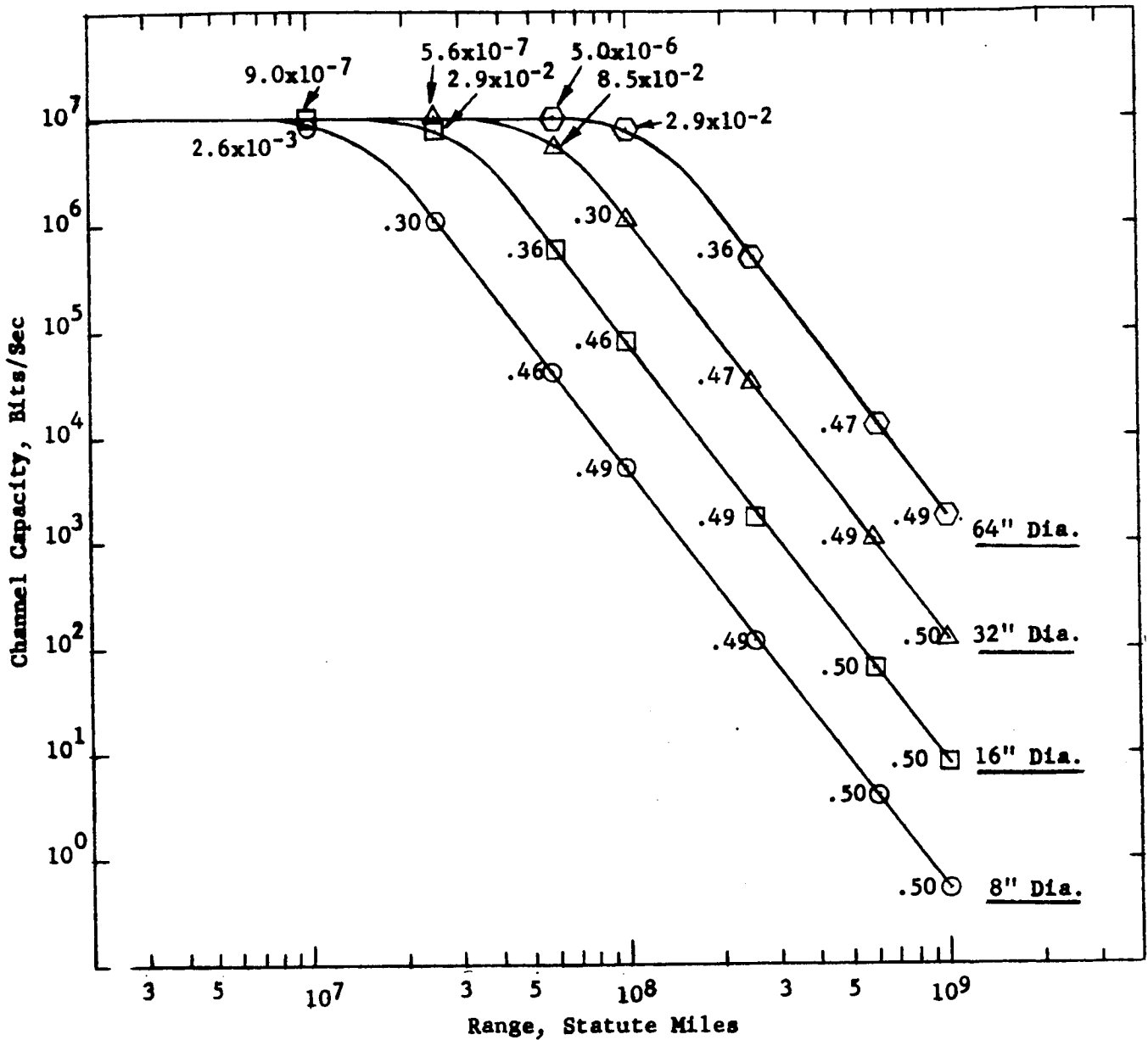
Notes: Photomultiplier Quantum Efficiency = 100%

Nyquist Period = 5×10^{-7} sec , 5 Bit Code

Nighttime on Earth.

See Table 5-1 for System Parameters.

The Number Shown at Each Calculated Point is the

Error Rate per Bit

Figure 5-4.   Earth Reception of Space Transmission

Notes: Photomultiplier Quantum Efficiency = 100%

Nyquist Period = 5 x 10^{-7} sec, 5 Bit Code

Daytime on Earth.

See Table 5-1 for System Parameters.

The Number Shown at Each Calculated Point is the

Error Rate per Bit.

Figure 5-5.   Earth Reception of Space Transmission

Notes: Photomultiplier Quantum Efficiency = 8%

Nyquist Period = 5 x 10^{-7} sec, 5 Bit Code

Nighttime On Earth

See Table 5-1 for System Parameters.

The Number Shown at Each Calculated Point is the

Error Rate Per Bit.

Figure 5-6. Earth Reception of Space Transmission

Notes: Photomultiplier Quantum Efficiency = 8%

Nyquist Period = 5×10^{-7} sec., 5 Bit Code

Daytime On Earth

See Table 5-1 for System Parameters.

The Number Shown at Each Point is the

Error Rate Per Bit

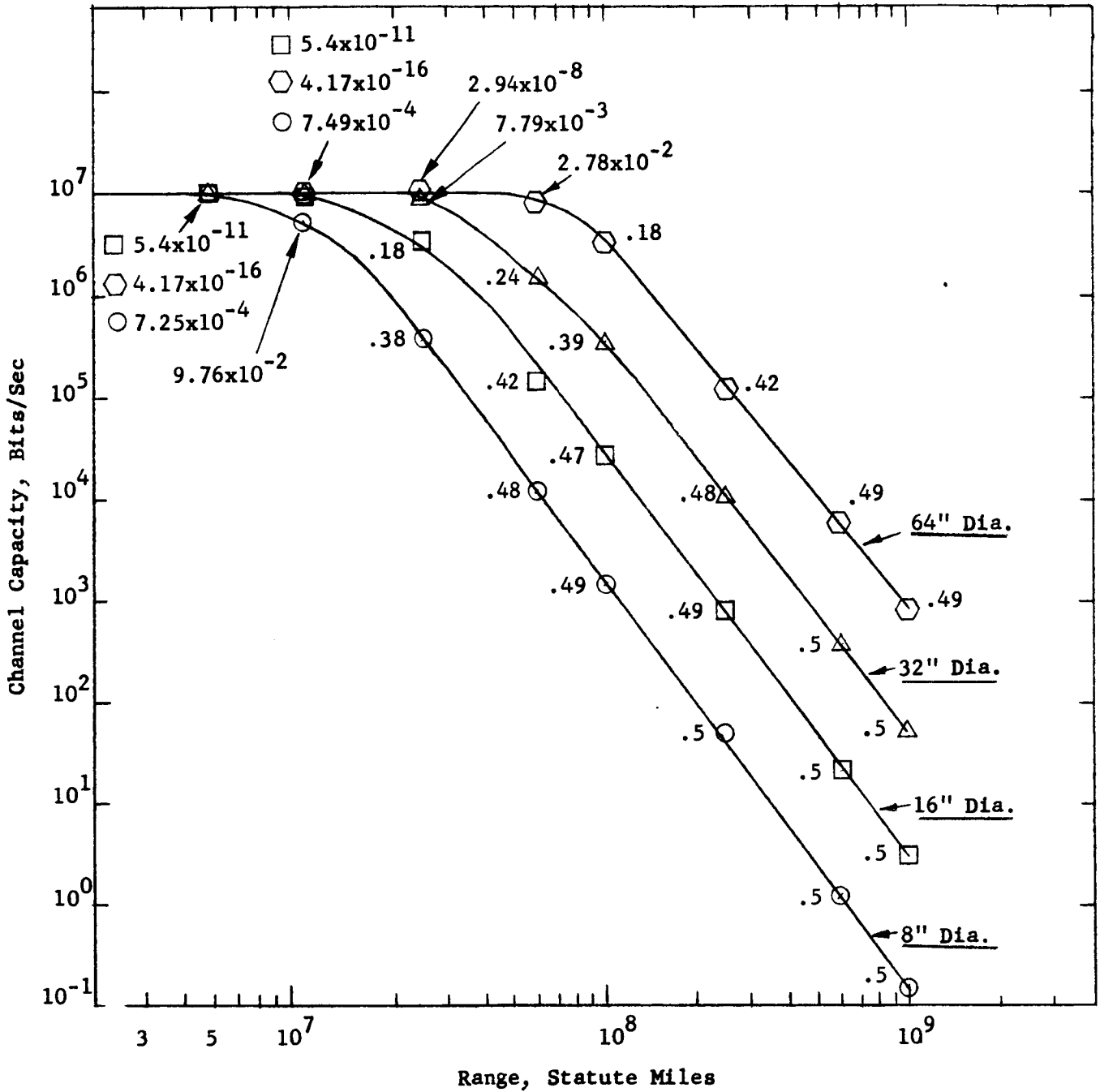Figure 5-7. Earth Reception of Space Transmission
(Expansion of Figure 5-5)
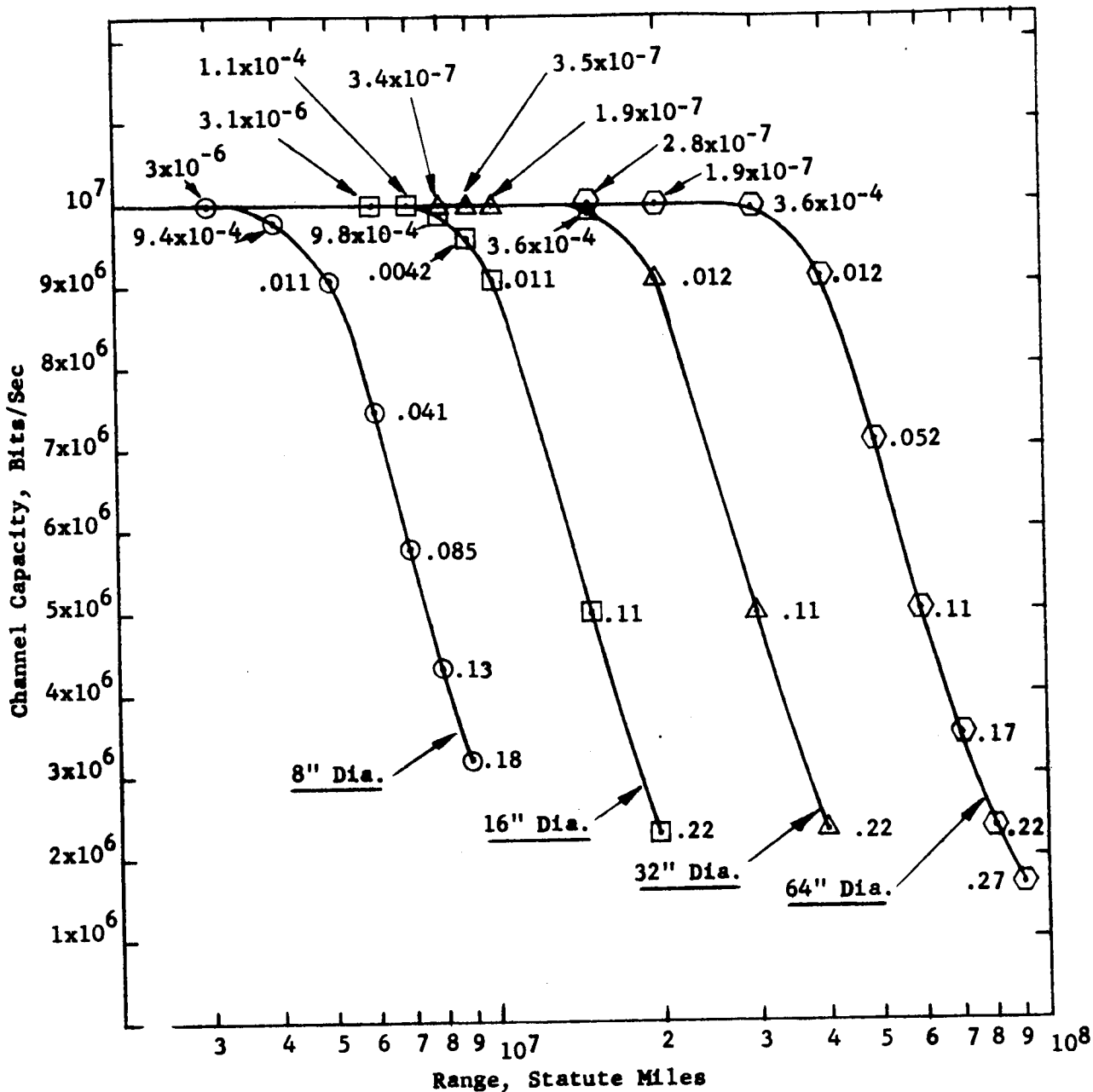
Notes: Photomultiplier Quantum Efficiency = 8%

Nyquist Period = 5×10^{-7} sec, 5 Bit Code

Nighttime On Earth

See Table 5-1 for System Parameters

The Number Shown at Each Calculated Point is the
Error Rate Per Bit
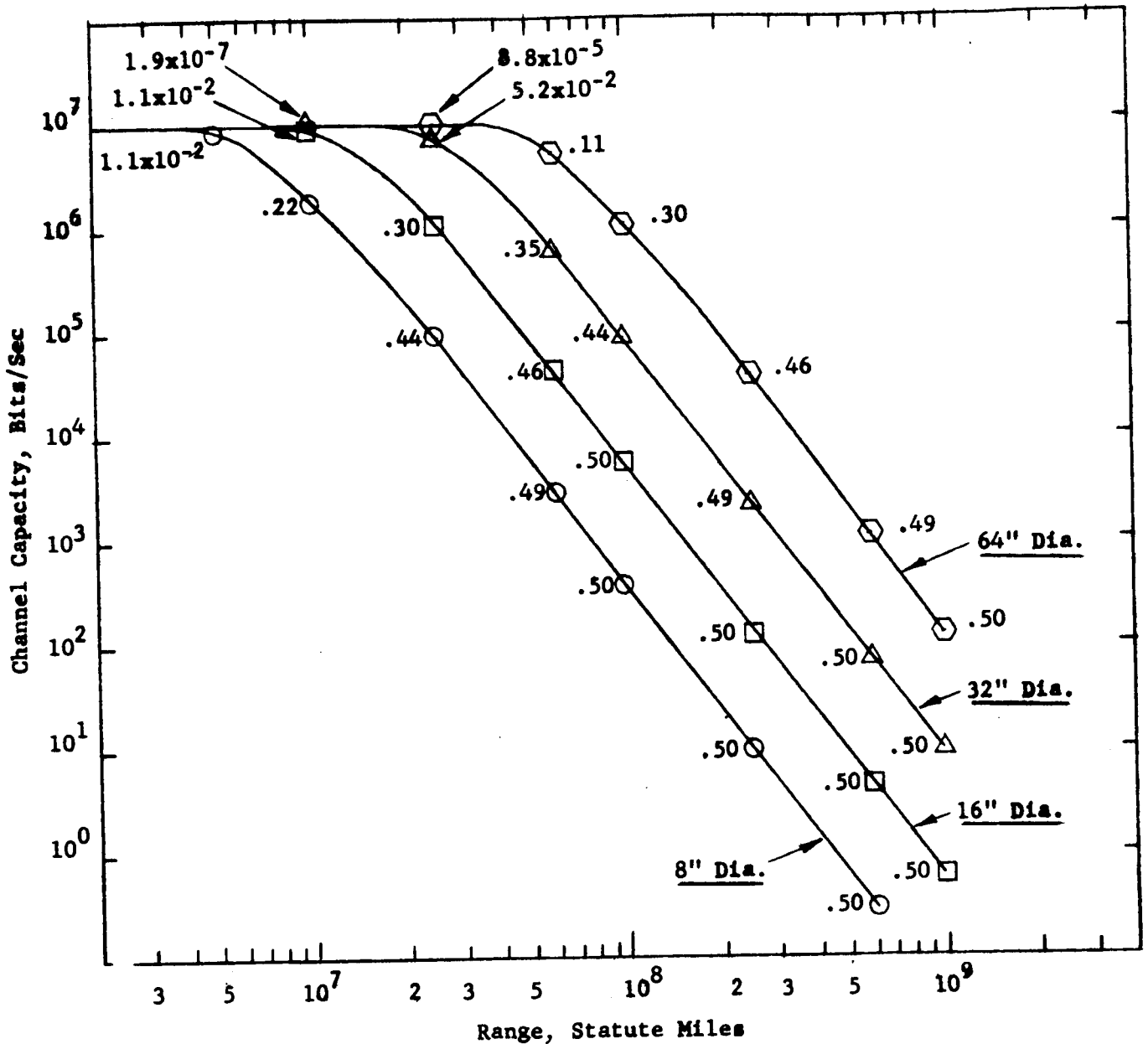
Figure 5-8. Earth Reception of Space Transmission
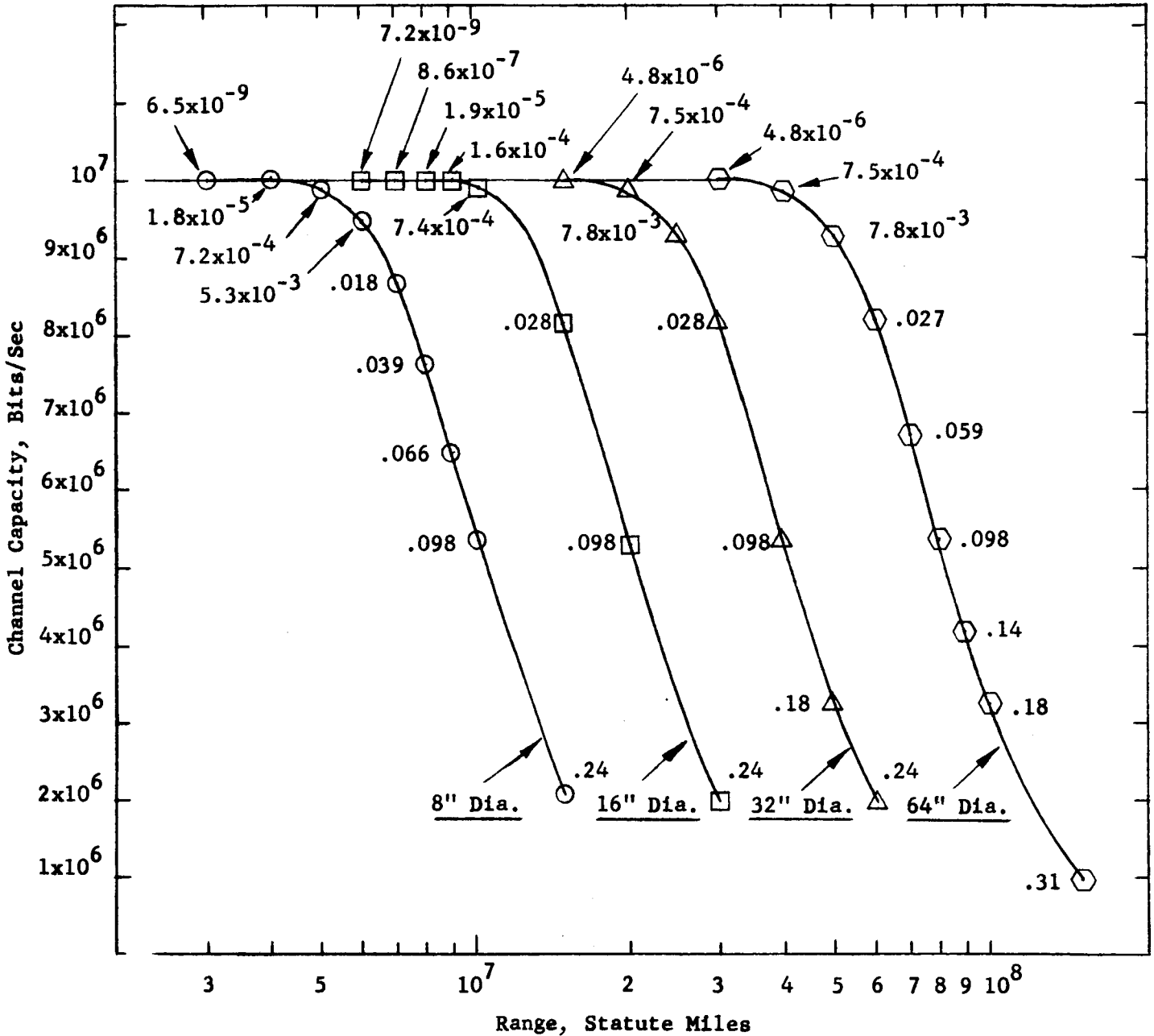(Expansion of Figure 5-6)

Notes: Photomultiplier Quantum Efficiency = 8%

Nyquist Period = 5×10^{-7} sec, 5 Bit Code

Daytime on Earth

See Table 5-1 for System Parameters

The Number Shown at Each Calculated Point is the
   Error Rate per Bit.

The shape of the channel capacity curve for the low error rate (less than 10^{-3}) is well approximated by Equation 5 on page 5-4. However, as soon as the error increases beyond 10^{-3}, the second term on the right side of Equation 1 on page 5-2, which is negative, becomes significantly large and channel capacity falls rapidly.

Thus, the maximum range at which high bandwidth communications are practical is sharply defined as shown by the break in the curves.

Figure 5-7 and 5-8 are expansions of Figure 5-5 and 5-6 in the region of interest (where channel capacity begins to drop and error rate increases).

SECTION VI

REFERENCES

[1] Determination of Optical Technology Experiments for a Satellite - Phase I Report, Engineering Report No. 7846. Norwalk: Perkin-Elmer Corporation, November 1964.

[2] Tatarski, V.I., Wave Propagation in a Turbulent Medium. New York: McGraw Hill Book Co., 1961.

[3] Reiger, S.H., Atmospheric Turbulence and the Scintillation of Starlight, Report No. R-406-PR. Santa Monica: The Rand Corporation, September 1962.

[4] Optical Space Communication System Study - Final Report, NASA Report No. CR-53466. Philadelphia: Missile and Space Division, General Electric Co., 1964.

[5] Ross, Monte. "Optical Receiving Devices," Electro-Technology. April 1964.

[6] McMurtry, B.J., Research on Techniques for Light Modulation. AD-284453.

APPENDIX A

ACQUISITION CONSIDERATIONS

APPENDIX A

ACQUISITION CONSIDERATIONS

We will assume that the deep-space vehicle has been detected by the earth terminal in the sense that all that is known is that the vehicle is more likely to be at certain point 0 than at any other point in the search region, but the vehicle may not be at 0 but only within an error circle at 0, all points at the same separation r from 0 being equally likely, and the probability falling rapidly to a ·negligible value as the angular separation r increases. This mode of initial acquisition can occur when the ground terminal is floodlighting the deep-space vehicle, and has computed trajectory data at its disposal.

Let p(r)dA denote the probability that the vehicle be in the region dA, an angular separation r from point 0. A circular normal probability density will be assumed as an approximation to the desired density function. It is further assumed that p(r) is proportional to $\exp(-r^2/2\,\sigma^2)$ where the constant of proportionality is determined by the realization that since the target is surely somewhere, the integral $\iint p(r)dA$ extended over the whole surface has the value unity.

The form of the probability density will then be equal to

$$p(r) = \frac{1}{2\pi\,\sigma^2} \exp\left(-r^2/2\,\sigma^2\right)$$

where the standard deviation σ increases the more the graph of p(r) is spread out, i.e., the more indefinite the knowledge of the deep-spaced vehicles' position.

We will now suppose that t minutes have elapsed after the time of
the observation. The deep-space vehicle will have moved along its trajectory
and the distribution will no longer be the same. Again from computed trajec-
tory information, assume that the angular rate of the vehicle can be estimated
with satisfactory accuracy, but not its direction. The magnitude of $\vec{\omega_v}$ is
known but not ϕ, where ϕ is the angular direction. We will further assume
that all directions are equally likely and are independent of the actual
position of the target. This assumption could be questioned since the direc-
tion of the deep-space vehicle will be known to lie in some smaller uncertainty
region. However, to obtain an approximation to the actual case this simpli-
fying assumption will be used. The new probability density function $p(r,t)$
after t minutes is now required.

Refer to Figure 1 for a sketch of the pertinent geometry.
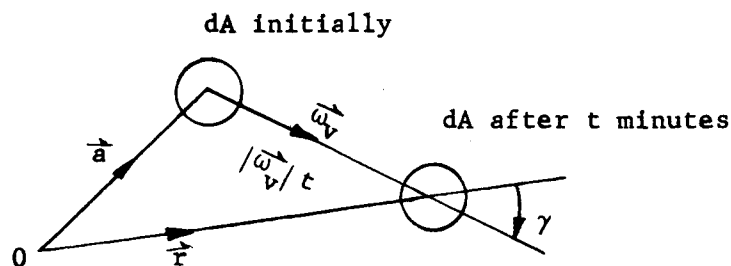
Figure A-1 Acquisition Geometry

Here we have considered the case of the vehicle whose $\vec{\omega_v}$ makes a
given angle γ with the direction from 0 to the contemplated position. The
angle γ is measured from vector $\vec{r}$ to vector $\vec{\omega_v}$. The vehicle will be in the
area dA if and only if it had initially been in a region congruent to dA
and situated $|\vec{\omega_v}|t$ away in the direction of the reversed vector $-\vec{\omega_v}$.

A-3

The probability of this event is:

$$\frac{1}{2\pi\sigma^2}\exp(-a^2/2\sigma^2)dA = \frac{1}{2\pi\sigma^2}\exp\left(-\frac{[r^2+|\vec{\omega_v}|^2t^2-2r|\vec{\omega_v}|t\cos\gamma]}{2\sigma^2}\right)dA$$

The probability that $\vec{\omega_v}$ makes an angle with $\vec{r}$ between γ and $\gamma + d\gamma$ is $d\gamma/2\pi$.
The probability of both these events is the product of these two probabilities,
and to obtain the required total probability $p(r,t)$ we must integrate over
all possible initial positions of dA, i.e., over all values of γ from 0 to
2π.

$$p(r,t) = \frac{1}{2\pi\sigma^2}\cdot\frac{1}{2\pi}\int_0^{2\pi}\exp\left(-\frac{[r^2+|\vec{\omega_v}|^2t^2-2r|\vec{\omega_v}|t\cos\gamma]}{2\sigma^2}\right)d\gamma$$

$$= \frac{1}{2\pi\sigma^2}\exp\left(-\frac{[r^2+|\vec{\omega_v}|^2t^2]}{2\sigma^2}\right)\cdot\frac{1}{2\pi}\int_0^{2\pi}\exp\left(\frac{2r|\vec{\omega_v}|t\cos\gamma}{2}\right)d\gamma$$

But $\frac{1}{2\pi}\int_0^{2\pi}\exp\left(\frac{r|\vec{\omega_v}|t}{\sigma^2}\cos\gamma\right)d\gamma = \frac{1}{2\pi}\int_0^{2\pi}\exp\left(-\frac{[r|\vec{\omega_v}|t\cos\gamma]}{\sigma^2}\right)d\gamma$

$$= \frac{1}{2\pi}\int_0^{2\pi}\exp\left(i\frac{[i\,r|\vec{\omega_v}|t\cos\gamma]}{\sigma^2}\right)d\gamma$$

$$= J_0\left(ir|\vec{\omega_v}|t/\sigma^2\right) = I_0\left(r|\vec{\omega_v}|t/\sigma^2\right)$$

where Jo denotes the ordinary Bessel function of zeroth order, and Io its
value for pure imaginary values of the argument. Therefore the probability
density function is equal to:

$$p(r,t) = \frac{1}{2\pi\sigma^2}\exp\left(-\frac{[r^2+|\vec{\omega_v}|^2t^2]}{2\sigma^2}\right)I_0\left(r|\vec{\omega_v}|t/\sigma^2\right)$$

Refer to Figure A-2 taken from Reference 1, for a plot of $2\pi \sigma^2 p(r,t)$ as a function of angular separation from an initial fix point with time as a parameter. The probability density spreads outward in r with time, so that the target is most likely to be in an expanding ring about 0. Since the peaks of the probability densities shift outward in r with increasing time it appears that one possible way of optimizing acquisition and tracking is to utilize an annular search pattern with the center of the annulus tracking the peak of the probability density. The cost of searching with an annular region instead of a circular one is that a greater received power is required to maintain a constant received power density since the annular area will be greater than the inner circular area.

The probabilistic model allows one to establish the parametric relationship between probability of containment of the deep space vehicle, elapsed time from the initial fix, angular velocity of the vehicle, rms vehicle angular uncertainty, and angular separation from the initial fix point.

The above probabilistic model although fraught with simplifying assumptions gives an indication of the type of analysis required to optimize the acquisition process.

In comparing various deep-space laser acquisition techniques it will also be necessary to determine the séarch or acquisition time required by the Earth and vehicle terminals to achieve a state of knowledge whereby the transmit-receive beams of both terminals are pointed in the required directions, signals are mutually recognized and the communication
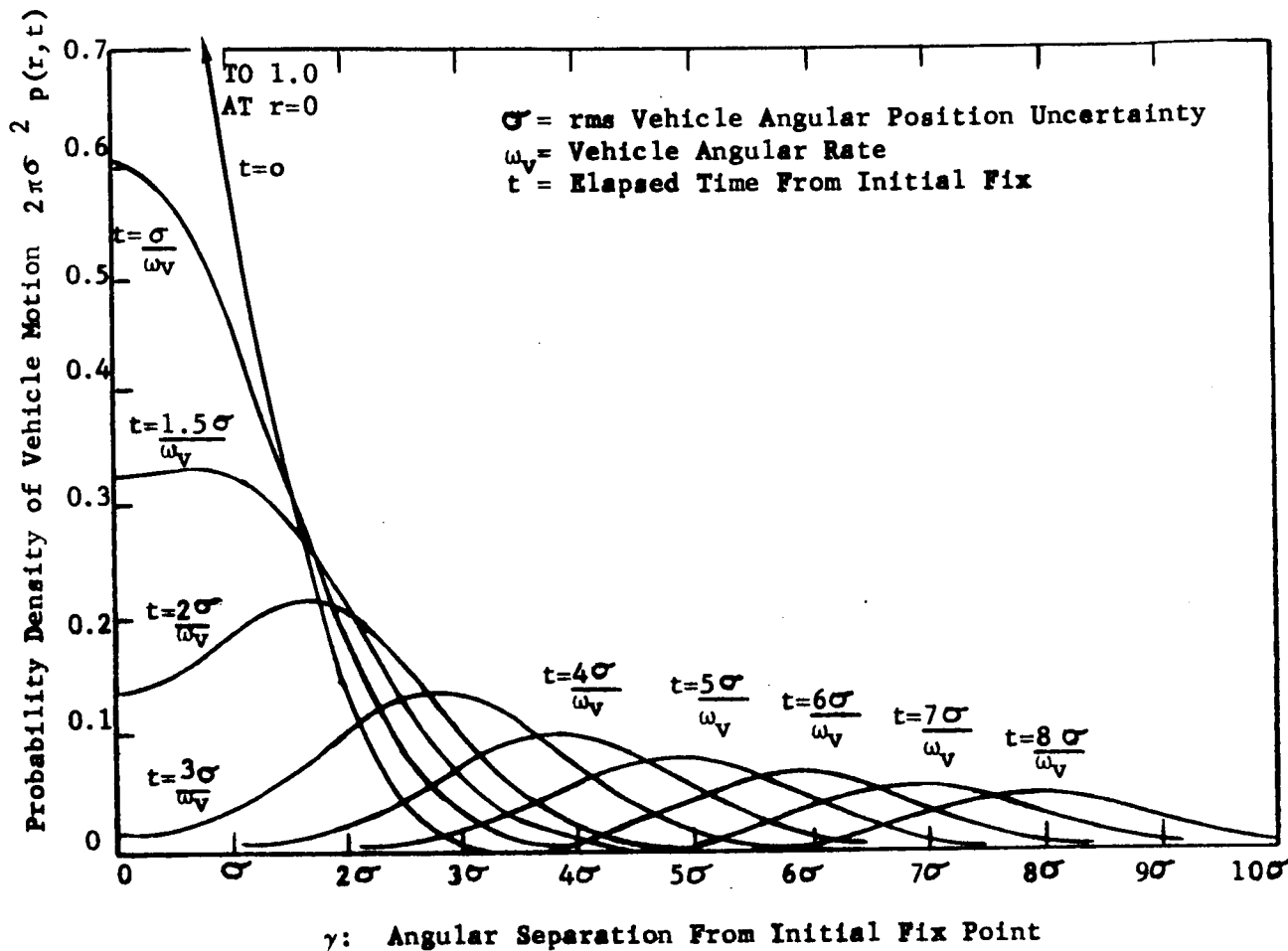
Figure A-2. Probability Densities of Deep Space Vehicle About An Initial Fix Point

link is thereby established. Search time and the expenditure of search

effort are especially at a premium for the deep-space case where one way

transit times are of the order of 7 to 10 minutes.

The establishment of a high capacity communication link between

two distant transmit-receive terminals (separation distances of the order of

10^8 miles), each having narrow beamwidths and specified uncertainty as to

relative angular locations makes it necessary to take into account any

change or relative angular uncertainty due to any motion of the Earth or

vehicle terminals as well as light aberration effects during the acquisition

time. The solid angle to be searched is not invariant during the acquisition

time. Also the propagation time delay between both terminals is quite large

in comparison to the least time spent per beam position during the acquisition

phase.

Since the narrow beam communication acquisition problem is a

statistical one in nature it is suggested that such mathematical techniques

as Markov chain concepts be employed to derive the equations for the expected

acquisition time and standard deviation of the acquisition time in terms of

such system parameters as relative angular uncertainty, beamwidth, atmospheric

caused angular jitter, pointing accuracy, probability of detection of a

tracking signature in noise, false alarm probability, etc.[2] The optimization

of search effort and system performance for various acquisition schemes can

then be assessed.

REFERENCES

[1] Koopman, B.O., "The Theory of Search, Part I, Kinematic Bases," Journal of the Operations Research Society of America, June 1956.

[2] Greenberg, J.S., "On the Narrow Beam Communication Systems Acquisition Problem," IEEE Transactions on Military Electronics, January 1964.

PERKIN-ELMER

APPENDIX B

DETERMINATION OF ROTATION ABOUT THE LINE OF SIGHT BY POLARIZATION AND DIRECTION

APPENDIX B

DETERMINATION OF ROTATION ABOUT THE
LINE OF SIGHT BY POLARIZATION AND DIRECTION

METHODS

This appendix contains a derivation of the signal-to-noise ratio required for the optical determination of the orientation of a light source about an axis parallel to the line of sight.[1]

For this discussion, the signal shall be considered to be that generated by a 1 arc-minute rotational error. This appears to be a reasonable assumption if one considers a deep space vehicle positioned at a distance of R from the earth, a vehicle transmitter beamwidth of σ, and a point ahead angular magnitude requirement of ρ radians.

At the earth vehicle range, the point ahead angle is measured by a distance of ρR and similarly the beamwidth is equivalent to a distance of σR -- this is as shown in Figure B-1.
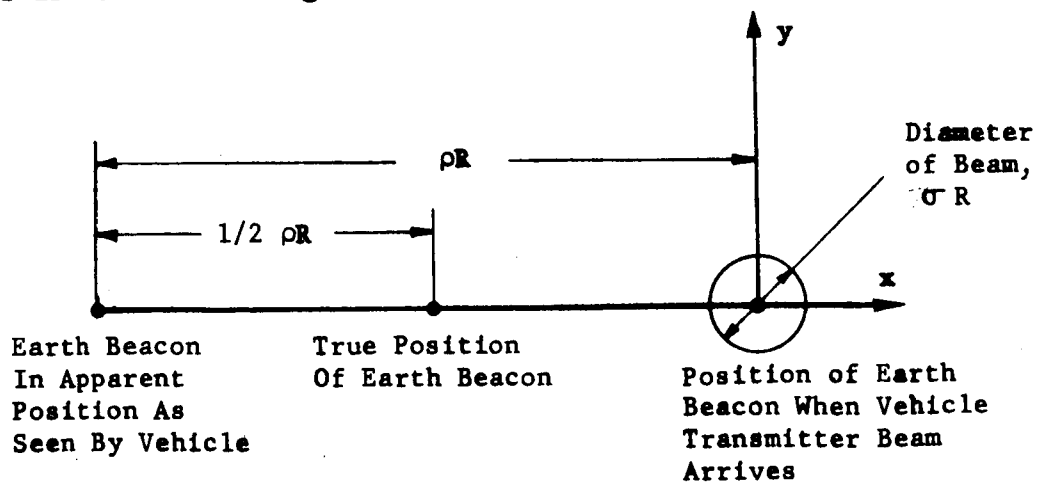
Figure B-1.

If some portion of the beam is to hit the beacon, and equal x any
y errors are allowed, then the offset magnitude of 36 $\widehat{sec}$ may be in error by
$\frac{\sigma R}{2\sqrt{2}} = \epsilon$ (or an angular magnitude error of $\frac{\sigma}{2\sqrt{\epsilon}}$)

Similarly, it is clear that some rotational error $\Delta\theta$ about the
line of sight will generate a y error which should be limited also to a distance
of $\frac{\sigma R}{2\sqrt{2}}$ (refer to Figure B-2).
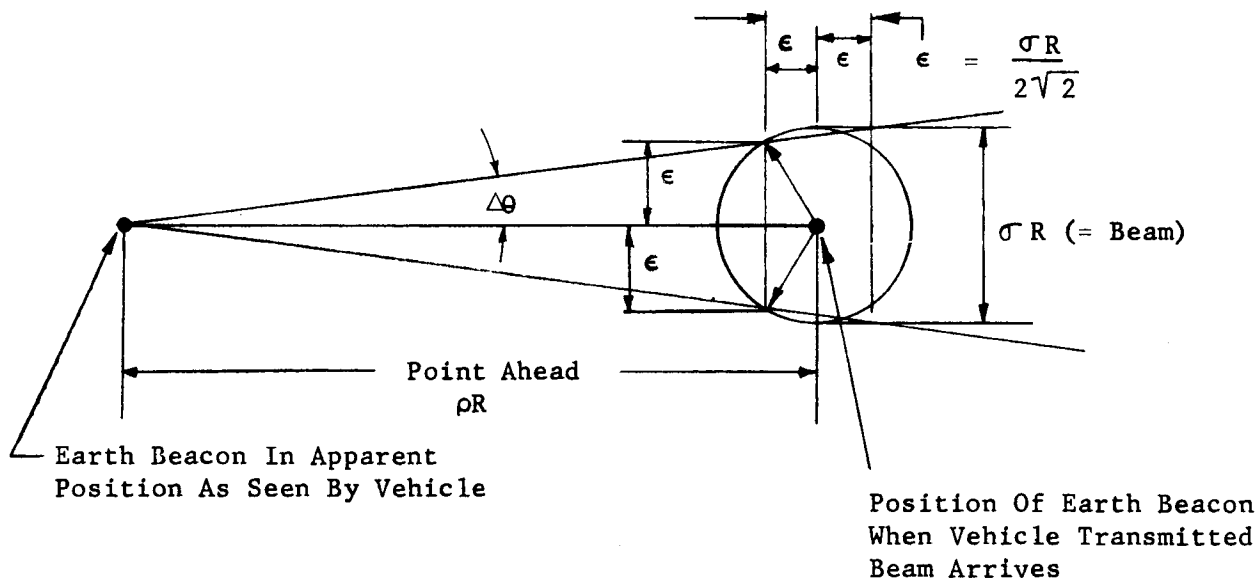
Figure B-2.

The maximum allowed value of $\Delta\theta$ is then closely equal to

$$\Delta\theta = \frac{\frac{\sigma R}{2\sqrt{2}}}{\rho R} = \frac{\sigma}{2\rho\sqrt{2}} \quad \text{radius}$$

Numerically for the OTS case,

$$\Delta\theta = \frac{0.1 \ \widehat{sec}}{2(36 \ \widehat{sec})\sqrt{2}} \times 57.3° = \underline{.0562°} = \underline{3.38 \ \widehat{min}}$$

B-3

for the case where

$$\sigma = .1 \widehat{\sec} \text{ and } \rho = 36 \widehat{\sec}.$$

These assumed values are considered appropriate for deep space considerations and, in addition, for the OTS experiments.

Two techniques for the optical determination of the orientation of a light source about an axis parallel to the line of sight are presented below.

1. Polarization Technique

The signal from the earth station beacon arriving at the vehicle is assumed to pass through a polarizer such as a calcite prism which has a fixed orientation with respect to the satellite structure. The polarizer is used to develop rotational references about the line of sight to the ground beacon. It will be assumed that the earth laser beacon beam which arrives at the vehicle telescope is plane polarized. Rotation about the line of sight will cause the signal received by the satellite to vary in intensity as a function of the angular rotation about the line of sight. In Figure B-3, a plane polarized earth laser beam of n_s photons per second enters a calcite prism and is split into two component beams, (ordinary and extraordinary rays). Background photons due to earthshine will accompany the signal beam and, in general, have a random state of polarization. Rotations about the line of sight of the incident signal beam causes intensity changes that are detected by two photomultipliers. The outputs of the two photomultipliers are subtracted by a difference signal ampli-fier and provide a control signal for the roll gimbal. A high degree of precision will be required for rotation about the line of sight for the point ahead of the transmit beam.
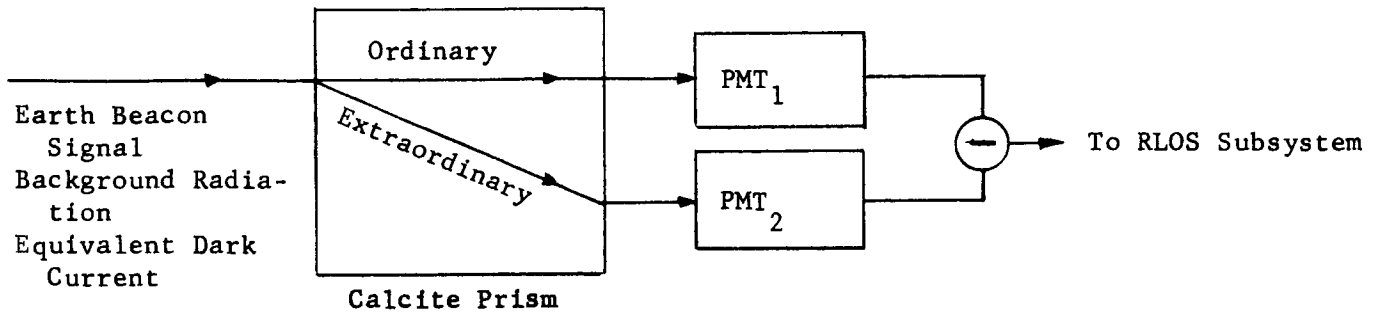
Figure B-3. Measurement of Rotation of Line of Sight
By Use of Polarized Light

The intensities of the exit beam from the calcite prism are:

$$n_s \cos^2\alpha + \frac{n_B}{2} + n_D \text{ for the ordinary channel, and}$$

$$n_s \sin^2\alpha + \frac{n_B}{2} + n_D \text{ for the extraordinary channel where:}$$

n_s = earth laser beacon photon arrival rate

n_B = background photon arrival rate

n_D = equivalent dark current arrival rate

α = angle between the principal plane of the calcite

crystal and the plane of polarization of the

incident signal beam.

A small rotation about the line of sight $\Delta\alpha$ of the incident earth laser beacon signal beam is detected by intensity changes of the two exit beams. These intensity changes are:

$-2 \, n_s \, \sin\alpha \, \cos\alpha \, \Delta\alpha$ for the ordinary channel

$+2 \, n_s \, \sin\alpha \, \cos\alpha \, \Delta\alpha$ for the extraordinary channel

To convert the intensity changes into number of photons we multiply the intensity changes by $1/2\Delta f$ where Δf is an electrical filter bandwidth in cycles per second. These number of photons are further multiplied by the quantum efficiency ϵ of the photodetector to obtain the number of photoelectrons. There will be $4 \, n_s \, \dfrac{\epsilon}{2\Delta f} \, \sin\alpha \, \cos\alpha \, \Delta\alpha = \dfrac{n_s \, \epsilon}{\Delta f} \sin 2\alpha \, \Delta\alpha$ signal photoelectrons at the output of the difference amplifier. The signal shot noise, the background noise contribution and the two detectors dark current noise produce an overall photoelectron uncertainty at the output of the difference amplifier or

$$\left[\frac{\epsilon}{2\Delta f} \left[\left(n_s \cos^2\alpha + \frac{n_B}{2} + n_D \right) + \left(n_s \sin^2\alpha + \frac{n_B}{2} + n_D \right) \right] \right]^{1/2}$$

which is equal to

$$\left[\frac{\epsilon}{2\Delta f} \left[n_s + n_B + 2n_D \right] \right]^{1/2}$$

The signal to noise ratio at the output of the difference amplifier is therefore:

$$\left. \frac{S}{N} \right]_{DIFF} = \Delta\alpha n_s \left[\frac{2\epsilon}{\Delta f \left[n_s + n_B + 2n_D \right]} \right]^{1/2}$$

where $\alpha = 45°$ maximizes S/N $\Big]_{DIFF}$

In terms of the respective incident powers, $\dfrac{S}{N}\Big]_{DIFF}$ may be expressed as:

$$\frac{S}{N}\Big]_{DIFF} = \Delta\alpha P_s \left[\frac{2\epsilon}{h\nu\,\Delta f\left[P_s + P_B + 2P_D\right]}\right]^{1/2}$$

Plots of RLOS signal to noise ratio versus range with low pass filter bandwidths (0.1, 1.0 and 10 cps) as a parameter are presented in Figure B-4 through B-10. The RLOS uncertainty $\Delta\alpha$ is taken at 1 arc-minute and the diameter of the satellite receiver aperture is set at 32 inches. The earth transmitter power is set at 200 watts, average. The earth transmitter beam divergence varies over the range 3, 5, and 10 arc-seconds. Also three values of quantum efficiency are chosen: $\epsilon = 0.0036$, 0.036 and 0.08.

One sees immediately that RLOS determination by this polarization technique at Martian ranges (10^8 miles), appears to be not feasible. However, performance at a tenth of this range (10^7 miles), may be possible with the narrow transmitter beam divergences and increased quantum efficiency and increased receiver aperture diameters. At synchronous satellite altitudes the polarization technique appears to be quite attractive. In any event, this method requires further investigation as the state of the art progresses.

2. Direction Method

Figure B-11 shows an alternate method whereby a small rotation angle change, $\Delta\beta$, of a distant source pair, (star and earth beacon) may be measured by a star tracker and telescope without the use of polarization methods. Assume

Diameter of Satellite Receiver = 32 inches
Transmitter Beam Divergence = 3 arc sec
Quantum Efficiency = 0.0036
RLOS Uncertainty = 1 arc minute
Refer to Table 8-2 of Phase I Report
    for Other System Parameters

$\Delta f = 0.1$ cps

$\Delta f = 1$ cps

$\Delta f = 10$ cps

RLOS Signal to Noise Ratio

Range in Millions of Statute Miles
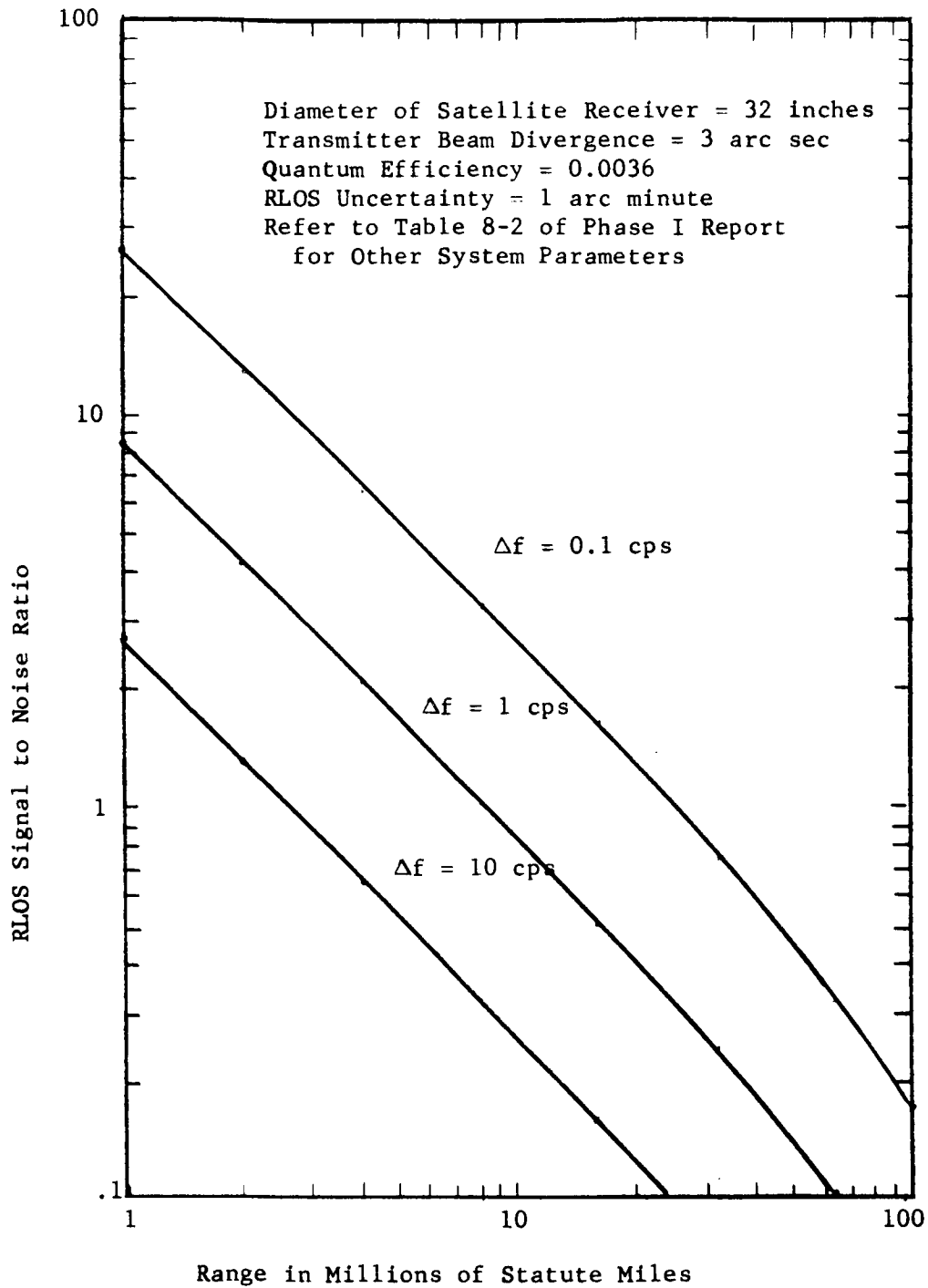
Figure B-4. RLOS Signal to Noise Ratio With Beam
            Divergence of 3 Arc Seconds

PERKIN-ELMER

Diameter of Satellite Receiver = 32 inches
Transmitter Beam Divergence = 5 arc seconds
Quantum Efficiency = 0.0036
RLOS Uncertainty = 1 arc minute
Refer to Table 8-2 of Phase I Report for
  Other System Parameters

Δf = 0.1 cps

Δf = 1 cps

Δf = 10 cps

Range in Millions of Statute Miles

Figure B-5. RLOS Signal to Noise Ratio with
              Beam Divergence of 5 Arc Seconds

Diameter of Satellite Receiver = 32 inches
Transmitter Beam Divergence = 10 arc seconds
Quantum Efficiency = 0.0036
RLOS Uncertainty = 1 arc minute
Refer to Table 8-2 of Phase I Report for
   Other System Parameters

Δf = 0.1 cps

Δf = 1 cps

Δf = 10 cps

RLOS Signal to Noise Ratio

Range in Millions of Statute Miles

Figure B-6. RLOS Signal to Noise Ratio with
   Beam Divergence of 10 Arc Seconds

Range in Millions of Statute Miles

Figure B-7. RLOS Signal to Noise Ratio With Beam
Divergence of 3 Arc Seconds

Diameter of Satellite Receiver = 32 inches
Transmitter Beam Divergence = 5 arc seconds
Quantum Efficiency = 0.036
RLOS Uncertainty = 1 arc minute

Δf = 0.1 cps

Δf = 1 cps

Δf = 10 cps

RLOS Signal to Noise Ratio
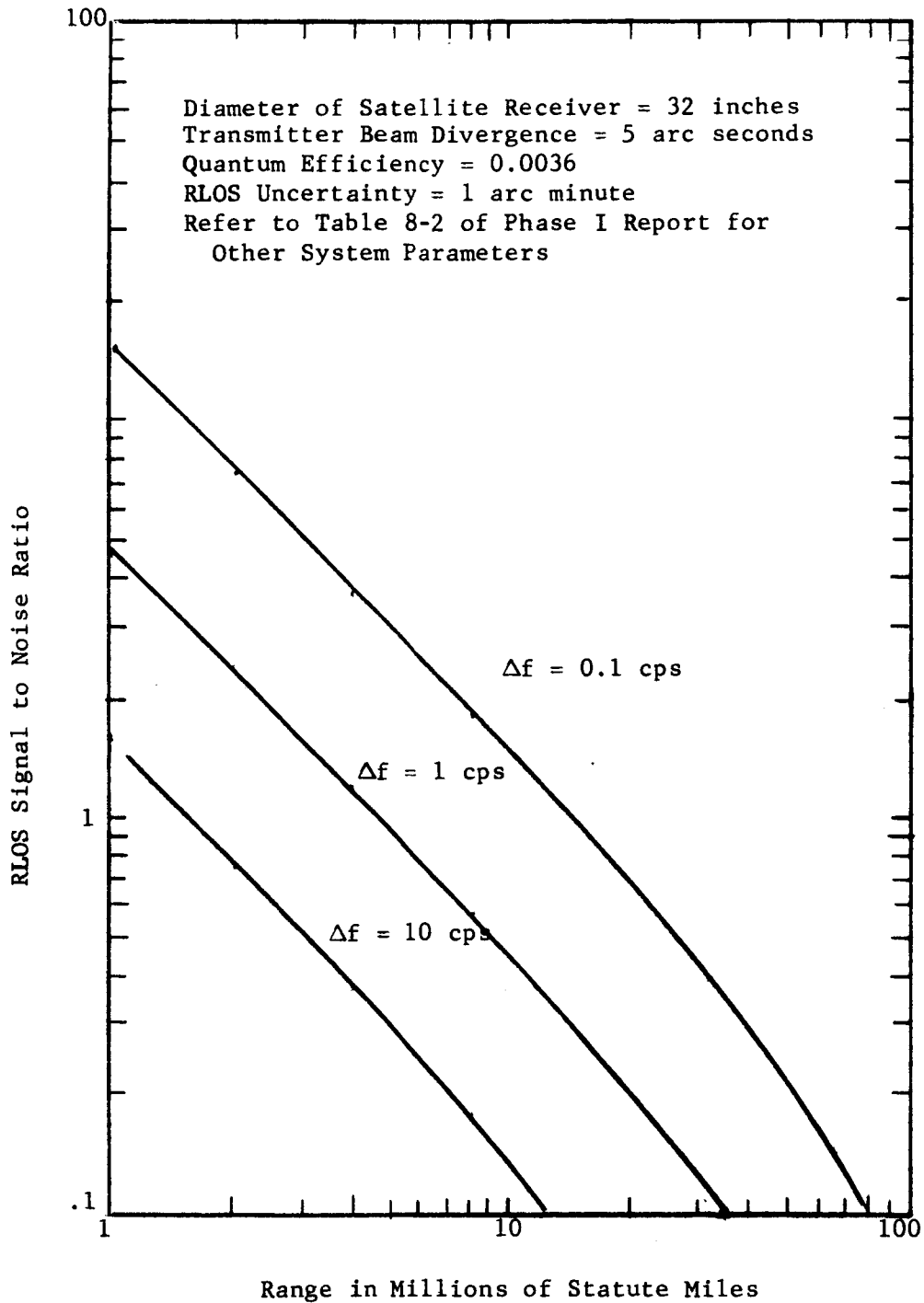
Range in Millions of Statute Miles

Figure B-8. RLOS Signal to Noise Ratio with
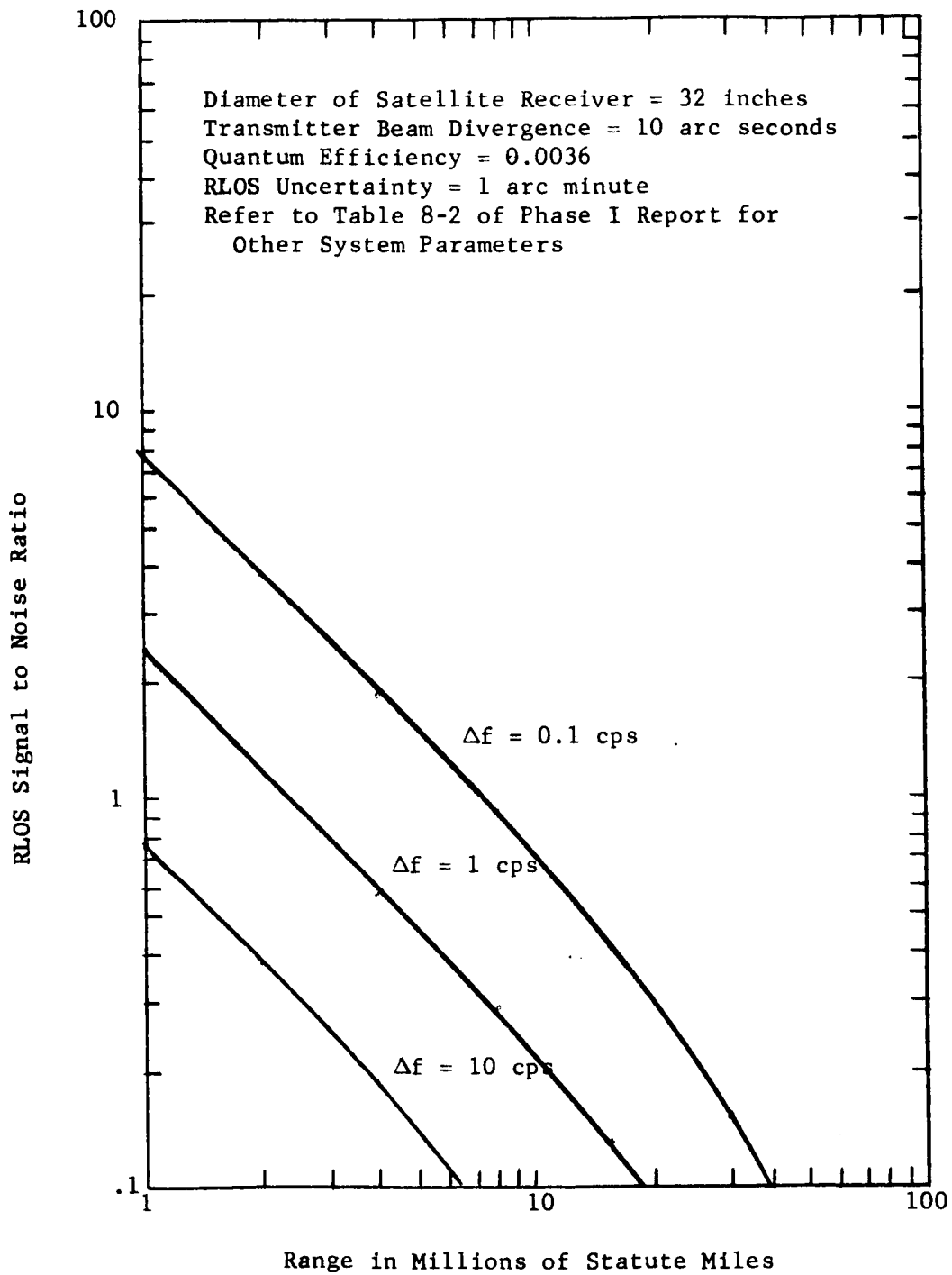Beam Divergence of 5 Arc Seconds
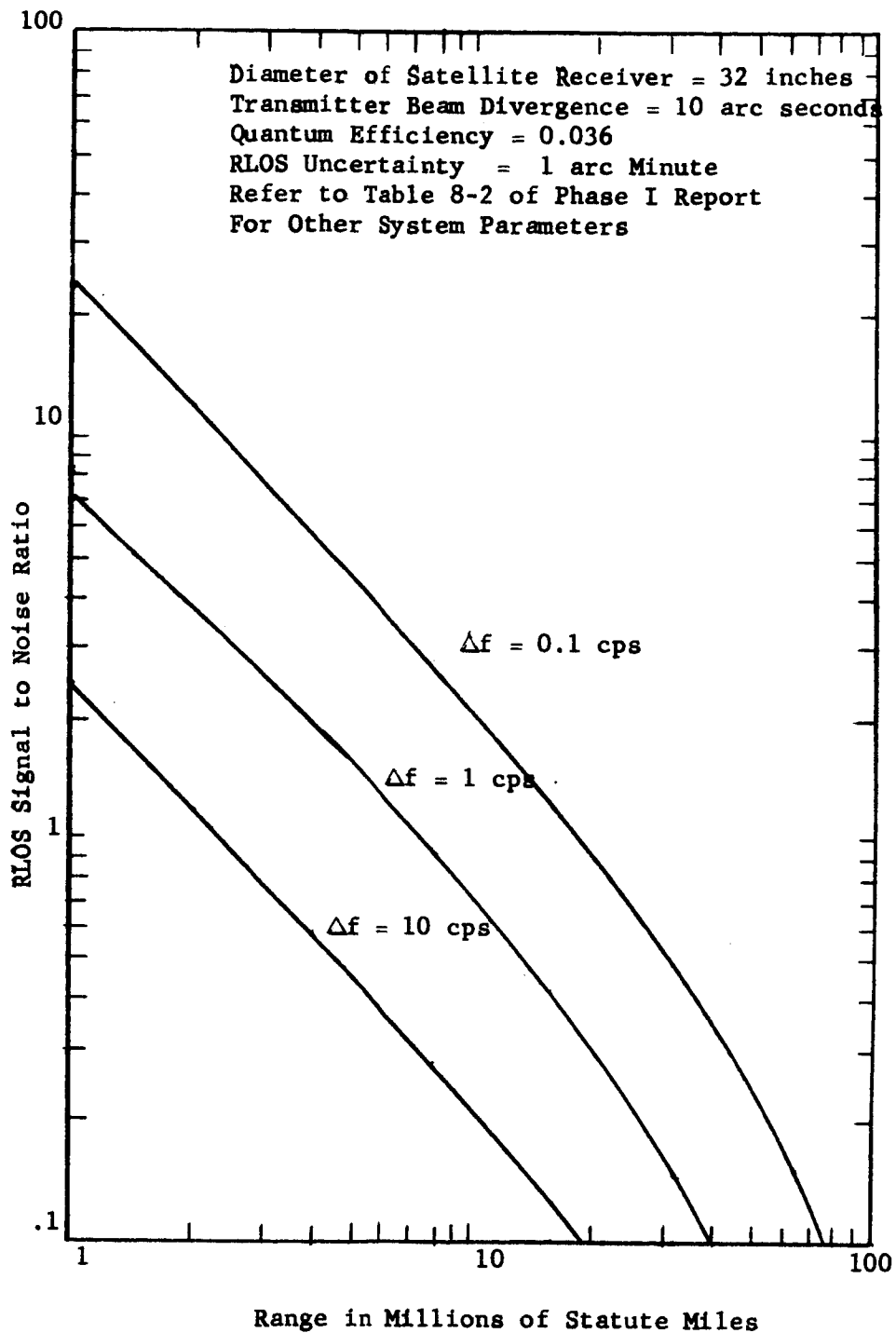
Figure B-9. RLOS Signal to Noise Ratio with Beam
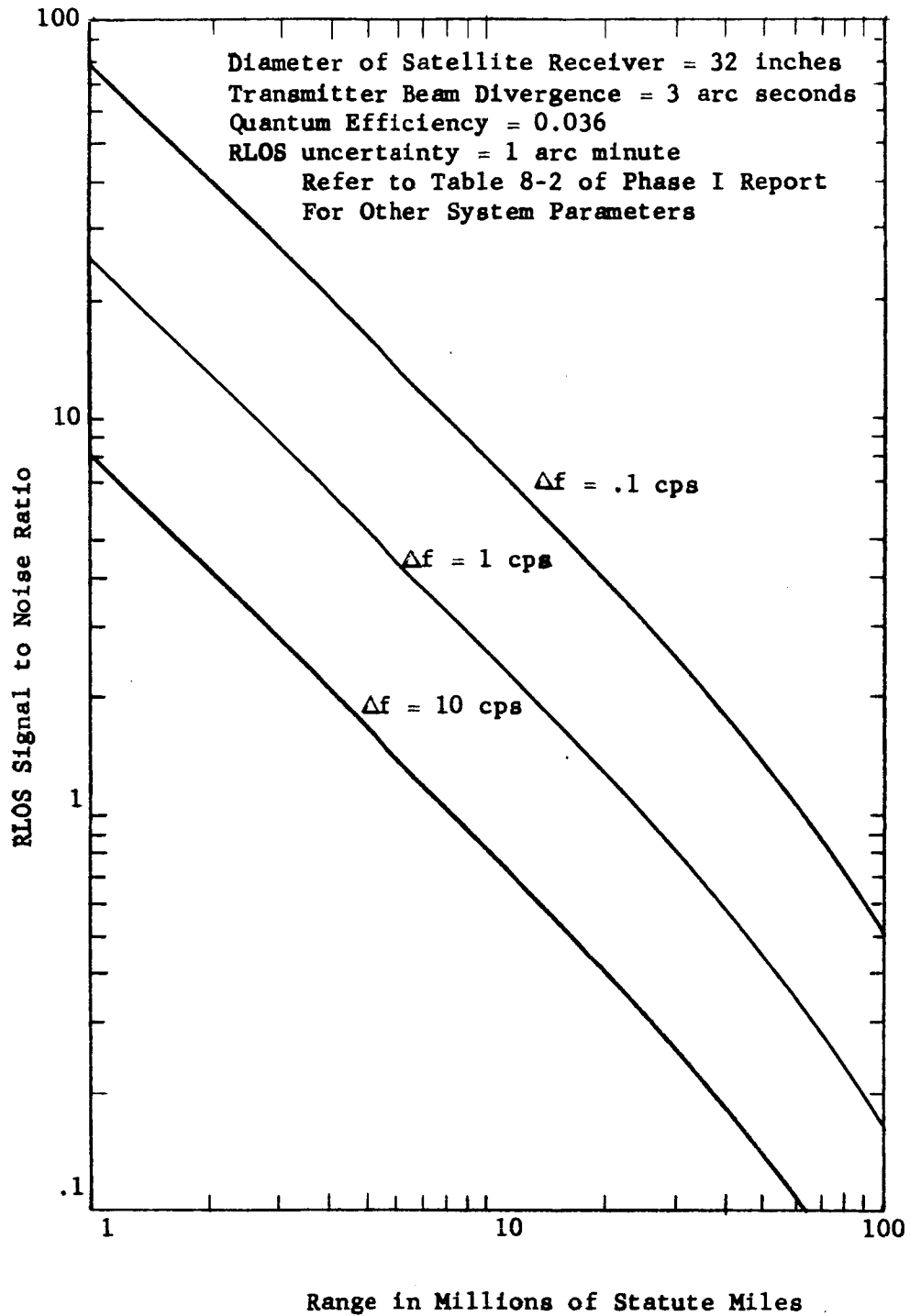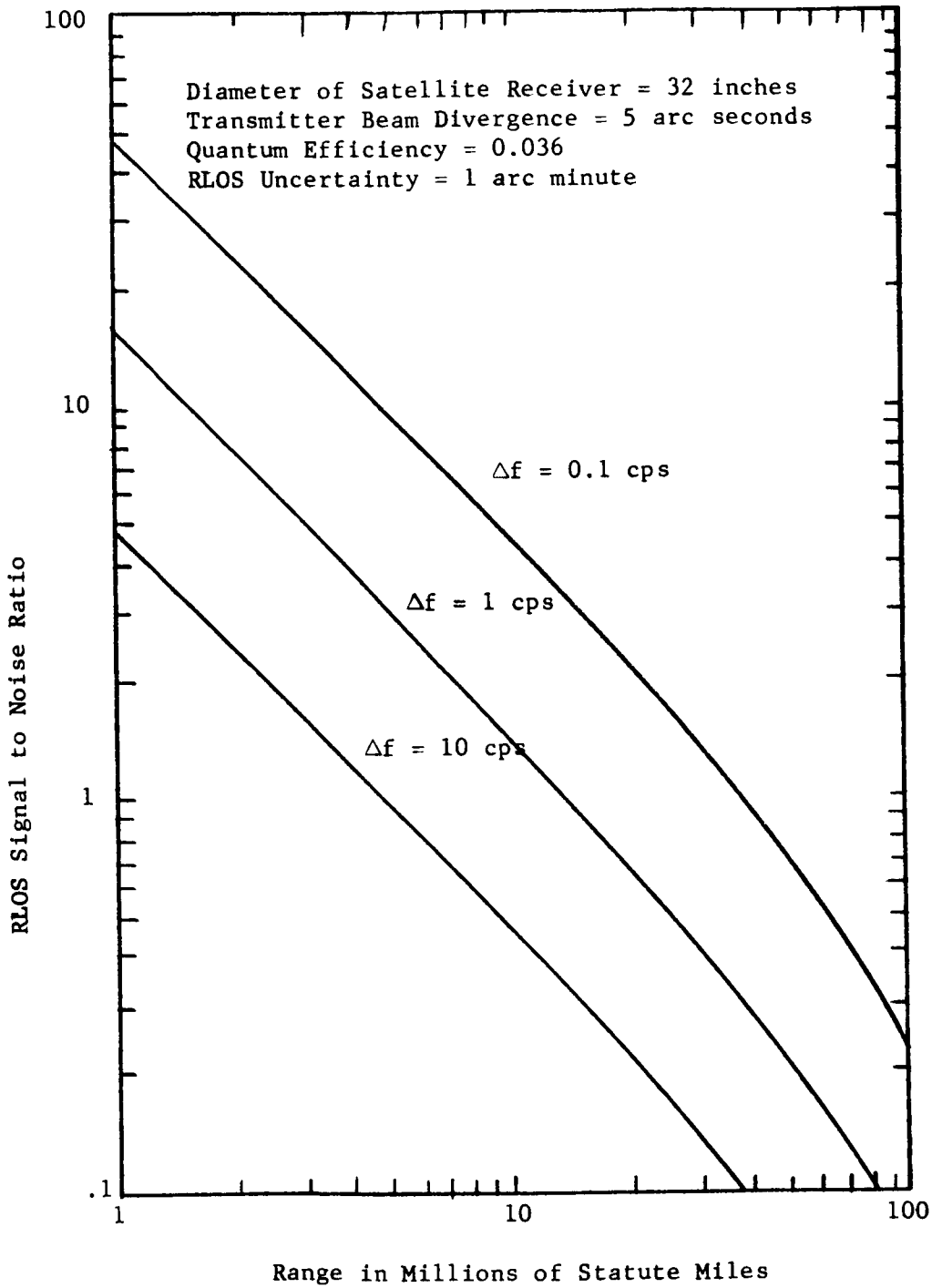Divergence of 10 Arc Seconds

Figure B-10. RLOS Signal to Noise Ratio With
Beam Divergence of 3 Arc Seconds

T_E Vehicle Telescope Pointing at Earth

T_S Star Tracker Pointing at Star in Galactic Plane

$\triangle\beta$ Angular RLOS Uncertainty

$\triangle\emptyset$ Angular Star Tracker Uncertainty

γ Angular Separation Between Star Tracker and Vehicle Telescope

Figure B-11. RLOS Measurement Using Star Tracker and Telescope

that the star tracker can determine the direction of a star S in the galactic

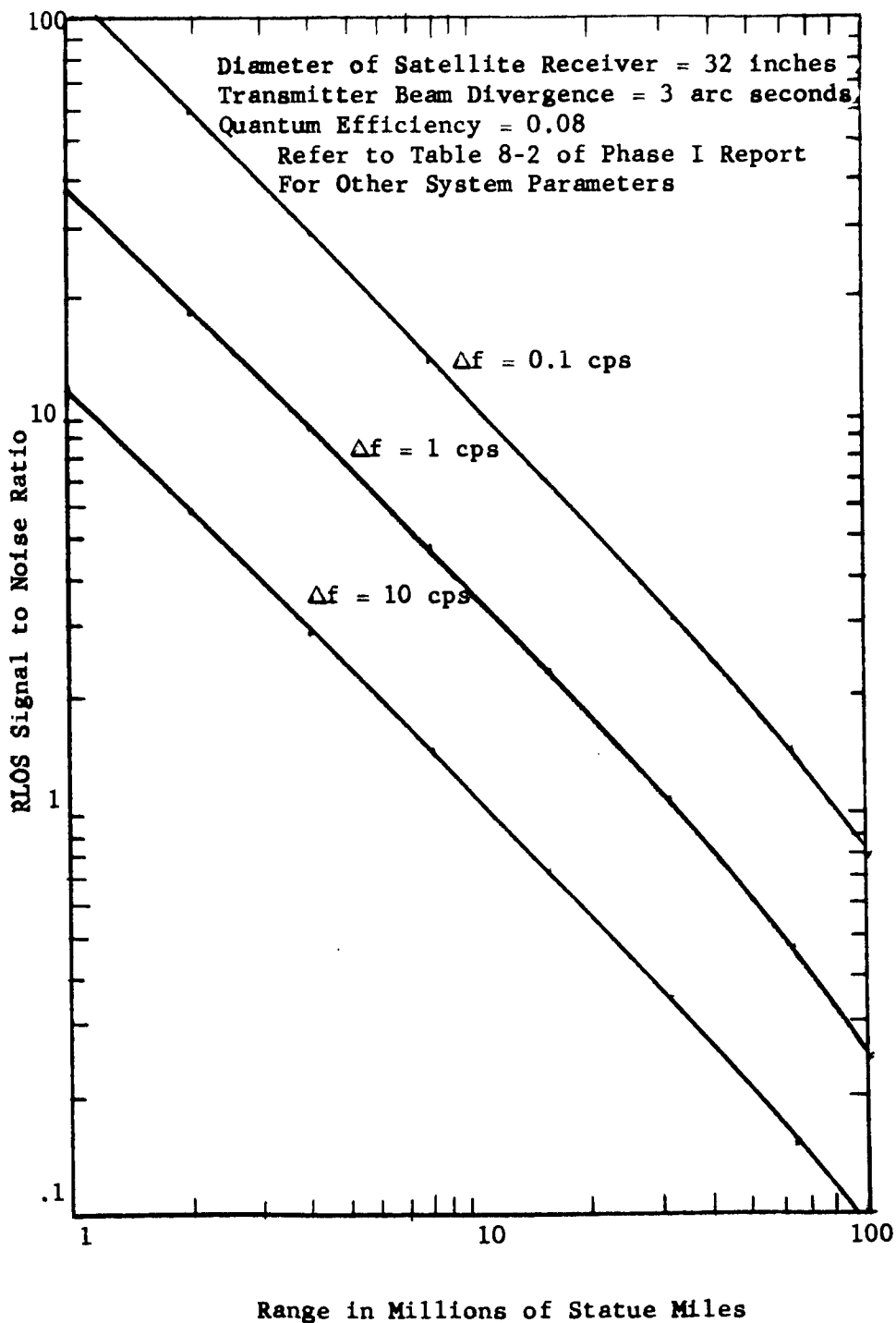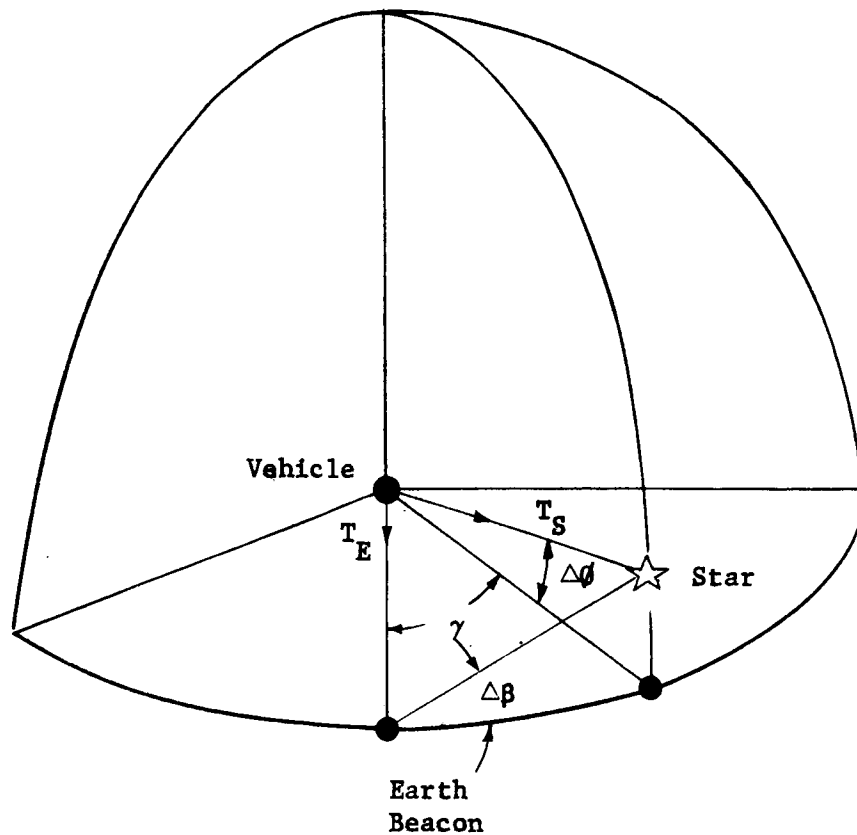plane to an angular uncertainty of $\Delta\phi$. Then the angular uncertainty of RLOS

as determined by the star tracker, assuming that the earth beacon is stationary,

is $\Delta\beta = \Delta\phi/\gamma$ where γ is the separation angle between the star tracker and

telescope viewing the earth. If the angular uncertainty in RLOS, $\Delta\beta$, is to be

held to 1 arc-minute and the angular separation, γ , is 6 degrees, then the star

tracker must determine the direction of the star to a reasonable angular uncer-

tainty of approximately 6 arc-seconds.

This simplified discussion ignores the effect of air shimmer on the

vehicle telescope performance, and assumes that the star tracker and vehicle

telescope can each resolve the two sources.

It appears from the above discussion that the direction method is

much more sensitive than the polarization method. However, there is the require-

ment of a star tracker to achieve the 1 arc-minute RLOS angular uncertainty.

References:

[1] Falconi, O., "Maximum Sensitivities of Optical Direction and Twist
    Measuring Instruments," J.O.S.A., Vol. 54, No. 11, Nov. 1964, pages
    1315-1320.

PERKIN-ELMER

APPENDIX C

POWER CONSUMPTION ESTIMATE FOR THE OPTICAL
TECHNOLOGY SATELLITE - EXPERIMENTS ONLY

APPENDIX C

POWER CONSUMPTION ESTIMATE FOR THE OPTICAL
TECHNOLOGY SATELLITE - EXPERIMENTS ONLY

AVERAGE POWER CONSUMPTION
(WATTS)

MODE OF OPERATION	TELESCOPE NO. 1	TELESCOPE NO. 2
Quiescent	0	0
Acquisition	78	143
Tracking	84	149
Communications	180	264

Duty cycle estimated at 50 percent.

POWER CONSUMPTION ESTIMATE FOR TELESCOPE NO. 1

COMPONENT	AVERAGE POWER DISSIPATION (WATTS)	OPERATIONAL MODE			
		QUIESCENT OPERATION	ACQUISITION	TRACKING	COMMUNICATIONS
Transmit Laser	10				10
External Optical Modulator	50				50
10^7 cps Signal Generator	2				
Diagnostic Electronics	15		15	15	15
Gain Adjust Loop	1		1	1	1
Very Fine Pointing Subsystem	6		6	6	6
Sum Signal Amplifier, Demodulator, Detector, RLOS Detector	6		2	2	2
Telescope Gimbals and Torquer Subsystem	10		10	10	10
Computer Programmer	5		5	5	5
Power Supplies	50		25	30	50
Power Supply Controls	1		1	1	1
Caging	5				
Subtotal (Watts)		0	65	70	150
Unidentified Misc. (20% of Subtotal)		0	13	14	30
Total Power Consumption, Telescope No. 1 (Watts)		0	78	84	180

POWER CONSUMPTION ESTIMATE FOR TELESCOPE NO. 2

OPERATIONAL MODE

COMPONENT	AVERAGE POWER DISSIPATION (WATTS)	QUIESCENT OPERATION	ACQUISITION	TRACKING	COMMUNICATIONS
Transmit Laser	10				10
Optical Modulator	50				50
10^7 cps Signal Generator	2				
Diagnostic Electronics	30		30	30	30
Gain Adjust Loop	1		1	1	1
Very Fine Pointing Subsystem	10		10	10	10
Sum Signal Amplifier, Demodulator, Detector, RLOS Detector	2		2	2	2
Telescope Gimbals and Torquer Subsystem	10		10	10	10
Computer Programmer	10		10	10	10
Power Supplies	60		30	35	60
Power Supply Controls	1		1	1	1
Predetection Filter Thermal Control	10		10	10	10
Magnetic Suspension	10		10	10	10
In-Line Alignment and Focus	5		5	5	5
Point Ahead Subsystem	11				11
Caging	5				
Subtotal (Watts)		0	119	124	220
Unidentified Misc. (20% of Subtotal)		0	24	25	44
Total Power Consumption, Telescope No. 2 (Watts)		0	143	149	264

PERKIN-ELMER

APPENDIX D

PRELIMINARY WEIGHT ESTIMATE
FOR THE OPTICAL TECHNOLOGY EXPERIMENTS

APPENDIX D

PRELIMINARY WEIGHT ESTIMATE
FOR THE OPTICAL TECHNOLOGY EXPERIMENTS

PRELIMINARY WEIGHT ESTIMATE FOR TELESCOPE NO. 1

	POUNDS
Primary	90
Primary Cell	56
Telescope Structure	230
Secondary and Support	27
Quartz Rods	20
Gimbal Ring and Associated Mechanisms	20
Gimbal Torquers (2)	6
Transmit Laser Assembly (With Frequency Stabilization)	12.5
Modulator (KDP) Assembly	1.0
Power Inverter	19.0
Modulator Electronics	10.0
Four Quadrant Detector Assembly	4.5
Transfer Lens Electronics	1.5
Transfer Lens Subassembly	29.0
Gimbal Torquer Electronics	2.0
Diagnostic Electronics	6.0
Control Computer	6.0
Telemetry Leads, Cables and Interconnections	12
Field Stop (Variable) Mechanism	1.0
Coarse Acquisition Sensor	5.0
Hi-Volt Power Supply	3
Spectral Filters (2)	3
Polarizer Sensing Assembly and Electronics	2.3
Miscellaneous Optical Elements and Supports	18
	650.8

PRELIMINARY WEIGHT ESTIMATE FOR TELESCOPE NO. 2

<u>POUNDS</u>

Basic Telescope No. 1		650.8 (From Former Sheet)
Plus (A)	8400Å Transmit Laser With 5 lbs. frequency control equipment with closed cycle cryogenic cooling.	16
(B)	Ga-As Modulation Electronics	.5
(C)	Laser (Third) and Modulator with Stabilizer	15
(D)	Transmit Beam Deflector	29
(E)	Piezo Tilt Mirror and Electronics	1.5
(F)	Risley Prism Deflector	2.5
(G)	Laser A Local Oscillator 6328Å (With Frequency Stabilizer)	12.5
	Laser B Local Oscillator 8400Å	.5
(H)	Four Quadrant Detector B	4.5
(I)	Point Ahead Electronics	2.0
(J)	Magnetic Suspension with Flexures	15
(K)	Additional Cabling	4
(L)	Additional Spectral Filters and Selector Mechanism	3
(M)	Caging 84 lbs. - 66 lbs. =	18 (Additional)
(N)	Alignment Mechanism - 3 at 2 lbs. each	6
(O)	Low Bandwidth Acquisition Sensor Auxiliary	15

TOTAL   795.8

PERKIN-ELMER

APPENDIX E

TELESCOPE DYNAMICS (SIMPLIFIED)

APPENDIX E

TELESCOPE DYNAMICS (SIMPLIFIED)

Dynamic Model

The telescope mounts were examined by considering the telescope in the simplest dynamic model possible. A single mass spring system in each of the principal directions can provide valuable initial parameter information. The elasticity of housing was considered as acting in series with the shock isolators. See Figure E-1.
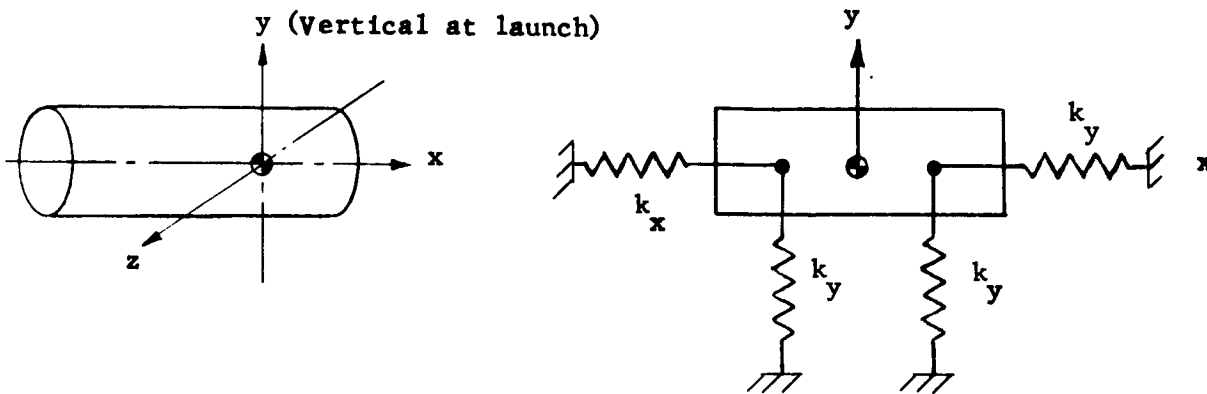

Figure E-1. Telescope Dynamic Model

The equivalent dynamic model to determine the required stiffness and damping in the y and z directions can be simplified to arrangement shown in Figure E-2.
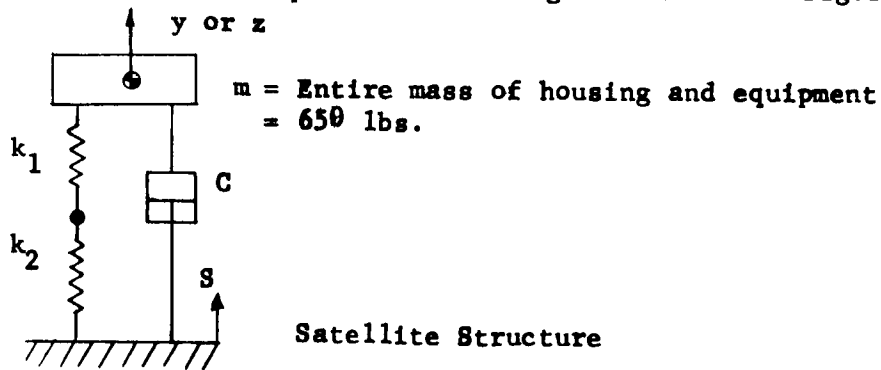

m = Entire mass of housing and equipment
= 650 lbs.

Satellite Structure

Figure E-2. Equivalent Telescope Dynamic Model

E-2

The spring rate of the housing in bending (and shear) is K_1 and is determined by extrapolating data from tests conducted on a similar structure with somewhat different parameters. By conducting a parametric study, it has been determined that the fundamental frequency of the telescope housing (without shock mounts) in the y and z directions is 189cps. The shear deflection will be about 3 times the flexural deflection for this assembly. The equivalent spring rate of the telescope can then be calculated as 2.2×10^6 pounds/inch.

The equation of motion for this system in the y direction is:

$$m\ddot{y} + C\dot{y} + \left(\frac{K_1 K_2}{K_1 + K_2}\right) y = f(t)$$

$$\text{Let } f(t) = -m\ddot{s}$$

then,

$$m\ddot{y} + C\dot{y} + K_{eq}. y = -m\ddot{s}$$

The assumptions implicit in this equation are:

1) The telescope housing and all equipment can be represented as a single rigid mass.

2) There is no elastic coupling between coordinates (either translational or rotational).

3) The principal axis of the housing is aligned with the coordinate axis.

4) Elasticity and damping are linear.

In the region of the fundamental frequency (10 - 200 cps) the excitation is assumed to be

$$s = 4.6 \text{ g's (0 to peak)}$$

This excitation was obtained by extrapolation from existing booster environment data. Assume a rattle space of $\pm 1/4$ inch is available.

$$\frac{y}{s} = \frac{1}{2\beta}$$

$$s = s/\omega_f^2$$

$$\frac{y\omega_f^2}{s} = \frac{1}{2\beta}$$

Let the damping ratio $\beta = 0.1$ (a reasonable value).

$$\frac{y\omega_f^2}{2} = \frac{1}{2(0.1)} = 5 = \text{Transmissibility}$$

$$\omega_f = 188 \text{ rad/sec}$$

$$f = 188/2\pi \text{ cps} = 30 \text{ cps (Resonant frequency)}$$

Therefore, if the system has a fundamental frequency of 30 cps and a damping ratio of 0.1, the transmitted g load will be the transmissibility times the forcing acceleration or (5) (4.6) equals to 23 g's.

The required spring rate of the shock mounts, k_2, is:

$$\omega_n = \frac{\omega_d}{\sqrt{1-\beta^2}} = \frac{188}{\sqrt{1-0.01}} = 189 \text{ rad/sec}$$

$$keq = m\omega_n^2 = \frac{651}{386} (189)^2 = 60,500 \text{ lb/in}$$
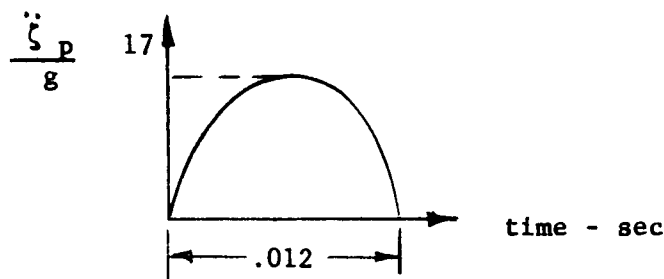
$$\frac{k_1 k_2}{k_1 + k_2} = 60,500$$

since

$$k_1 = 2.2 \times 10^6 \text{ lb/in}$$

$$k_2 = 6.2 \times 10^4 \text{ lb/in}$$

The spring rate for each mount in the y direction can now be found.

$$k_2' = \frac{1}{4}(6.2 \times 10^4) = 1.55 \times 10^4 \text{ lb/inch}$$

In addition to the steady state environment, this system must also withstand a shock pulse in the y direction of 17g - 12 millisecond half sine pulse:

Using the notation from the "Shock and Vibration Handbook."[*]

$$\frac{m}{k}\ddot{v} + v = \zeta(t) \quad \text{(see eq. 8.2 of above reference)}$$

where

$$\zeta(t) = \zeta_p \sin \frac{\pi t}{\tau}$$

$$\omega_n = 189 \text{ rad/sec} \qquad T = \frac{2\pi}{\omega_n} = \text{Natural period}$$

$$\frac{\tau}{T} = \frac{\omega_n}{\omega_f} = \frac{189}{262} = 0.721$$

where

$$\tau = 0.012 \text{ sec} = \text{Forcing period}$$

$$f_f = \frac{1}{2(0.012)} = 41.6 \text{ cps}$$

$$\omega_f = 41.6(2\pi) = 262 \text{ rad/sec}$$

From the curves presented on pages 8-23,[*] the response is found by interpolation between $\frac{\tau}{T} = 0.5$ and 1.0

[*]
Shock and Vibration Handbook, Harris and Crede, Vol. I - Pages 8-23.

$$\frac{v}{\zeta_p} = 1.5$$

$$\zeta_p = \frac{\ddot{\zeta}_p}{\omega_f^2} = \frac{17(386)}{(262)^2} = 0.0956 \text{ inch}$$

Rearranging the equation of motion

$$\ddot{v} = \omega_n^2 \left[\frac{\ddot{\zeta}_p}{\omega_f^2} \sin\left(\frac{t}{\tau}\pi\right) - v \right] .$$

At resonant point $t/\tau = T/\tau = 0.72$ the acceleration is the maximum.

$$\ddot{v} = (189)^2 \left[\frac{17(386)}{(262)^2} \sin\left(0.721\,\pi\right) - 1.5 \ (0.0956) \right]$$

$$\ddot{v} = -2160 \text{ in/sec}^2$$

$$\frac{\ddot{v}}{g} = \frac{2160}{386} = 5.6 \text{ g's}$$

Since this g level is relatively low, it is possible to stiffen the system appreciably if required for steady state conditions. The displacement is within the allowable tolerance of ±1/4 inch.

$$v = y = 1.5 \ (0.0956) = 0.144 \text{ inch}$$

In order to allow for coupling effects, non linearities and the effects of internal suspension, a more elaborate dynamic model is required involving many more degrees-of-freedom. However, the above values provide good starting point data.

Acoustic Mirror Loading

The primary mirror is further softened within the housing by elastic mounts in three points which are desengaged after launch as discussed in

Section 3.0. In addition to withstanding the shock and vibration environ-
ment transmitted through the satellite structure, the mirror must withstand
an acoustical environment. The steady state and transient sound pressure
levels for Centaurs have been specified.[*] The maximum steady state pressure
level is 132 db which is effectively constant from a frequency of 30 cps to
1000 cps. The fundamental frequency (f) of the primary mirror mounted on a 3
point support is approximated by the following equation:

$$f = \frac{0.67}{a^2} \sqrt{\frac{gD}{\rho h}}$$

a = mirror radius - in

g = 386 in/sec^2

D = flexural rigidity

$\quad = \dfrac{E\, h^3}{12(1 - \mathscr{H})}$

h = plate thickness in.

ρ = density, lb/inc^3

For the OTS mirror, the frequency (f) is equal to 800 cps.

The sound pressure is $db = 20 \log_{10} \dfrac{P}{4.2 \times 10^{-7}\ lb/ft^2}$

$P = 1.8\ lb/ft^2$ at sound pressure of 132 db.

The total force exerted on the mirror surface is:

$$F = PA = \frac{(1.8)}{1.44}\ \frac{\pi}{4}\ (32)^2 = \underline{\underline{10.4\ lb}}$$

Consider the following first approximation of the mirror model as sketched in
Figure E-3.

Assume $\qquad \beta = \dfrac{c}{c_c} = 0.01$ at resonance

$$\text{Transmissibility} = \frac{m\ddot{x}}{F} = \sqrt{\frac{1 + 4\beta^2}{4\beta^2}} = \sqrt{\frac{1 + 4(.01)^2}{4\,(0.01)^2}} = 500$$

$$m\ddot{x} = 500 \ (10.4) = 5200 \ \text{lb.}$$

$$\ddot{x} = 20,000 \ \text{in/sec}^2$$

$$\frac{\ddot{x}}{g} = 52 \ \text{g's} = \text{Resonant steady state response to 132 db of sound.}$$
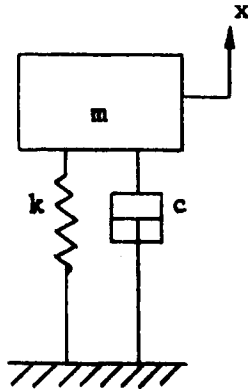

Figure E-3. Equivalent Mirror Model

It is anticipated that the quartz mirror will be able to survive this loading perhaps with additional internal damping of the mirror obtained by use of appropriate materials.

The mirror must also survive the shock environment. As presented in the reference previously indicated for the Centaur environment, the maximum sound level is 136 db and the period is approximately 100 seconds. The shape is shown in Figure F-4.
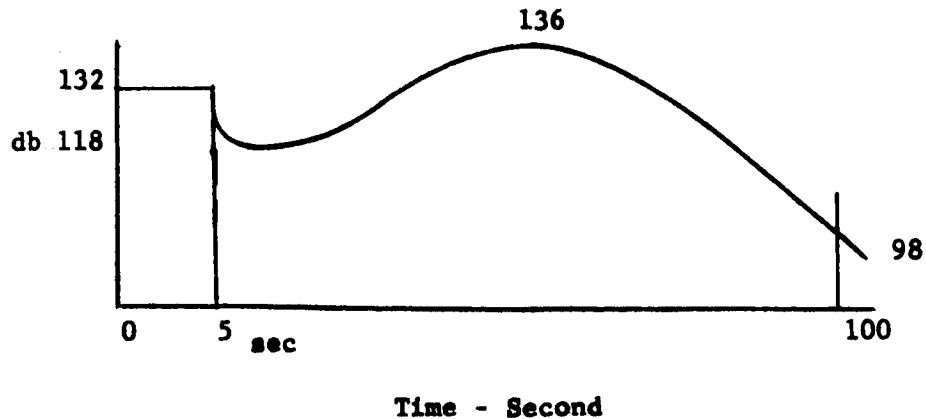

Figure E-4. Centaur Acoustical Shock Environment

To simplify the analysis, assume the shock can be represented by two distinct

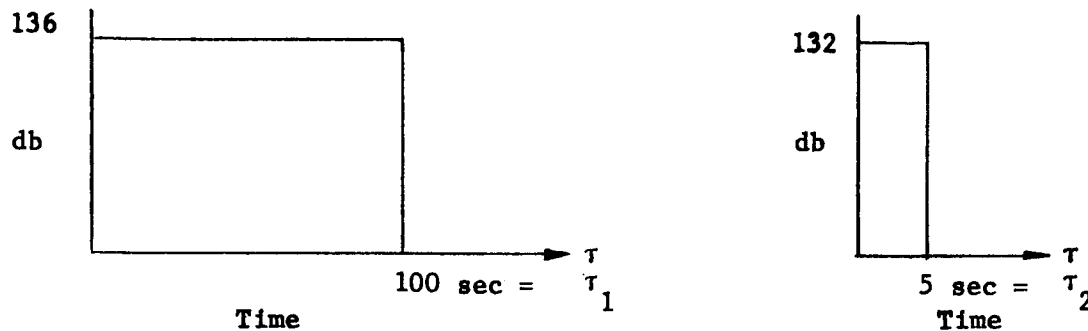rectangular pulses in Figure E-5.

Figure E-5.

The assumption of rectangular pulses is conservative. Again utilizing the

notation in the "Shock Mount Handbook,"

Natural freq. of mirror = 800 cps

$T = \dfrac{1}{800} = 0.00125$ sec. = natural period

$T/2 = 0.00063$ sec

τ = Forcing Period

$\tau_1 = 100$ sec

$\tau_2 = 5$ sec

$\dfrac{\tau_1}{T} = \dfrac{100}{0.00125} = 80,000$

$\dfrac{\tau_2}{T} = \dfrac{5}{0.00125} = 4,000$

Since these values of $\dfrac{\tau_1}{T}$ and $\dfrac{\tau_2}{T}$ are so large, the system behaves like a

rigid body and there is no magnification of the input pulse. The maximum

force on the mirror due to the transient acoustic impulse is:

$P = 3$ lb/ft^2 at a sound level of 136 db

$F = \underline{\underline{16.7 \text{ lb.}}}$

$m\ddot{x} = F = 16.7$

$\ddot{x} = 64.5$ in/sec^2

$\dfrac{\ddot{x}}{g} = \underline{\underline{0.167}}$ g's

This 0.167 g value is insignificant when compared to the allowable loads for the mirror.

APPENDIX F

CONSIDERATIONS OF SIGNAL TO NOISE RATIO
IMPROVEMENT IN TRACKING PULSED LASER BEACONS

APPENDIX F

CONSIDERATIONS OF SIGNAL TO NOISE RATIO IMPROVEMENT IN TRACKING PULSED LASER BEACONS

The S/N ratio in an optical communication system utilizing a pulsed beacon was examined to determine the effect of duty cycle for the assumption that average laser power is a constant. It appears that no improvement is possible for cases where only the signal is present. However, when degradation due to background light is present, decreasing the duty cycle can improve S/N ratio substantially and, in the limit, the S/N ratio will essentially become that obtainable without background light. The S/N ratios computed are those corresponding to perfect photosensors (viz: unit quantum efficiency, zero dark current, etc). Since other sources of system noise are often equivalent to background light, the effects on S/N from such sources can be reduced.

Pulsed Beacon Operation - The improvement in S/N utilizing low duty cycle laser pulses can be determined over CW beacon operation assuming that average laser output power is a constant. The first approach shall be for a system in which the background light photon arrival rate uncertainty is determined by averaging the total number of photons received between pulses over the interval T-t (see Figure F-1).
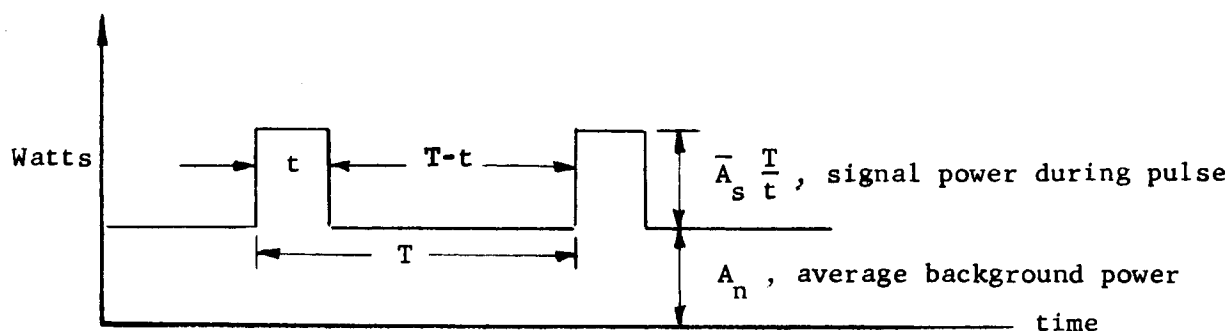
Figure F-1

The magnitude of the signal plus background power during the pulses shall similarly be determined by averaging over the interval, t.

The average photon arrival rate for background light is

$$\frac{A_n}{10^{-7}hc} \stackrel{\triangle}{=} A_n K,$$ while the average photon arrival rate

for signal is given by $\bar{A}_s \frac{T}{t} K$:

The uncertainty in determining the true height of the background level and signal plus background photon arrival rates are,

$$\sqrt{\frac{A_n K (T-t)}{T-t}} \qquad \text{and} \qquad \sqrt{\frac{(\bar{A}_s \frac{T}{t} T + A_n t)K}{t}} \quad \text{respectively.}$$

The rms error in correctly determining the signal pulse height is equal to the rms sum of the two preceeding quantities and signal to noise ratio can be expressed as.

$$S/N = \frac{\bar{A}_s \frac{T}{t} K}{\left(A_n K \left[\frac{1}{T-t} + \frac{1}{t}\right] + \frac{\bar{A}_s TK}{t^2}\right)^{1/2}} \tag{1}$$

which for the case of $A_n = 0$ reduces to

$$S/N = \sqrt{A_S TK} \qquad (2)$$

indicating that S/N cannot be altered by varying the duty cycle. This is a logical result since each pulse corresponds to a given average number of electrons, $\bar{N}_S$, with an rms uncertainty of $\sqrt{\bar{N}_S}$. Hence, the percent rate uncertainty can be expressed as,

$$\frac{\sqrt{\bar{N}_S}/t}{\bar{N}_S/t} \quad \times \quad 100\%,$$

which is not a function of t.

That S/N improvement for cases where background light is not negligible can be demonstrated by considering two cases. The first shall assume that $t = T/2$ and the second shall assume that $t \ll T$.

For the first case equation one reduces to

$$S/N = \frac{\bar{A}_S K}{\sqrt{(A_n + A_S)\frac{K}{T}}} \qquad (3)$$

while for the second case the equation becomes

$$S/N = \frac{\bar{A}_S K}{\left[\left(\frac{A_n t}{T} + \bar{A}_S\right)\frac{K}{T}\right]^{1/2}} \qquad (4)$$

The S/N improvement factor, Z, due to reducing duty cycle while holding average laser power fixed, is obtained by dividing equation 4 by 3; i.e.,

$$Z = \sqrt{\frac{A_n + \bar{A}_S}{A_n \frac{t}{T} + \bar{A}_S}} \qquad (5)$$

F-4

Examination of this equation and equation 2 indicates that as t approaches zero, the signal to noise ratio approaches that corresponding to the case wherein $A_n = 0$.

This is an especially significant result for cases where background light power exceeds the signal power and, in addition, since many other sources of guidance system noise are equivalent to additional components of background light.

It is noteworthy that if one considers a system in which the number of photons in each of the intervals $T-t$ and t are counted and then differenced to obtain signal level, there is no improvement of S/N with t reduction. The basic reason for this is that, in contrast with the method above, the contribution to signal magnitude uncertainty due to photon discreteness in the interval $T-t$ is not weighted by $\frac{1}{T-t}$.

Consider next a system in which background light level is determined by determining the photon arrival rate during a period, t_n, between the signal pulses intervals, t_s. Here the signal photon rate is given by $\bar{A}_s TK/t$, and the background light photon rate is given by $A_n K$.

The uncertainty in determining the signal magnitude is the rms sum of the uncertainties in the background photon arrival rate and signal plus background photon arrival rate or,

$$\sqrt{\frac{A_n K}{t_n}} \qquad \text{and} \qquad \sqrt{\frac{(\bar{A}_s \frac{T}{t_s} + A_n)K}{t_s}}$$

and the S/N ratio becomes

$$S/N = \frac{\overline{A}_s \frac{T}{t_s} K}{\left\{ \left(\frac{A_n}{t_n} + \frac{A_n}{t_s} + \frac{\overline{A}_s T}{t_s^2} \right) K \right\}^{1/2}} \qquad (6)$$

For the case where $A_n = 0$, this reduces to

$$S/N = \sqrt{A_s T K} \qquad (2)$$

showing that S/N is not a function of t_s.

For the case of $A_n \neq 0$ and $t_s = t_n = t$, equation 6 becomes

$$S/N = \frac{\overline{A}_s K}{\sqrt{\left(\frac{2A_n t}{T^2} + \frac{A_s}{T} \right) K}} \qquad (7)$$

Computation of the improvement factor Z' for this case (as was done to obtain equation 5) leads to

$$Z' = \sqrt{\frac{(A_n + \overline{A}_s)}{2A_n \frac{t}{T} + \overline{A}_s}} \qquad (8)$$

which is similar to equation 5 and differs only in that a factor 2 appears preceeding the A_n term in the demoninator of the radical. This result indicates that significant S/N improvement is possible in cases where A_n exceeds A_s. It is noteworthy that systems which count pulses over the intervals t_n and t_s and utilize the differences to establish signal magnitude lead to exactly the same result if $t_n = t_s$.

Equation 8 is applicable to systems utilizing bandpass amplifiers to provide filtering action. The output of the amplifier sampled between signal pulses subtracted from the output of the amplifier during the signal pulse will be the estimated height of the signal pulse.

A typical system utilizing this method is indicated by the block diagram of Figure F-2.

The single axis tracking error sensor utilizes a two sided roof prism, situated in the optical focal plane, and two phototubes to sense the light reflected from the two sides. The PMT signals are separately filtered and the sum sent to the pulse sensor and gate generator which generates the t_n and t_s gate signals. Each filtered output is fed to two sample and hold circuits which sample the magnitude of background light in interval t_n, and the magnitude of signal plus background light during the interval t_s. The outputs of the hold circuits are summed and differenced to:

(1) Determine the signal pulse amplitude differences of the PMT output signals.

(2) Determine the total signal amplitude received.

The total signal amplitude is utilized as a gain control signal for the error amplifier to achieve a pointing error signal of stabilized scale factor.
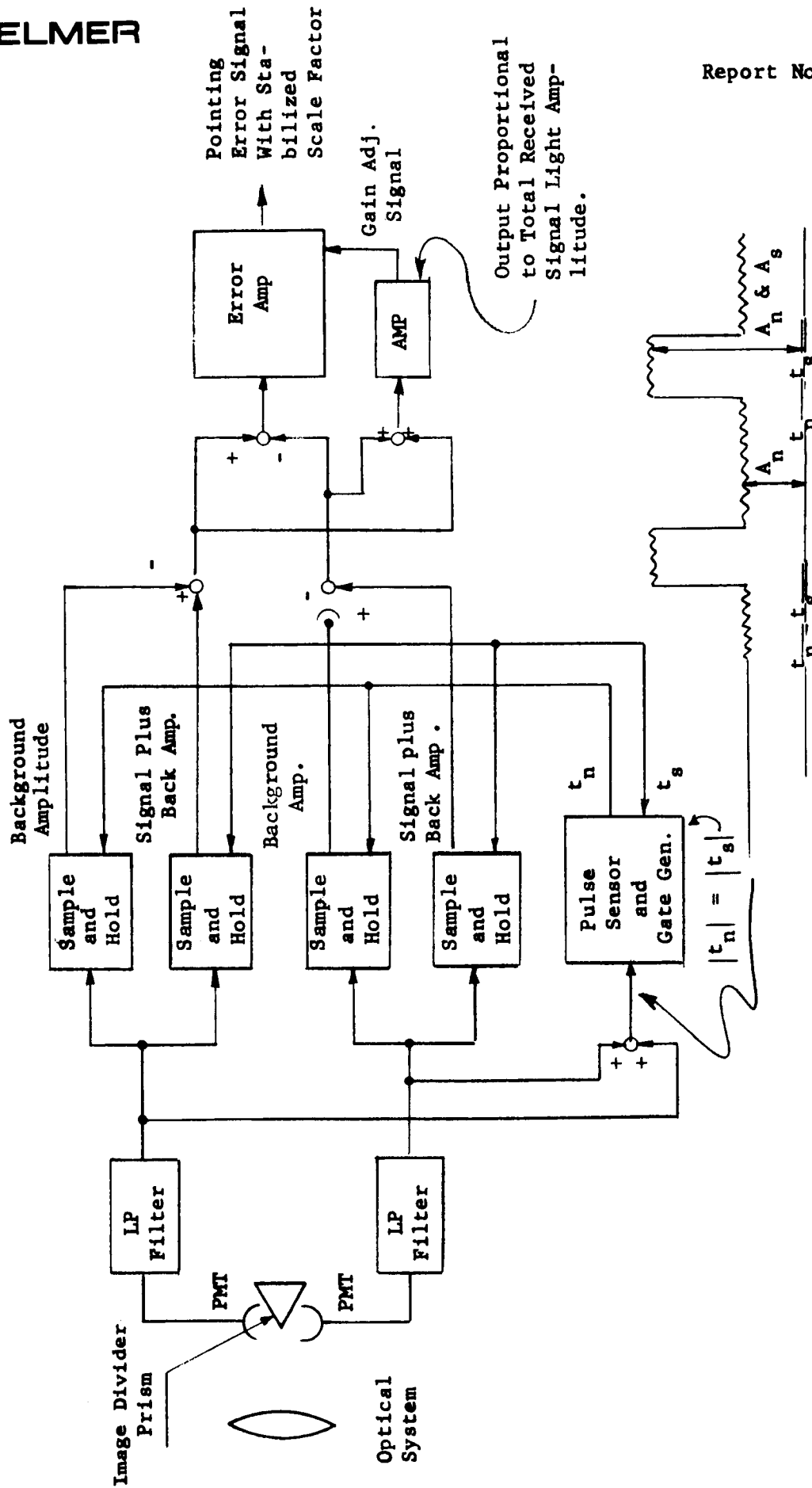
Figure F-2. Single Axis Tracking Error Sensor for Pulse Beacon Operation